

**SAN PEDRO CREEK WATERSHED
SEDIMENT SOURCE ANALYSIS**

**Volume II:
Hillslope Sediment Source Assessment**

Stephanie Sims



San Francisco
State University

Abstract

The hillslopes and tributaries within San Pedro Creek Watershed are covered mainly by coastal scrub, chaparral, and dense riparian vegetation while the lower elevation valley is urbanized. Sediment is generated predominately from mass wasting processes as the hillslopes are highly prone to landslide activity from steep slopes with unconsolidated bedrock and are frequently subjected to heavy rainfall. Surface erosion is also significant within the watershed primarily on areas heavily influenced by land use practices resulting in little to no vegetative cover and compacted soils, both modifying flow and increasing runoff. Sediment sources were identified by examining land use change and landslide mapping from historic aerial photography combined with primary field data and GIS modeling. Most sediment produced from landslides was triggered by natural sources while surface erosion was largely generated from anthropogenic triggers. The Middle and Sanchez subwatersheds were found to produce the highest levels of sediment for which sediment abatement techniques were then proposed.

Table of Contents

List of Tables.....	v
List of Figures	vi
1. Introduction.....	1
1.1 Purpose and objectives	1
1.2 Project overview	1
2. Study Area	2
2.1 Geomorphology	3
2.2 Geology.....	8
2.3 Soils	12
2.4 Land use.....	14
2.5 Land cover.....	19
2.6 Climate	23
3. Sediment Production.....	25
3.1 Geomorphic and fluvial processes.....	25
3.1.1 Mass wasting.....	25
3.1.2 Surface erosion	31
3.2 Anthropogenic influence.....	34
3.3 Influence of vegetation	38
4. Methodology	41
4.1 Aerial photographic interpretation	42
4.2 Field surveys.....	47
4.3 GIS models	48
4.4 Previous work in SPCW	52
4.5 Synthesis	53
5. Results	55
5.1 General patterns: Landslide and gully distribution.....	55
5.1.1 Impacts of land use change on sediment production	57
5.1.2 Effective drainage	68
5.1.3 Perennial flow	73
5.1.4 SEM	76
5.1.5 SHALSTAB	78
5.1.6 Connectivity	80
5.2 Subwatershed prioritizations	91
5.2.1 North subwatershed	93
5.2.2 Middle subwatershed	101
5.2.3 Middle/South subwatershed	109
5.2.4 South subwatershed	112
5.2.5 Sanchez subwatershed	122
5.2.6 Shamrock subwatershed.....	130
5.2.7 Pedro Point I subwatershed	136
5.2.8 Pedro Point II subwatershed	141
5.2.9 Crespi subwatershed	146
5.2.10 Unnamed subwatersheds	149

6. Conclusions.....	156
6.1 Changes in sediment sources	156
6.2 Proposed recommendations for sediment mitigation	157
6.3 Limitations	163
6.4 Possibilities for future research	165
6.5 Contributions of the study	165
References	166
Appendices	
A: Aerial photograph inventory	172
B: GIS layers used	176
C: Past and current land use cover per subwatershed	178
D: Current effective drainage density per subwatershed	182

List of Tables

1. Soil erodibility ratings derived from the K- factor and slope	51
2. Landslide and gully sources in SPCW categorized by number of events and % of total	56
3. Break down of anthropogenic landslide and gully sources categorized by number of events and % of total	56
4. Years landslides and gullies were first visible on aerial photographs categorized by number of events and % of total	57
5. Landslide “age” at first visible year on aerial photographs categorized by number of events and % of total	57
6. General land use patterns per year observed for the entire SPCW in hectares and percent	58
7. Total sum of all streams, roads, trails, and drainage channels per subwatershed	68
8. Total effective drainage density per subwatershed.....	71
9. Known areas of perennial flow initiation along tributary branches.....	74
10. Level of connectivity of possible sources to the stream network as a factor of buffer distance and percent hillslope.....	80
11. SEM model merged with connectivity values from Table 11 to determine the level of connectivity of the SEM.....	81
12. Current land use by subwatershed	91
13. Total landslide and gully inventory from those identified on aerial photographs between 1941 and 1997	92
14. Total landslide volume delivery estimates based on levels of connectivity of landslide scars to the stream network.....	92

List of Figures

1. San Francisco, CA, 15 miles north of study area	3
2. San Pedro Creek Watershed	3
3. SPCW draining northwest to the Pacific Ocean	4
4. Slope of SPCW in degrees	6
5. Pacifica State Beach looking northwest from Montara Mountain Trail	7
6. Terraced hillslopes altering the geomorphology of natural slopes	8
7. Surficial geology and fault lines of SPCW	10
8. Tributary following San Pedro Mountain Fault and draining into Brooks Creek in the upper South subwatershed	11
9. Soil complexes of SPCW	13
10. USGS topography map of SPCW in 1896 with little urban development and few roads	15
11. USGS topography map of SPCW in 1997	15
12. Roads, trails, and public lands of SPCW	16
13. Remnant bare soil and erosion from previous off-road use in Pedro Point II subwatershed	17
14. Shamrock Ranch with nearby open space and residential development	17
15. Urbanization in the North subwatershed from the valley floor encroaching on the toe slopes of hillsides	18
16. Land cover of SPCW	20
17. Native evergreen and deciduous scrub assemblages of south-facing hillslopes of the Middle subwatershed from Hazelnut trail	21
18. Non-maintained trail in the exotic blue gum eucalyptus and Monterey pine forest in Shamrock subwatershed	22
19. Mixed grassland and native deciduous scrub of the upper North subwatershed	23
20. Average daily temperatures and precipitation per month displayed on Table 1	24
21. Select landslides triggered from January 1982 storm event that were studied in detail	27
22. Oddstad slide in the North subwatershed	28
23. Slope angle and properties for nine landslides within Pacifica triggered by the January 1982 storm event	29
24. Landslides triggered from January 1982 storm event with corresponding geological units, Pacifica, CA	30
25. Rills on the nearly vertical face of an uphill trail cut in the South subwatershed	32
26. Gullies along a trail on Cattle Hill in the upper North subwatershed	32
27. Gullies upslope from a trail in the Middle subwatershed	33
28. Fluvial erosion causing incision through a former landslide deposit in an intermittent tributary draining into Sanchez Fork	34
29. Severe surface erosion from concentrated Horton overland flow downslope of Coastside Boulevard	35
30. Concentrated flow creating surface erosion and increasing the effective drainage density along the Hazelnut Trail draining to South Fork	35

31. Mountain bike trails and constructed features along an otherwise unmaintained trail draining to Shamrock Fork	36
32. Burrow hole that may soon lead to piping along the upper edge of complex in a gully the Middle subwatershed.....	37
33. Riparian corridor along Pedro Point I channel.....	39
34. Tree throw from an overturned blue gum eucalyptus	40
35. Generalized relative slope susceptibility map of SPCW	43
36a. Pre-1982 debris flow scars and tracks mapped from aerial photographs.....	44
36b. Landslides and tracks from the 1982 storm event superimposed on a 1977 susceptibility map previously created by the author	45
36c. Debris flow susceptibility map updated from the 1977 version with likely debris flow runout paths	46
37a. Land use in 1941 with existing roads and trails.....	59
37b. Land use in 1955 with existing roads and trails.....	61
37c. Land use in 1975 with existing roads and trails.....	63
37d. Land use in 1983 with existing roads and trails.....	65
37e. Land use in 1997 with existing roads and trails.....	67
38. Total sum of the stream network, roads, trails, and urban drainage channels per subwatershed displayed in meters	70
39. Effective drainage density of the individual subwatersheds displayed in km/km ²	72
40. Sample tributaries surveyed to determine the area required to maintain perennial flow.....	75
41. Sediment erosion model of SPCW	77
42. Relative shallow slope stability measured as a unitless ratio of effective precipitation/transmissivity.....	79
43. Connectivity at concentric distances in meters from the stream network	82
44. Results of Table 12 displaying areas significantly susceptible to surface erosion with direct connectivity to the drainage network	83
45. SHALSTAB displayed with results of Table 11 displaying relative landslide potential connectivity	84
46a. Landslide and gully connectivity to the stream network in Crespi and Pedro Point I and II subwatersheds	85
46b. Landslide and gully connectivity to the stream network in Sanchez subwatershed	86
46c. Landslide and gully connectivity to the stream network in South subwatershed.....	87
46d. Landslide and gully connectivity to the stream network in Middle subwatershed	88
46e. Landslide and gully connectivity to the stream network in North and Crespi subwatersheds	89
47. North subwatershed outlined in red indicating significant sediment sources in yellow	95
48. Trail network along the upper slopes of the Picardo Ranch	96
49. Landslide deposit downslope from trail on Picardo Ranch subjected to surface erosion	97
50. Trail eroding into drainage culvert of terraced hillslopes	98

51. Rilling upslope of trail on terraced hillslope contributing to the sediment delivered to the drainage ditch	99
52. Trail channeling flow and creating a moderate gully draining toward the North Fork	100
53. Middle subwatershed outlined in red indicating significant sediment sources in yellow	102
54. Slump on terrace between Weiler Ranch Road and the Middle Fork	104
55. Deeply incised drainage in colluvium with repeat history of landslides	105
56. Gully incising through landslide deposit along Weiler Ranch Road	106
57. Incision at culvert from uphill ephemeral drainages	107
58. An ephemeral drainage along a portion of Hazelnut trail	108
59. Middle/South subwatershed outlined in red indicating significant sediment sources in yellow	110
60. Surface erosion along an upslope roadcut draining to ditch and culverted under the road directly to the Middle/South fork	111
61. South subwatershed outlined in red indicating significant sediment sources in yellow	113
62. Erosion along uphill section of lower Hazelnut Trail	115
63. Surface erosion along uphill section of trail	116
64. Surface erosion on barren hillslope along Brooks Creek Trail upslope of upper trail	117
65. Barren loose soil from upper trail dumping onto lower trail and further downslope	118
66. Surface erosion on Brooks Creek Trail with rilling in unconsolidated landslide deposits on the upper trail cut	119
67. Surface erosion along Brooks Creek Trail	119
68. Channel along Brooks Creek Trail draining on the upper slopes	120
69. Surface erosion upslope from road eroding directly to drainage ditch	120
70. Control structures implemented after a slide	121
71. Sanchez subwatershed outlined in red indicating significant sediment sources in yellow	123
72a. Severe mass wasting and subsequent surface erosion downslope of Coastside Boulevard draining to Sanchez Fork	124
72b. Same source as shown in Figure 70a taken over 8 months later after one complete rainy season	124
73. Rutted trail heavily utilized by mountain bikers	125
74. Surface erosion along compacted and gullied trail on the ridgeline between Sanchez and Shamrock subwatersheds	126
75a. Loose unconsolidated soil exposed from significant recreational use	126
75b. Loose unconsolidated soil exposed from significant recreational use	127
76. Channel with significant incision and very exposed tree roots adjacent to heavily compacted trail	127
77. Deep channel incision into landslide deposit	128
78. Trail cut eroded to bedrock with sediment accumulation along the base from surface erosion along upslope soils	129
79. Shamrock subwatershed outlined in red indicating significant sediment sources in yellow	131

80. Shamrock Ranch in the base of the Shamrock valley with sparsely vegetated fields used for grazing	132
81. Incision in trail routing sediment directly into stream	133
82. Gully formed from culverted flow downslope of Highway 1	134
83. Sediment in excavated culvert draining directly to stream along the trail upslope from the Shamrock Ranch	135
84. Nearly impervious compacted trail used significantly by mountain bikers	135
85. Pedro Point I subwatershed outlined in red indicating significant sediment sources in yellow	137
86. Channel incision from culvert draining the urbanized hillslope	138
87. Channel incision from another culvert draining the urbanized hillslope and accumulated flow from culvert	139
88. Severe surface erosion on trails that have not yet established connectivity in the upper Pedro Point I subwatershed	140
89. Pedro Point II subwatershed outlined in red indicating significant sediment sources in yellow	142
90. Surface erosion along former trails	143
91. Surface erosion along former trails	144
92. Erosion to bedrock exposing tree roots along upper trail cut	145
93. Crespi subwatershed outlined in red indicating significant sediment sources in yellow	147
94. Surface erosion over unconsolidated material delivering sediment to the downslope trail and adjacent drainage	148
95. Unnamed subwatersheds outlined in red indicating significant sediment sources in yellow	150
96a. Severe gully in drainage downslope of paved Coastside Boulevard	151
96b. Severe gully in drainage downslope of paved Coastside Boulevard	152
97. Convergence of flow from rutted upper trail and partially paved lower trail	153
98. Undercut vegetation and exposed tree roots on upper trail cut along Coastside Boulevard	154
99. Erosion control tarps washed downslope of trail on landslide deposit	154
100. Ephemeral drainage from upslope switchbacks	155
101. Existing and apparently effective sediment control measures implemented in Pedro Point II subwatershed	158
102. Tree and shrub cuttings (at arrow) placed along trail in an area with deep incision to reduce erosion and promote vegetation growth	159
103. Large gravels spread onto the nearly impervious surface of the road	160
104. Ineffective erosion control structures	161
105. Tarps proving to be ineffective control measures have washed downslope of an area of an eroding area along the Coastside Boulevard	161
106. The partially paved surface of the Coastside Boulevard	162
107. Unconsolidated landslide material along the upper hillslope of the Valley View Trail in the Middle subwatershed	163

1. Introduction

Excess sedimentation of waterbodies is problematic and prevalent worldwide. While natural geomorphic processes generate sediment, land uses including urbanization, agriculture, and grazing significantly enhance the amount produced. Elevated levels threaten fish and amphibious species populations, reduce overall water quality, and can even alter the morphology of a stream.

Select California watersheds are among the highest worldwide in levels of sediment production (Mount 1995). In San Pedro Creek Watershed (SPCW) mass wasting and surface erosion processes act on these sources to dislodge large materials and entrain finer sediments. Aware of these geomorphic processes acting on SPCW, the search for specific sources of sediment through a detailed analysis of the watershed was conducted. A comprehensive assessment of past, current, and potential future sediment sources was conducted with analyses of the subwatersheds. This highly localized breakdown was designed to reveal site-specific problems that could be modified in order to decrease delivery of sediment to San Pedro Creek.

1.1 Purpose and Objectives

The primary purpose of this research is to identify spatial and temporal variations of hillslope sediment sources occurring from natural processes and enhanced by changes in land use. Upon completion the following objectives will be met:

1. Qualitatively and where possible quantitatively identify natural and anthropogenic hillslope sources delivering sediment to San Pedro Creek;
2. Prioritize anthropogenic source areas for management and;
3. Propose management recommendations for mitigating sediment from anthropogenic sources.

1.2 Project Overview

This study begins with a general overview of the study area. The following sections identify sediment-generating processes occurring in SPCW and review methods used for similar studies as well as those used for this study. The general patterns and site-specific prioritizations resulting from the various methods are then analyzed in the Results section. Finally management recommendations to abate sediment delivery to San Pedro Creek are proposed in the Conclusions section.

2. Study Area

San Pedro Creek is confined within a steep drainage with urbanization comprising about 33% of the total watershed area (SPCWC 2000). The remainder is composed of forest, grassland, chaparral, and coastal scrub vegetation communities mainly designated as open and recreational space. Situated roughly 24 km south of San Francisco, CA (Figure 1) within the coastal community of Pacifica in San Mateo County (Figure 2) the creek drains a total of 21.3 km² or 8.2 mi² northwest into the Pacific Ocean.

The majority of the drainage area, 18.9 km² or 7.3 mi², is composed of fourteen distinct subwatersheds: the North, Middle, South, combined Middle/South, Sanchez, Shamrock, Crespi (labeled Hinton), Pedro Point I and II, and five groups of subwatersheds collectively titled unnamed 1-5 (Figure 3). The unnamed subwatersheds drain directly to the main fork of San Pedro Creek and are composed of numerous smaller subwatersheds. Breaking San Pedro Creek Watershed (SPCW) into subwatersheds provides an effective means to isolate from which tributaries sediment is entering the stream system. Land uses vary significantly in the subwatersheds and factors generating sediment can also be effectively attributed to the distinct subwatersheds. This subwatershed system follows that established by the SPCWC varying only by adding the unnamed subwatersheds and dividing Pedro Point into two subwatersheds. The remainder of the drainage, 2.4 km² or 0.9 mi², is urban development on the valley floor and runoff mainly funnels into storm drains and channels from the overlying urban environment (SPCWC 2000).

The ten subwatersheds are the focal zones of the study area. Hillslopes and tributaries are the predominant contributors of sediment to the main channel; however, the localized erosional processes occurring within each subwatershed vary significantly. The amount of sediment generated is mainly controlled by precipitation but also by geomorphology, geology, soils, land use, and land cover. These factors vary significantly within and between the many subwatersheds. The North fork, which is the largest, is also the most heavily influenced by urbanization and most of the drainage is channeled underground. Conversely, the Middle and South forks are radically different, heavily vegetated open space with minimal current land use impacts. The remainder of the subwatersheds comprising the study area consists of a variety of different land uses and land cover ranging between minimal to high levels of use.



Figure 1: San Francisco, CA, 15 miles north of study area (ESRI 2001).



Figure 2: San Pedro Creek Watershed (USCB 2001).

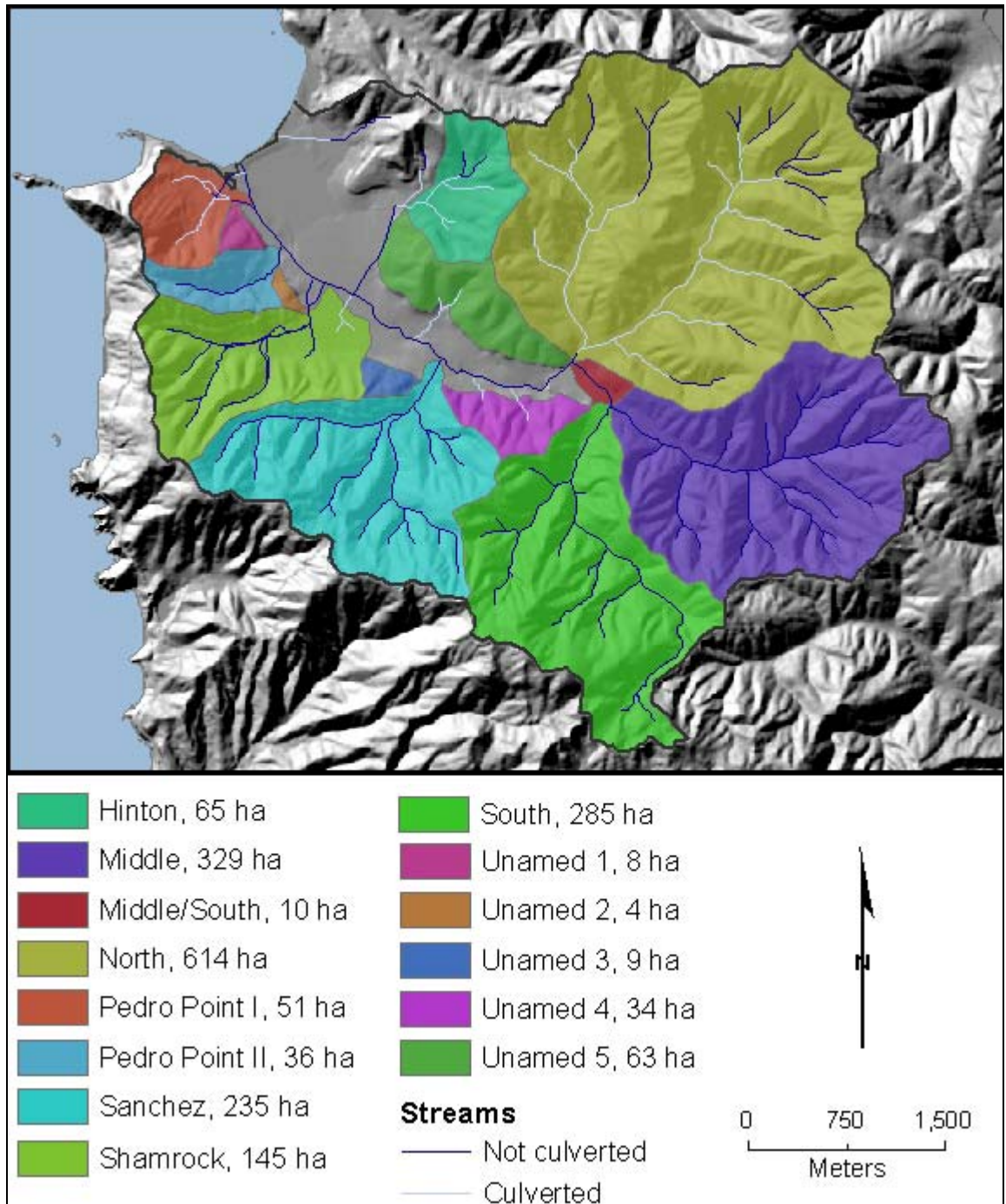


Figure 3: SPCW draining northwest to the Pacific Ocean. The subwatershed drainages shown are overlaying a gray-shaded topography layer representing the remainder of the watershed and surrounding areas. (SPCWC 2000).

2.1 Geomorphology

The Santa Cruz Mountain Range forming the eastern boundary of SPCW is situated only 5.8 km away from the Pacific Ocean to which San Pedro Creek drains (Figure 5). The proximity of this mountain range to the ocean with hillslopes up to 54° create drastic changes in relief that demarcate the distinct boundaries of SPCW (Figure 4). Montara Mountain sits at 578 m and extends west to San Pedro Mountain at 317 m and east to Whiting Ridge to form the entire southern extent of the drainage (USGS 1997). Sweeney Ridge constitutes the entire eastern extent of the watershed connecting to Cattle Hill on the northern boundary and extending west to the Pacific Ocean.

Urbanization has increased the gradient of some hillslopes. Pampeyan (1994) found that toe hillslope removal associated with increased development altered hillslope morphology and increased landslide potential within the Linda Mar neighborhood. To reduce this hazard, hillside terraces are now common throughout much of the North subwatershed (Figure 6) to prevent excess moisture and debris accumulation.

Perched on the edge of the North American plate, which is uplifted by the subducted Pacific plate, SPCW continues to rise. Situated at the junction of these plates, the area contains many faults creating a complex geologic structure. Combined with anthropogenic influences, SPCW is a highly failure-prone landscape.

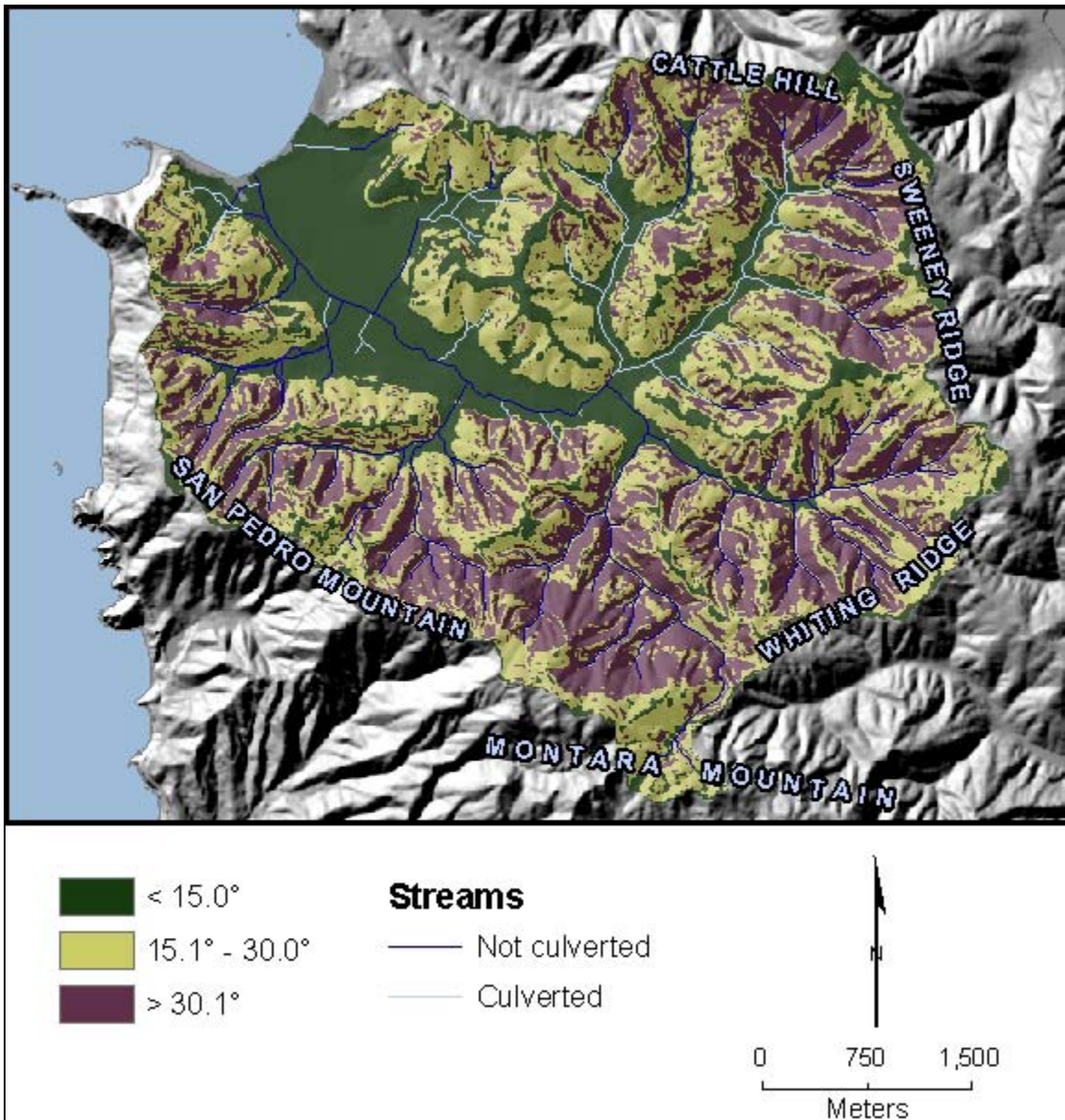


Figure 4: Slope of SPCW in degrees with labeled prominent range and mountain features (USGS 2003).



Figure 5: Pacifica State Beach looking northwest from Montara Mountain Trail. The beach forms the northwestern extent of SPCW and is the outlet of San Pedro Creek.



Figure 6: Terraced hillslopes altering the geomorphology of natural slopes.

2.2 Geology

The underlying geology of SPCW is relatively complex due to the abundance of faults (Figure 7). Unless otherwise noted all of the geology information in this section is based on Pampeyan (1994). The Pilarcitos fault, a strike-slip fault, is the largest and most structurally influential fault within the study area running along the center of SPCW. It demarcates the boundary between the Franciscan complex of the Pilarcitos block to the north and the granitic rocks of the La Honda block to the south. Running parallel to and south of the Pilarcitos fault lays the San Pedro Mountain fault (Figure 8) spanning through large portions of the Sanchez and South Forks. This fault further distinguishes the geology of the La Honda Block from sandstone shale and conglomerate to the north and granitics to the south. Many smaller inconspicuous faults predominately lay parallel to these larger faults but are not as influential in controlling geologic structure. One of these faults that has been significant in controlling the underlying sandstone and greenstone runs perpendicular to the others within the North fork subwatershed.

The geology of SPCW is composed mainly of older sedimentary rocks typical of those found in the western U.S. coastal ranges. The Franciscan complex in the Pilarcitos block contains some of the oldest sedimentary and igneous rocks in the San Francisco Bay area dating back to the Jurassic and Cretaceous periods. This complex is also the most diverse and fractured as a result of structural control from faults. Greenstone and sandstone, also known as graywacke, comprise the largest area of the complex including lesser amounts of conglomerate, limestone, chert, serpentinite, and sheared rock or *mélange*, which contains sheared shale, siltstone, and graywacke. The La Honda complex north of the San Pedro Mountain fault contains rocks from both the Tertiary-- sandstone shale and conglomerate-- and Quaternary periods, a geologic unit composed of slope wash, ravine fill and colluvium that is locally known to be up to 6 m deep with maximum accumulations near the bases of slopes. The bedrock within the same complex but south of the San Pedro Mountain fault is from the Cretaceous period predominately consisting of Montara Mountain granite interspersed with Quaternary slope wash, ravine fill and colluvium.

Many bedrock types within these two complexes are highly susceptible to surface erosion and slope failure based on intrinsic physical properties, proximity to other geologic units, or under certain geomorphic or climatic conditions. *Mélange*, slope wash, ravine fill, and colluvium, and weathered granitic rock comprise the underlying bedrock of roughly 80% of the study area and are all highly susceptible to slope failure. Highly weathered *mélange* erodes to badlands topography as is displayed in gullies intermingled with slope wash, ravine fill, and colluvium along the northern hillslopes of the Middle subwatershed. The upper part of the sandstone, shale, and conglomerate unit is prone to failure where oversteepened by faulting. This bedrock type demarcates much of the northern border of the San Pedro Mountain Fault opposing weathered granite creating a very landslide-prone area on the northern slope of Montara Mountain. The sandstone, sandstone, shale and conglomerate, and *mélange* units are all interbedded with shale, which increases the susceptibility to failure (Rib and Liang 1978). This partially accounts for instability of the limestone bands surrounded by either *mélange* or slope wash, ravine fill, and colluvium as landslides are more common in limestone where interbedded with soft rocks (Rib and Liang 1978). Known landslides indicated as active younger deposits and older deposits showing no movement in the past few decades often correspond to these failure-prone areas (Pampeyan 1994). Landslides, gullies, and areas of significant surface erosion in SPCW are expected to correspond with many of these areas.

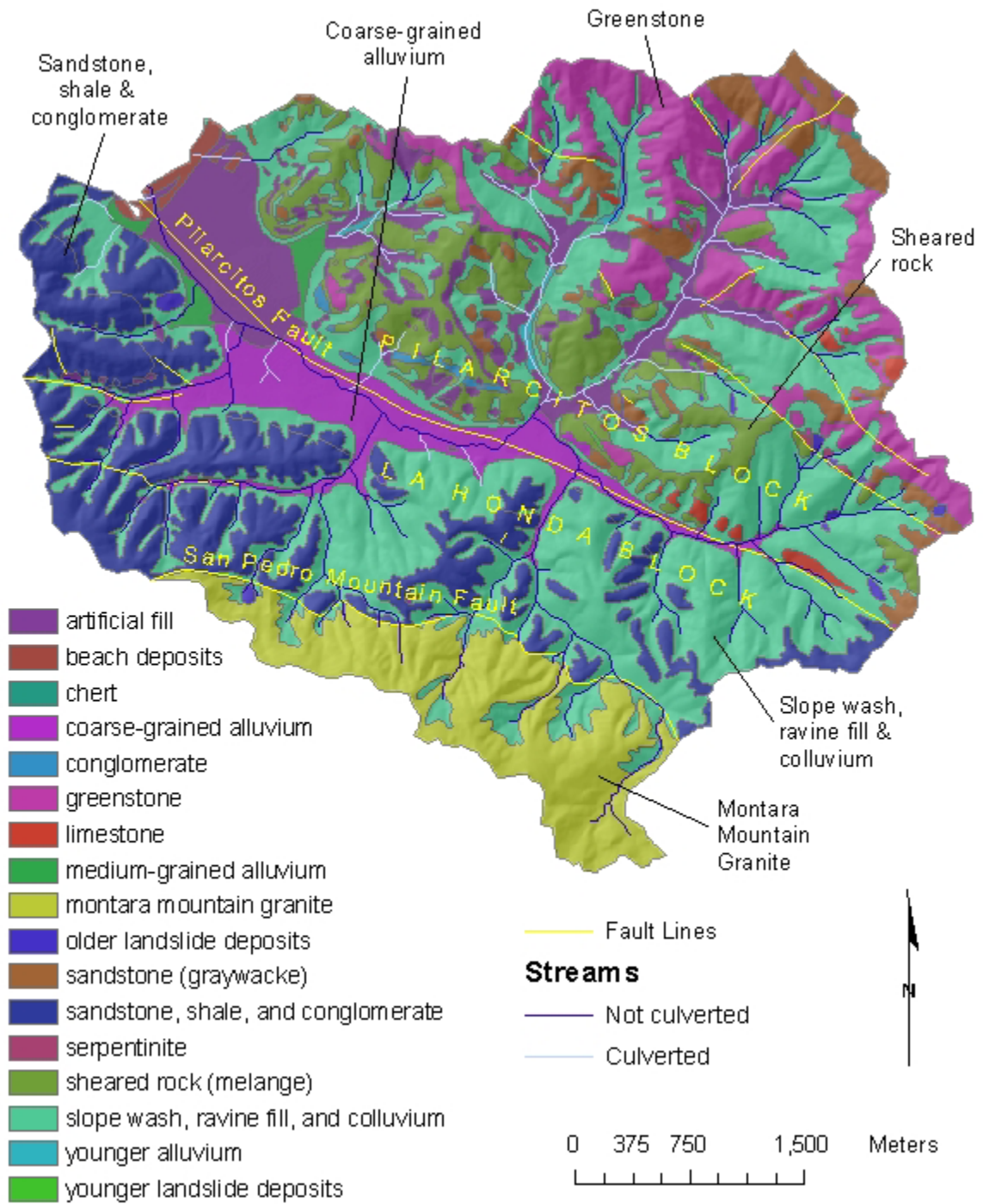


Figure 7: Geology and fault lines of SPCW (Pampeyan 1994).

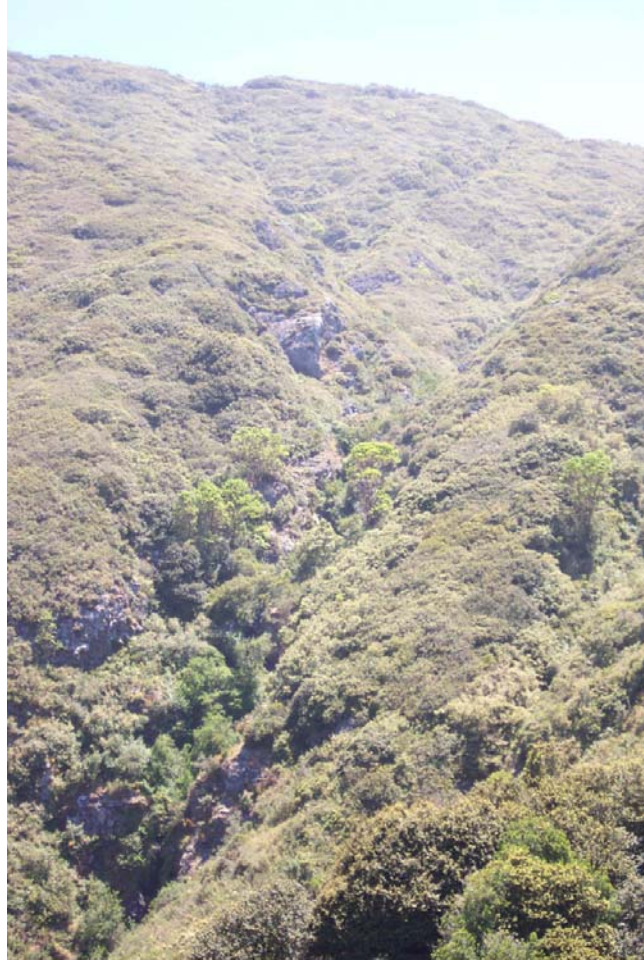


Figure 8: Brooks Creek, a tributary of the South Fork, crossing the San Pedro Mountain Fault at a waterfall.

2.3 Soils

The USDA Soil Conservation Service (now the Natural Resources Conservation Service) has categorized, grouped, and mapped soil types into complexes throughout San Mateo County to facilitate land use planning efforts (Kashiwagi and Hokholt 1991). Four complexes named by the predominant soil types cover hillslopes of the majority of the study area: Barnabe-Candlestick, Candlestick-Barnabe, Candlestick-Kron-Buriburi, and Scarper-Miramar (Figure 9). The most prevalent, the Barnabe-Candlestick complex, is highly susceptible to surface erosion and is composed of 35% Candlestick soil which is very prone to slippage when wet. Candlestick soils generally tend to be deep, possibly from the accumulation of landslide material delivered by unstable hillslopes. These same characteristics apply to the Candlestick-Barnabe and Candlestick-Kron-Buriburi complexes, which are not as widespread throughout the study area, but are composed of higher percentages of the deeper, landslide-prone Candlestick soil. The Scarper-Miramar complex is confined only to the southern extent of the study area overlying granitic bedrock and is highly susceptible to surface erosion.

The soil types of each complex vary by parent material and the extent of weathering. Hard, fractured sandstone, which is abundant throughout SPCW is the parent material for Barnabe, Candlestick, Kron, and Buriburi. Scarper and Miramar are derived from Montara Mountain Quartz. The composition of soils varies from the fine sandy loam of Candlestick to the gravelly coarse sandy loam of Scarper. Candlestick is the most relevant in potential sediment production because of its diffuse abundance, fine material composition, and relatively high susceptibility to surface erosion. Miramar, found in the upper headwaters of the South fork is also susceptible to surface erosion.

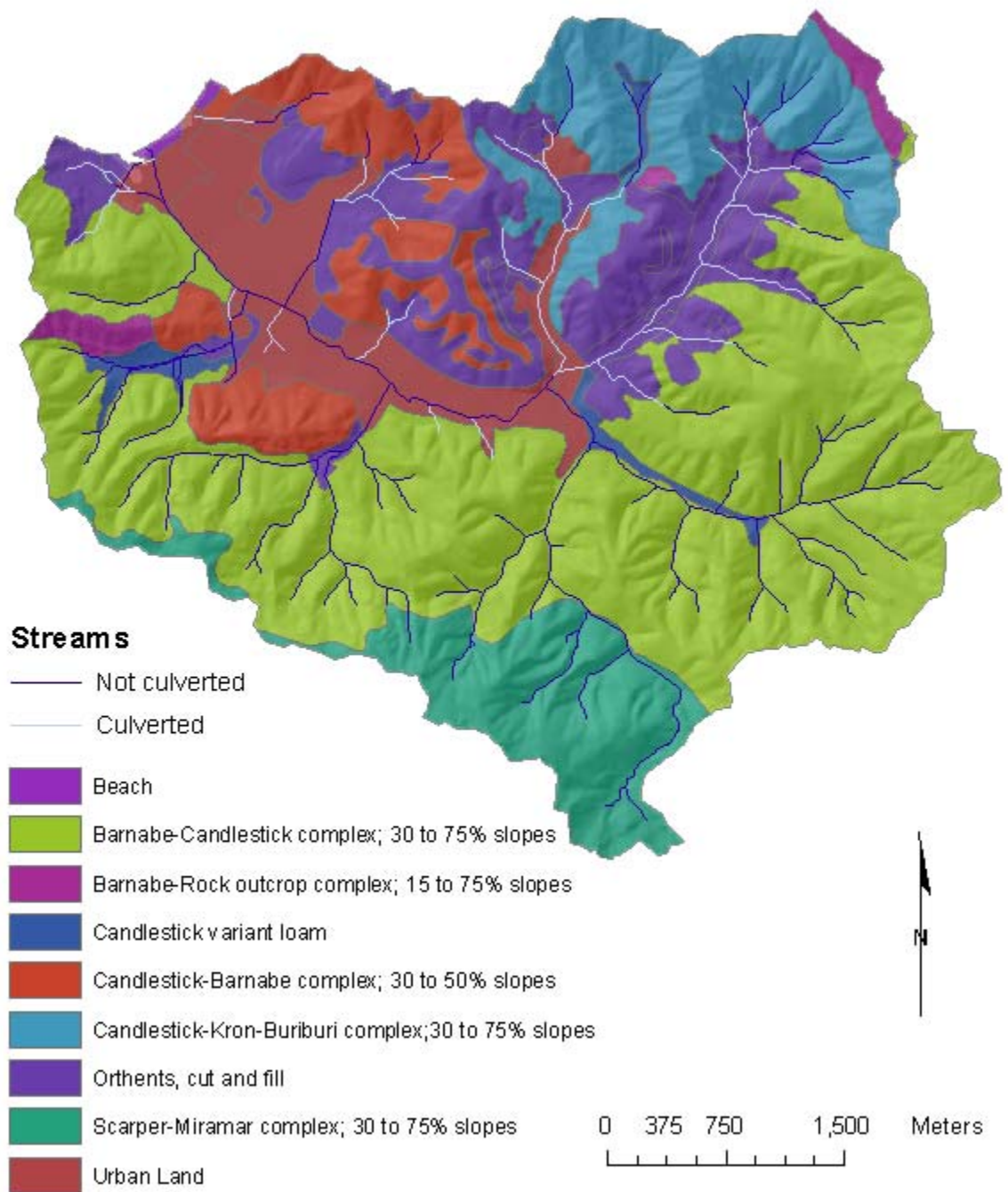


Figure 9: Soil complexes of SPCW (Kashiwagi and Hokholt 1991).

2.4 Land Use

San Pedro Valley has historically been influenced by several distinct cultures and practices. Beginning roughly 5,000 years ago with occupation by the native Ohlone tribes SPCW was subjected to a frequent fire regimen enhancing hunting and foraging (Collins *et al.* 2001). When Spanish settlers arrived the practice completely faded away along with the Ohlone population by the end of the 1800s (Collins *et al.* 2001). With the initial Spanish settlement in the late 1700s came agriculture, grazing animals, exotic plant species introduction, and increased population and development. Occupation by current U.S. citizens began in the mid 1800s as westward settlement intensified and expanded agriculture and urban development including structures, roads, and railroad lines (Figure 10).

Currently, most of the lower watershed of San Pedro Creek is urbanized with residential and commercial uses (Figure 11) while most of the upper watershed is designated as open space recreational use (Figure 12). The majority of the study area in the Middle, South, and Sanchez Forks is public land containing numerous maintained trails under the jurisdiction of San Mateo County as San Pedro Valley Park and McNee Ranch State Park. The Golden Gate National Recreation Area under the National Park Service controls a large portion of the North subwatershed and the North Coast County Water District manages significant portions of the Middle and South subwatersheds (SPCWC 2000). The Pacifica Land Trust recently acquired land on Pedro Point II that was previously utilized by off road motorcycle enthusiasts (Figure 13) causing severe alteration of vegetative cover and soil characteristics (Davis 2002). Current access to this restoration site is available on a number of trails. In addition to the public open space land, there are private facilities operating on sizeable amounts of land in SPCW: the Shamrock (Figure 14), Picardo, and Hinton Ranches and the Park Pacifica Stables. Nearby trails on both surrounding public and private lands are regularly accessed on horseback from some of these facilities.

Land use impacts of the upper watershed are predominately from current recreational access. These trails and surrounding roads are displayed in Figure 12 with public land ownership designations. Included in the trails designation are any roads that are not readily accessible to cars as a result of land ownership or decommissioning. Trails are categorized as “maintained” if undertaken by the land manager or otherwise indicated as “not maintained”. Detailed information on specific trails is covered in the Results section under individual subwatershed assessments.

While lower portions of the Middle, South, Sanchez, and Shamrock Forks remain relatively undeveloped, residential development has encroached up the valley along the North, Hinton, and Pedro Point I forks culverting most of the flow. Urbanization has overtaken several hillsides primarily in the North fork and has extended as far up the valleys as possible. This development has pressured toe slopes of adjacent hillsides and increased the potential hazard for landslides (Figure 15).

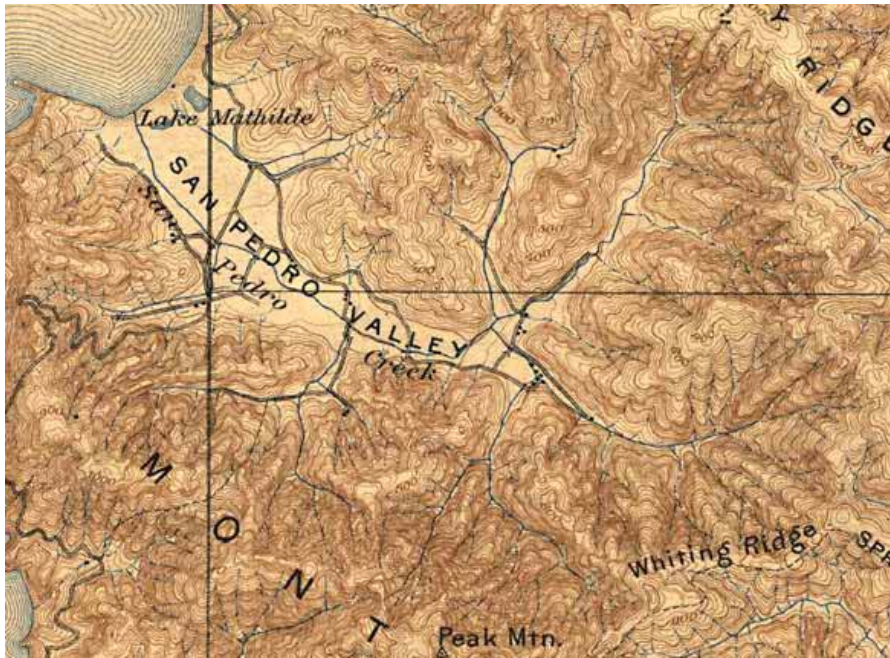


Figure 10: USGS topography map of SPCW in 1896 with little urban development and few roads (OMC 2003).



Figure 11: USGS topography map of SPCW in 1997 showing extensive development throughout most of the valley floor as indicated by the gray fill and the broad road system (USGS 1997).

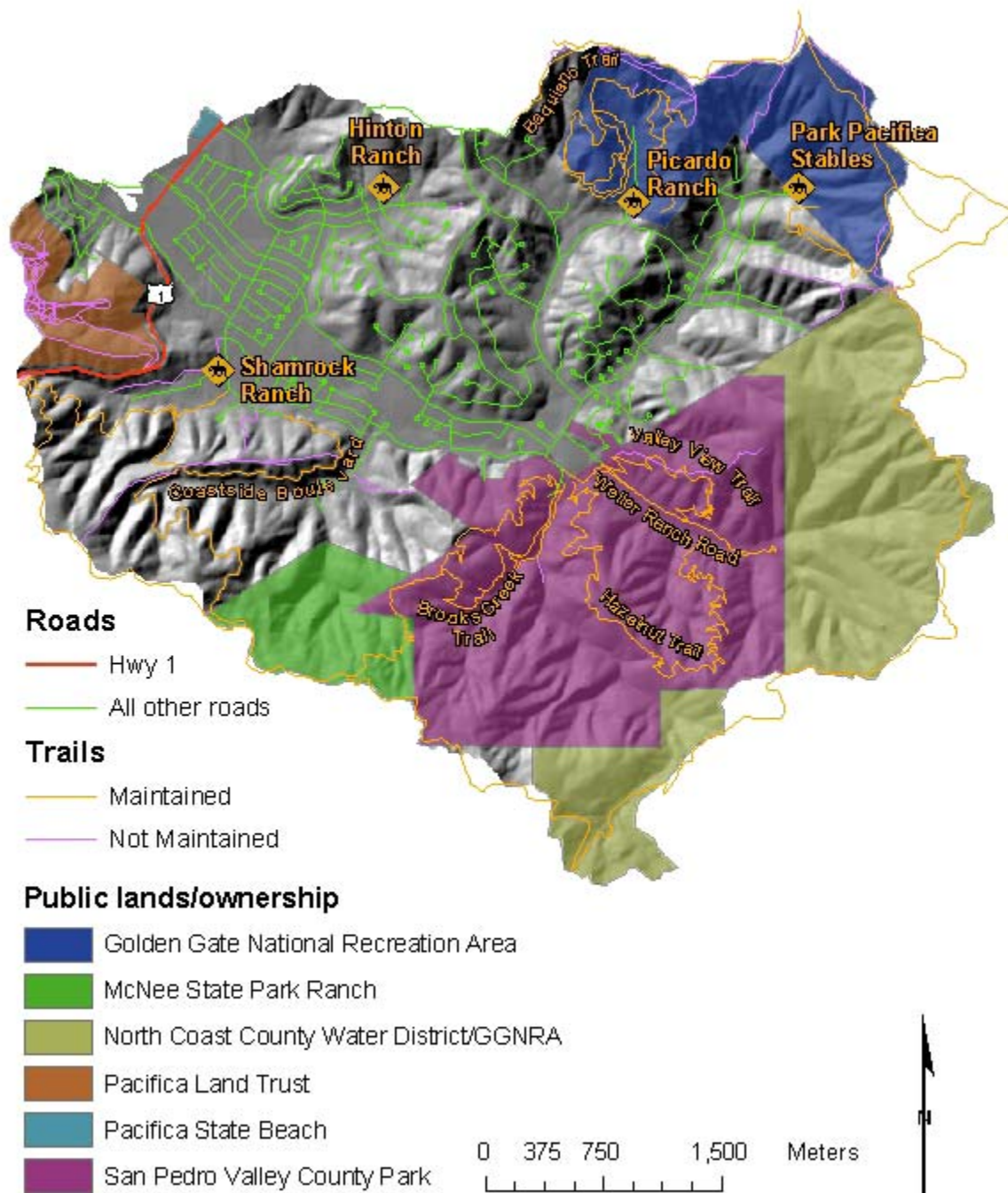


Figure 12: Roads, trails, and public lands of SPCW. Some of the more prominent trails that were surveyed are labeled. Ranches are labeled and the remainder of the gray areas is under private landownership (SPCWC 2000).



Figure 13: Remnant bare soil and erosion from previous off-road use in Pedro Point II subwatershed.



Figure 14: Shamrock Ranch with nearby open space and residential development.



Figure 15: Urbanization in the North subwatershed from the valley floor encroaching on the toe slopes of hillsides. The northern profile of the Oddstead landslide is shown covered in trees to stabilize the hillside.

2.5 Land Cover

The valley floor of SPCW is dominated by commercial and urban development while the upper hillslopes are blanketed with a combination of native, exotic, and mixed vegetation (Figure 16). This hillslope vegetation is composed of a combination of native and exotic grasses, forests, scrubs, and riparian areas. Vegetation types dominated by exotic and mixed species cover roughly 33% of the total study area while native vegetation comprises the remainder.

Only a few vegetation types dominate the non-urbanized land cover of SPCW. Coastal scrub and chaparral encompass roughly 90% of the total study area (SPCWC 2000). Both plant communities are densely distributed throughout hillslopes of the watershed (Figure 17). There are several coastal scrub assemblages in SPCW that differ by predominant species as a factor of underlying bedrock type, soil depth, slope, and aspect (Vasey 2001). These assemblages include gray-green, dominated by California sagebrush (*Artemisia californica*); semi-moist with toyon (*Heteromeles arbutifolia*), blue blossom (*Ceanothus thyrsiflorus*), coffee berry (*Rhamnus californica*), and silk tassel (*Garrya elliptica*); and fully-moist containing California hazelnut (*Corylus cornuta*) and cream bush (*Holodiscus discolor*). Although species variations among the local coastal scrub communities exist, all assemblages are dominated by Coyote brush (*Baccharis pilularis*). While the coastal, or deciduous, scrub assemblages thrive in areas with deep soil, the chaparral, or evergreen scrub, flourishes in rocky, shallow soils. The prevalent chaparral species include brittle-leaf manzanita (*Arctostaphylos tomentosa crinita*) and Montara manzanita (*Arctostaphylos montaraensis*), golden chinquapin (*Chrysolepis chrysophylla*), and California huckleberry (*Vaccinium ovatum*). Exotic forests also cover a large portion of SPCW and consist mainly of blue gum eucalyptus (*Eucalyptus globulus*) and Monterey pine (*Pinus radiata*) (Figure 18). The remaining area consists of grasslands that follow the ridgeline of the North fork (Figure 19) and riparian forests that follow the tributaries.

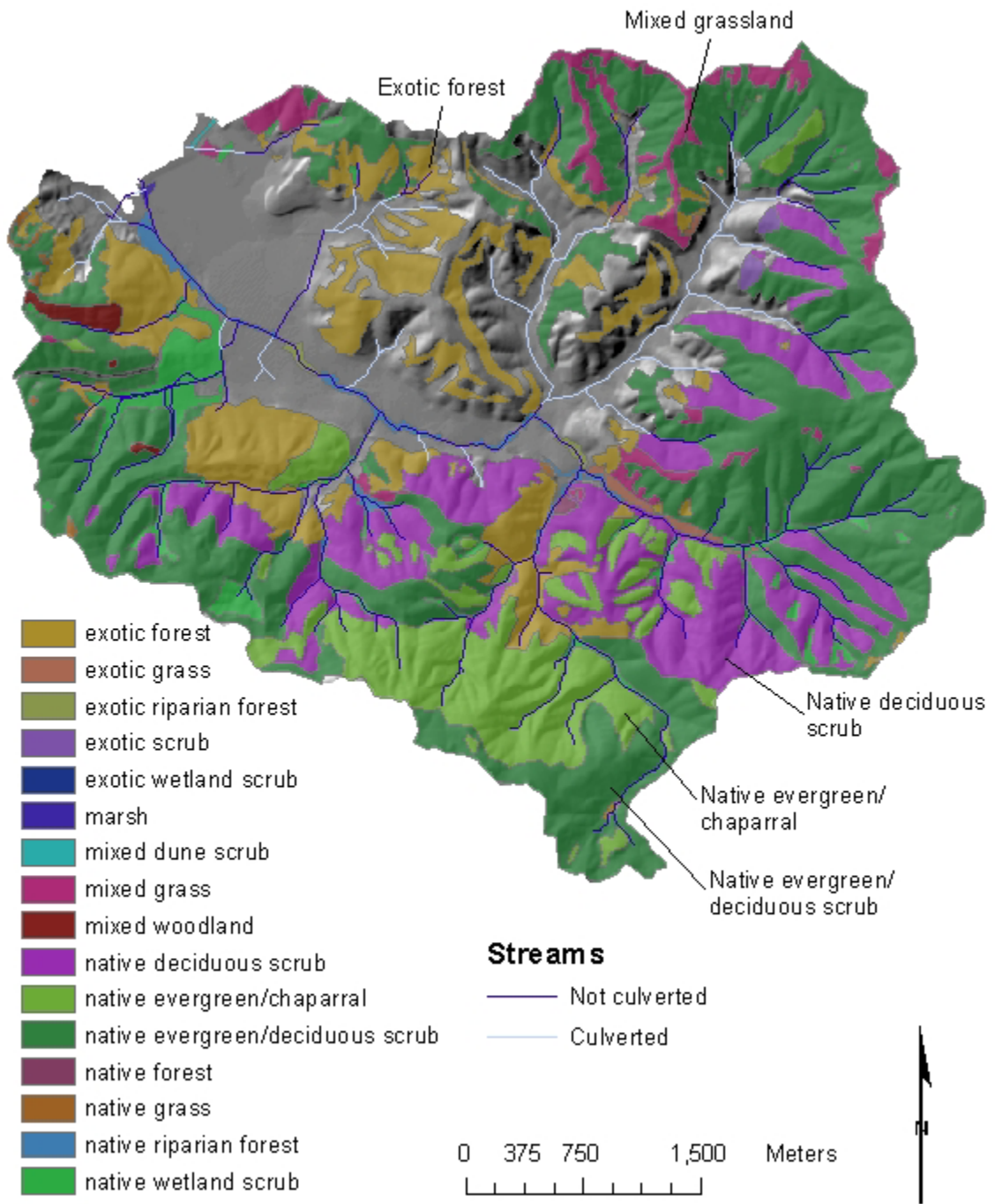


Figure 16: Land cover of SPCW. Vegetation data for the gray areas either was not collected or is urban land cover (SPCWC 2002)

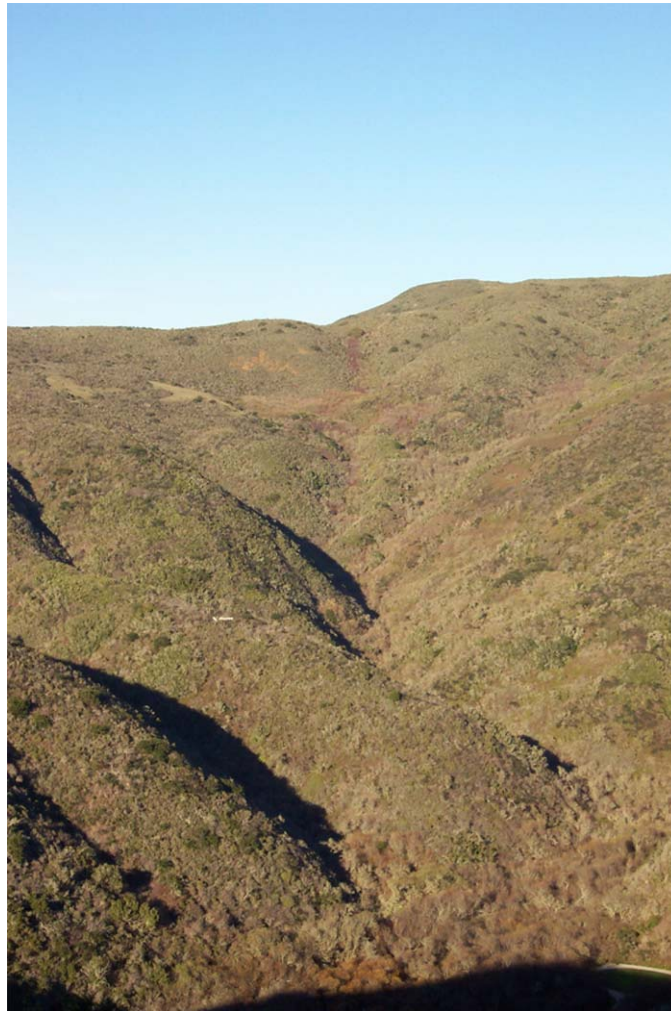


Figure 17: Native evergreen and deciduous scrub assemblages of south-facing hillslopes of the Middle subwatershed from Hazelnut trail.



Figure 18: Non-maintained trail in the exotic blue gum eucalyptus and Monterey pine forest in Shamrock subwatershed.



Figure 19: Mixed grassland and native deciduous scrub of the upper North subwatershed.

2.6 Climate

The Mediterranean climate of SPCW consists of cool, dry summers with regular fog and wet, mild winters with 90% of the rainfall occurring between the months of November and April (USACE 1998). Figure 20 displays precipitation and temperature from data collected in San Francisco between 1948-1988. Data suggests that SPCW has a higher annual precipitation than these values (Collins *et al.* 2001, Amato 2003, Howard *et al.* 1988) but the yearly patterns of the wet and dry season are effectively displayed with an annual variation in temperatures of only 6°C.

The most current precipitation data in SPCW has been collected from 13 rainfall gauges dispersed throughout the Pacifica area (Collins *et al.* 2001). Based on these data, the U.S. Army Corps of Engineers (USACE) have determined the annual precipitation to average 838 mm (33 inches) within SPCW. This value is significantly higher than that of San Francisco's annual precipitation of 517 mm (Kashiwagi and Hokholt 1991). SPCW borders the western side of this range collecting the majority of the precipitation. The mean annual precipitation of Pacifica has also been totaled at 635 mm/year (Monteverdi in Howard *et al.* 1988), data collected in February 2000 suggests a mean annual precipitation of 1000 mm/year (Amato 2003), and extensive records from a rainfall gage in San Pedro Valley Park collected since 1978 show an average 970 mm (38.2 inches). Based on data collected from the USACE rain gauges rainfall averages 584 mm (23 inches) west at the Pacific Ocean and 965 mm (38 inches) east along the higher elevations (Collins *et al.* 2001).

Most debris flow events in SPCW are triggered during the wet season generally ranging between November and April (Figure 20). Between October 1981 and April 1982 1,221 mm

of precipitation was recorded at Half Moon Bay Weather Station (Monteverdi in Howard *et al.* 1988). Rainfall data collected during a 27-hour storm period between January 3-5, 1982 indicates that with antecedent moisture of 500 to 760 mm, 8 hours of intense rainfall at 10 to 20 mm/hour is sufficient to initiate abundant debris flows (Cannon and Ellen 1988). With rainfall intensity between 5.0 and 6.6 mm/hr, 150 – 200 mm fell on January 4th, 1982 in less than 30 hours (Monteverdi in Howard *et al.* 1988) triggering 475 landslides throughout the greater Pacifica area (Howard *et al.* 1988).

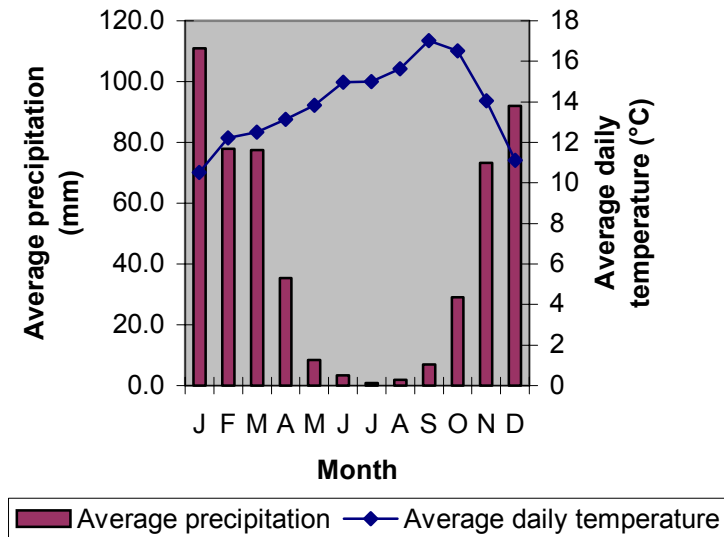


Figure 20: Monthly average temperature and precipitation for San Francisco between 1948-1988. The precipitation data is lower than that collected in SPCW but effectively displays the general yearly pattern of rainfall (Kashiwagi and Hokholt 1991).

3. Sediment Production

Excess sedimentation of waterbodies is a significant problem worldwide. Within California, sediment is considered the principal cause of water quality impairment along the northern coastal drainages (KRIS 2002). While sediment develops and occurs naturally, excess levels generally stem from the modification and intensification of land use practices and can create a multitude of associated problems. Intensified land use activities including silviculture, mining, and urban development significantly enhance sediment production elevating levels in drainages. The increased levels of sediment degrade the ecosystem by deteriorating water quality, changing a stream or river channel's morphology, and decreasing propagation rates of anadromous fish species including the threatened resident steelhead trout (*Oncorhynchus mykiss*) population in SPCW.

Multiple geomorphic processes generate sediment, with water acting as the primary erosion, transport, and deposition agent. Mass wasting and surface erosion were found to be the predominant sediment-generation processes occurring in SPCW, primarily from hillslopes and tributaries. Mass wasting includes rapid shallow and slow deep-seated landslide events. San Mateo County is highly prone to landslide activity, which is enhanced by land use practices (Brabb and Pampeyan 1972). Surface erosion, the detachment of soil by processes associated with fluvial transport, is most effective on bare soil making it an important factor on dirt roads and adjoining drainages, gullies, and in areas with disturbed vegetation including new development and off-road recreational use.

Sediment generation in a landscape is a factor of multiple natural and anthropogenic influences. Selby (1993) identifies climate and geology as the predominant factors of erosion with a close interdependency of soil type and vegetation. In SPCW however, the relief is steep and urbanization is encroaching on toe slopes increasing the potential for landslide failures. This is just one example underscoring the significance of anthropogenic influences on levels of local sediment production.

3.1 Geomorphic and Fluvial Processes

Finco and Hepner (1998) identify the first step in sediment mitigation as the assessment of a study area as a collection of small, contiguous sources of nonpoint pollution. Understanding how these localized processes function and relate to contribute to the overall sediment generation in SPCW is fundamental to accurate source identification. The total erosion within a watershed is widely variable as it is assessed as sediment generated from surface erosion (Walling 1983) and mass wasting processes. These occurrences constitute the dominant hillslope and tributary mechanisms supplying sediment to San Pedro Creek and are significantly enhanced by land uses.

3.1.1 Mass Wasting

Mass wasting in SPCW occurs in the form of landslides, slumps, and soil creep. Landslides occur along a shear plane of bedrock (Ahnert 1996) and represent

the predominant form of mass wasting occurring within SPCW. Soil creep is also a factor but due to the high levels of rainfall, not as effective as landslides and fluvial erosion. For this paper, landslides include numerous mass movements including shallow debris flows and slumps, which are explained in more detail below.

Sediment production within steep-sloped watersheds is often dominated by episodic mass wasting events (Kasai *et al.* 2001). Shallow rapid landslides, or debris flows, are the dominant geomorphic process delivering sediment to SPCW. With connectivity to the drainage network, significant amounts of sediment can be entrained.

Most landslide activity seems to take place within or adjacent to areas that have a history of landsliding (Brabb and Pampeyan 1972). Debris flows generally originate in zero order basins that maintain a recurring pattern of filling and sliding (Montgomery and Dietrich 1989).

Urban development in SPCW is encroaching on the fringe of hillslopes increasing landslide hazard potential. Partially as a result of this growth, various aspects of geomorphic features related to slope instability have been mapped (Nilsen 1986). Few counties have as thorough a slope stability mapping history as San Mateo. However, only the slow deep-seated flows, or earthflows, which are not the most significant sources of sediment, had previously been examined in detail (Ellen *et al.* 1988).

A severe storm event delivering intense rainfall occurred from January 3-5, 1982 triggering 475 landslides in the town of Pacifica, California alone. The storm initiated predominantly shallow debris flows with a high concentration in SPCW (Howard *et al.* 1988). As a result, the relevance of shallow landslides was revealed and landslides were subsequently mapped throughout the Bay area. Nine slides in Pacifica, five that occurred in the North subwatershed of SPCW (Figure 21), were studied in extensive detail. The Oddstad slide dislodged 2,290 m³ of material demolishing two homes and killing three children (Figure 22) (Howard *et al.* 1988).

Debris Flows

Debris flows occur from slope instability (Davis 2002) and are common in SPCW due to the steep terrain, poorly consolidated bedrock, and heavy rainfalls associated with Mediterranean climates (Brabb and Pampeyan 1972). Ellen *et al.* (1988) define debris flows as shallow, rapid, and complex events generating internal turbulence and moving downslope a significant distance often delivering a substantial amount of sediment to streams. Subsurface water flow is the predominant cause of slope failure (Collins *et al.* 2001) while geology and topography are also significant controls (WFPB 1997a). In San Mateo County, the distribution of debris flows is directly correlated to the underlying geology (Figure 22) (Wieczorek *et al.* 1988) and slides in Pacifica originate on slopes between 26-45° near the heads of first order drainages

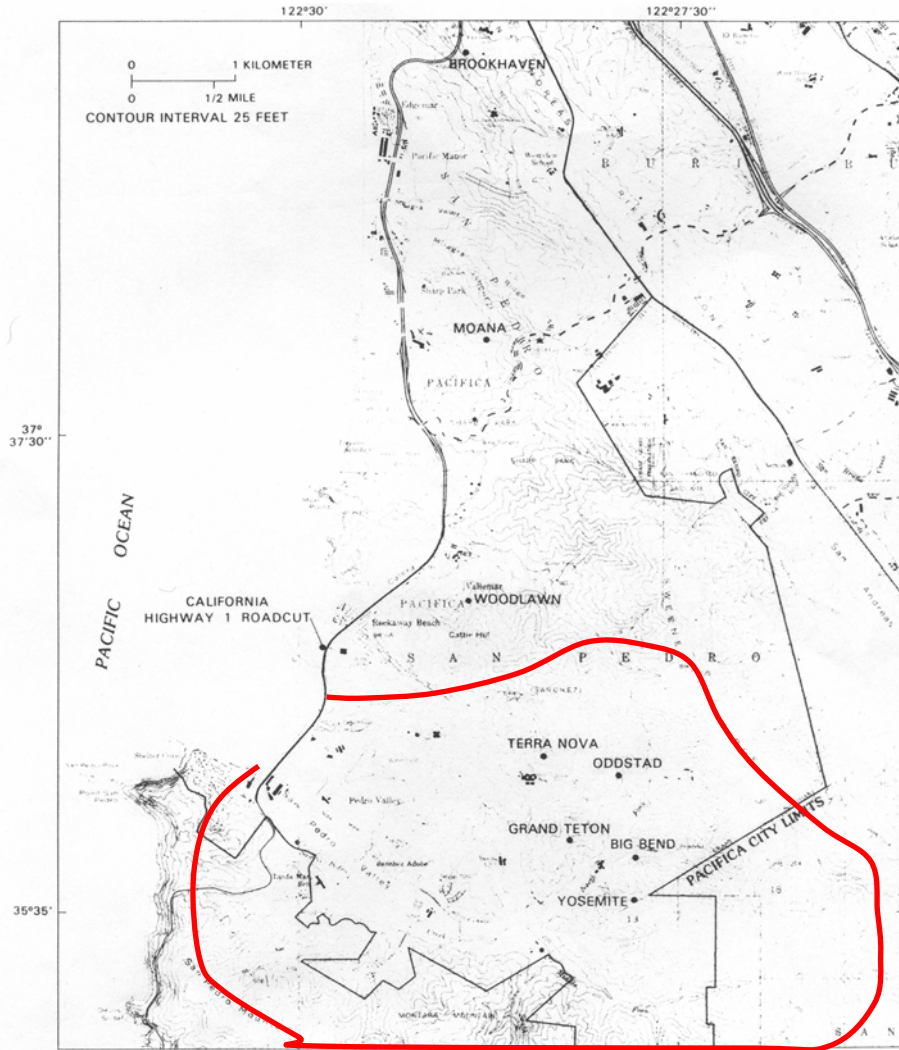


Figure 21: Select landslides triggered from January 1982 storm event that were studied in detail. Five of the nine occurred within the North subwatershed and fall within the generalized extents of SPCW outlined in red (modified from Howard *et al.* 1988).



Figure 22: Oddstad slide in the North subwatershed (USGS 1998).

(Figure 24). Within SPCW, the five landslides that received the greatest attention occurred between a narrow range of 26-308 (Howard *et al.* 1988). The ten subwatersheds are the focal zones of the study area. Hillslopes and tributaries are the predominant contributors of sediment to the main channel; however, the localized erosional processes occurring within each subwatershed vary significantly.

The amount of sediment generated is mainly controlled by precipitation but also by geomorphology, geology, soils, land use, and land cover. These factors vary significantly within and between the many subwatersheds. The North fork, which is the largest, is also the most heavily influenced by urbanization and most of the drainage is channeled underground. Conversely, the Middle and South forks are radically different, heavily vegetated open space with minimal current land use impacts. The remainder of the subwatersheds comprising the study area consists of a variety of different land uses and land cover ranging between minimal to high levels of use.

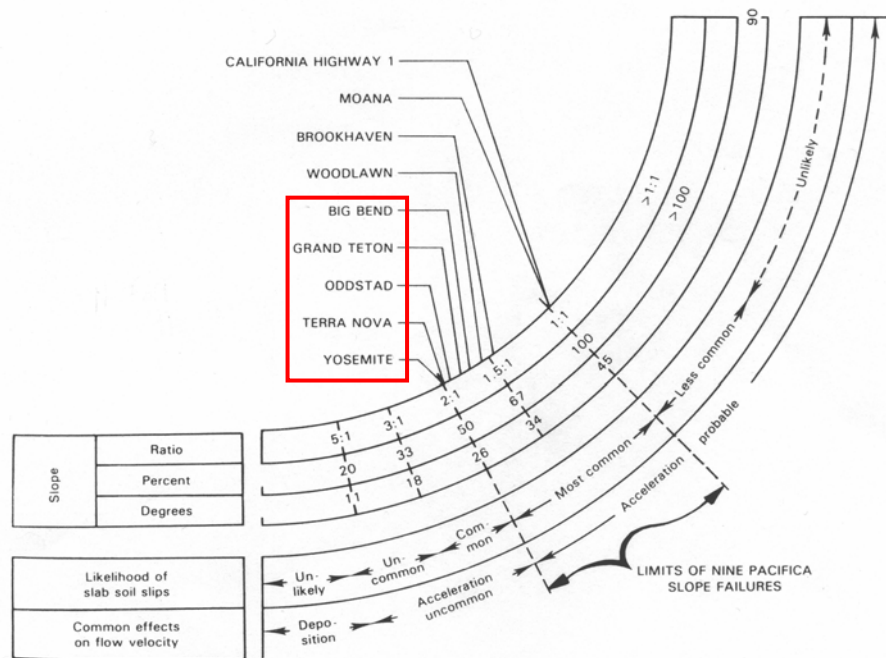


Figure 23: Slope angle and properties for nine landslides within Pacifica triggered by the January 1982 storm event. Landslides within red border occurred in the North subwatershed of SPCW and are located in Figure 3 (Howard *et al.* 1988).

Slumps

Slumps are failures along a shear failure plane in which the upper portion of material retains its original structure (Ahnert 1996). Commonly occurring downslope of trails and channel terraces near the creek, evidence of slumps was found throughout SPCW. Slumps are also episodic in nature but generally don't deliver as much initial sediment to the stream network as debris flows. Instead soils displaced from slump events are exposed to soil creep and surface erosion acting as long-term sediment sources. Areas prone to slumping are commonly recurring, ensuring future sediment supply.

Soil Creep

Creep is the process of unconsolidated material "creeping" downslope, either from continuous movement or expansion and contraction, up to a maximum rate of 1-2 cm per year (Ahnert 1996). Due to the mild climate, SPCW is not influenced by contraction and expansion generally associated with the freeze/thaw cycle reducing the rate of movement significantly. Other agents of creep include gravity and biogenic activity (Stillwater Sciences 1999).

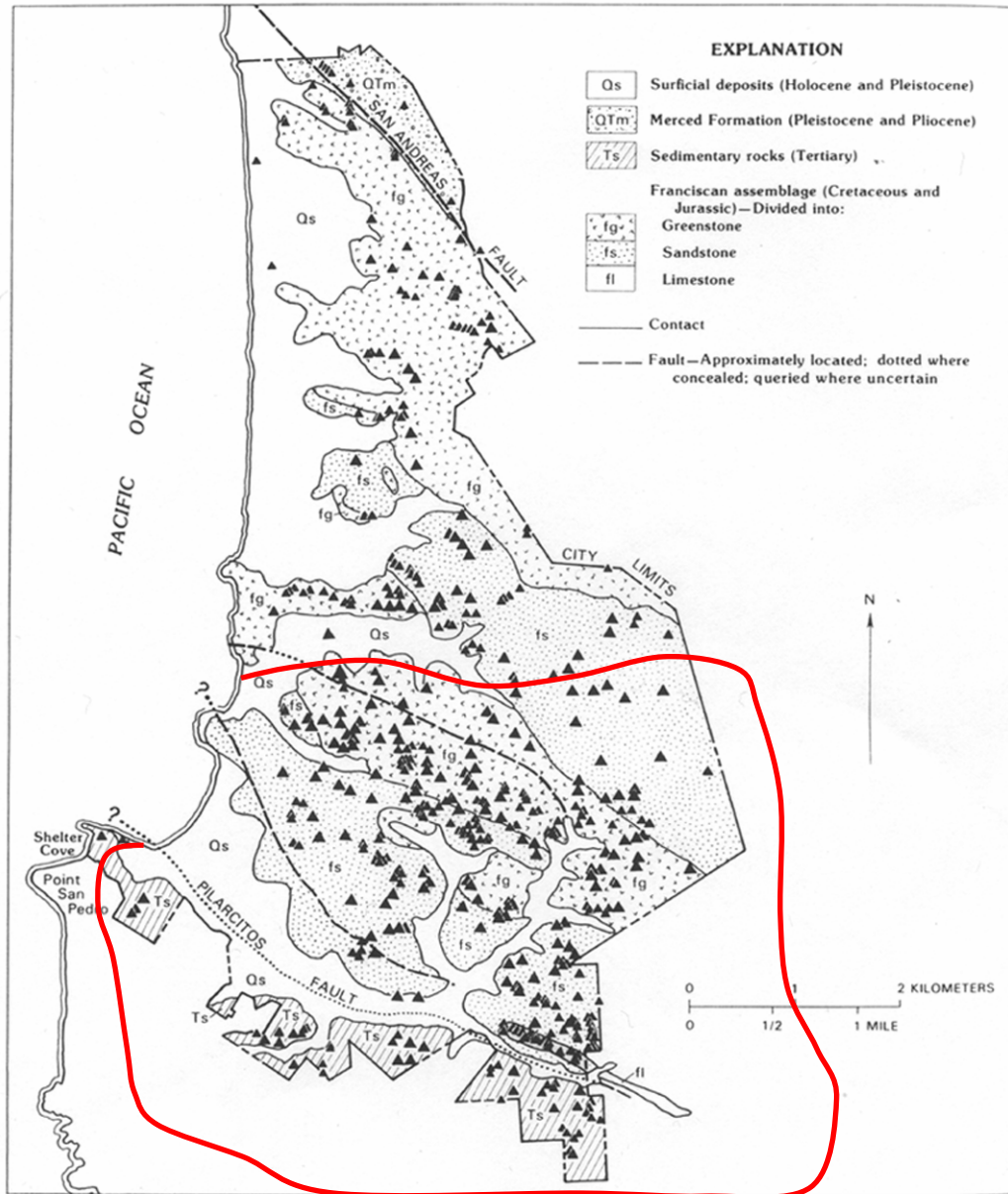


Figure 24: Landslides triggered from January 1982 storm event with corresponding geological units, Pacifica, CA. Generalized extents of SPCW outlined in red. (modified from Howard *et al.* 1988).

3.1.2 Surface Erosion

Displaced soils from surface erosion acting on bare slopes has been calculated up to several tonnes per hectare per year (Ahnert 1996). Surface erosion occurs from fluvial processes acting on the landscape to detach and entrain sediments and its effectiveness is highly dependant upon the level of soil compaction and exposure (WFPB 1997b). It is therefore most effective on areas with bare and compacted soil or sparsely vegetated cover, which is limited mainly to trails and roads throughout SPCW. In headwater catchments channel degradation and gully erosion, both forms of surface erosion, are known to be significant sources of sediment (Kasai *et al.* 2001). Mass wasting events enhance surface erosion processes by disturbing or removing vegetative cover exposing bare soil. Recent landslide scars provide bare soil, which are then subjected to surface erosion (WFPB 1997a).

Sheetwash and Overland Flow

Sheetwash is the process of water flowing over the landscape surface in a “sheet” during a rainfall event and is known as the most common process of soil erosion (Ahnert 1996). Sheetwash moves through two types of overland flows: Hortonian, which is initiated when the soil infiltration rate is exceeded by rainfall intensity triggering surface runoff, and saturation, when the underlying soil is already inundated from throughflow and interflow sources of antecedent moisture. Hortonian overland flow is intensified in areas surrounding impermeable surfaces such as urbanization or bedrock whereas saturation overland flow most commonly occurs on lower gradient slopes near channel margins (Parsons and Abrahams 1993).

Rainsplash Erosion

Rainsplash, the process of soil displacement from raindrops, acts differently from sheetwash, but its denudational effects can be significant in rills and gullies. Rainsplash erosion is most effective in dislodging sediments on bare soils. The full impact of a raindrop in producing this erosion is minimized by the presence of vegetation, low gradient slopes, the inherent resistance of soil to displacement, and the intensity of the raindrop (Mount 1995).

Rills and Gullies

Rills and gullies are physical features formed in areas with sparse or no vegetative cover or with heavily compacted soil. Rills are shallower and occur when saturation overland flow becomes concentrated from an increased slope gradient or where the surface roughness increases, both creating more turbulent flow (Figure 25) (Ahnert 1996). Gullies, which are formed from the same initial processes, are much deeper than rills and have incised into deep channels (Figures 26 and 27) (Collins *et al.* 2001).

Rilled and gullied slopes are potentially major sources of sediment, although the contribution from each varies greatly (Meyer 1986). Areas with bare soil cover occur in SPCW only where land uses have significantly altered vegetative cover and revegetation has not yet occurred. Sediment generated from surface erosion of gullies and rills are currently effective sources of sediment where connectivity to the drainage has been established.



Figure 25: Rills on the nearly vertical face of an uphill trail cut in the South subwatershed.



Figure 26: Gullies along a trail on Cattle Hill in the upper North subwatershed.

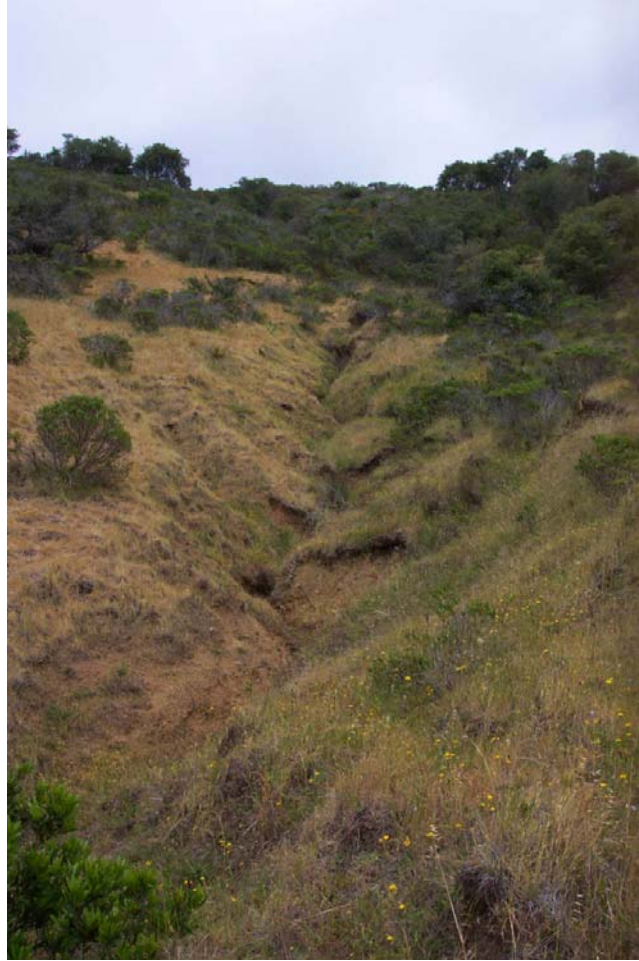


Figure 27: Gullies upslope from a trail in the Middle subwatershed.

Fluvial Erosion

Water flowing through a stream channel acts as the agent of fluvial erosion (Collins *et al.* 2001). Fluvial erosion, other surface erosion processes, and mass failure occur in conjunction to entrain sediment from channel banks (Prosser *et al.* 2000; Couper and Maddock 2001). These processes work together to cause weakening of the stream bank and are the dominant sediment-contributing processes in upper watersheds (Figure 28) (Couper and Maddock 2001). On the other hand, massive failures occurring along tributaries can stabilize the channel by reducing the bank gradient. Unless the critical shear stress to remove the material is exceeded, the bank will be reinforced (Thorne 1982). Erosion of channel banks is also influenced by water flow properties, bank material composition, climate, subsurface conditions, channel geometry, man-induced factors, and biology, including animal burrows and root systems (Knighton 1984).

Numerous researchers have determined that where fluvial erosion along channels, including adjacent valley sides, is the predominant source of sediment, the relationship between sediment yield and catchment area is positive (Kasai *et al.* 2001). This is important to SPCW as a whole because much of the main channel is straightened, which lead to major bank incision and headward erosion possibly causing bank erosion to be a major source of sediment.

3.2 Anthropogenic Influence

Sediment generated from natural processes in SPCW is often enhanced by land use practices (Figures 29 & 30). Agriculture, grazing, and a regular fire regime have historically influenced SPCW hillslopes and tributaries. Significant gullies have developed along some of the coastal hillslopes as a result of agriculture and subsequent grazing (Davis 2002). While a large portion of SPCW is currently urbanized, the main sediment influenced by anthropogenic activities is derived from concentrated and diverted flows from trails and roads on hillslopes and along the tributary.



Figure 28: Fluvial erosion causing incision through a former landslide deposit in an intermittent tributary draining into Sanchez Fork (Davis 2003).



Figure 29: Severe surface erosion from concentrated Horton overland flow downslope of Coastside Boulevard, draining to a culvert draining to the storm drain network near Sanchez Fork.



Figure 30: Concentrated flow creating surface erosion and increasing the effective drainage density along the Hazelnut Trail draining to South Fork.

Recreational use in the open space areas of the upper watershed has resulted in the establishment of maintained and unmaintained trails. Multiple user groups frequent the trails in designated areas including pedestrians, mountain bikers, equestrians, and even off-road vehicles. These trails increase the effective drainage density of SPCW diverting and concentrating flow creating high erosion areas and compact soil creating nearly impervious surfaces similar to those of urbanized areas. Mountain bikers have constructed courses on trails that may not have been previously established (Figure 31). Several ranch and stable facilities in the area frequently use the surrounding trails for horse riding. In at least one situation at Park Pacifica Stables, this has resulted in off-road vehicle use for trail maintenance. Previous use by off-road motorcyclists created a network of trails throughout Pedro Point II heavily compacting soils and removing substantial amounts of vegetative cover.

Biogenic activity accelerates the downslope movement of soil known as creep. Animals, such as the local deer, mountain lion, and bobcat populations, also contribute to this process. Biogenic activity from small burrowing animals often results in piping, which is the funneling of water through these holes causing erosion at the outlet (Figure 32). Piping, found along trails throughout most landscapes in the watershed, can significantly contribute to gully formation and trail erosion. Human activity on trails also expedites this process increasing the potential amount of sediment delivered to the stream network.



Figure 31: Mountain bike trails and constructed features along an otherwise unmaintained trail draining to Shamrock Fork.



Figure 32: Burrow hole that may soon lead to piping along the upper edge of a gully complex in the Middle subwatershed.

Large construction projects within SPCW have significantly impacted the creek and modified the sediment levels and delivery from upstream. One such project is the Devil's Slide Tunnel currently being constructed by Caltrans (Caltrans 2003). The tunnel is being bored within Shamrock subwatershed to divert Highway 1 from the current slide prone route along the coast. Rerouting of the highway will expose significant amounts of soil susceptible to erosion at least temporarily during construction. A long-term repercussion could include interbasin transfer or the routing of water from the natural drainage to another increasing the possibility for surface erosion where the diverted flow has been concentrated.

Many mitigation measures have been installed that reduce the sediment produced by some of the previously listed sources. Some of the trails frequented on horseback near the Park Pacifica stables were graded and regularly maintained to prevent soil compaction and channel formation. The restoration site at Pedro Point II formerly used by off-road motorcyclists has since been partially revegetated with netting and downed organic material promoting more growth on hillslopes prone to significant surface erosion. Water bars are commonly placed along trails diverting flow in efforts to reduce incision along the trail. Along Coastside Boulevard on which control measures such as tarps and sandbags have also been adopted, water bars were found to be ineffective or even significantly damaging areas downslope from the trails generating several landslides and gullies. Terraced hillslopes near residential areas stabilize hillslopes by diverting water and debris accumulation

preventing delivery of sediment from landslides. Sediment is instead delivered through the concrete channels and culverts routed directly to the storm drain system and ultimately to the stream network.

3.3 Influence of Vegetation

Vegetative buffers act as sinks preventing the delivery of most sediment transported by surface erosion and mass wasting processes to the channel (WFPB 1997b). While many studies have recognized the sediment filtering capabilities of riparian buffers (Budd *et al.* 1987; Lynch *et al.* 1985; Gilman and Skaggs 1988; Petersen *et al.* 1992), the minimum distance required to filter sediments from streams varies from 6.5 meters (Riley 1998) to 100 meters (Budd *et al.* 1987). This wide range of buffer distances is primarily a factor of variations in slope, land use, and vegetation cover. One study found the effectiveness of vegetation buffers in filtering sediment to be up to 90% (Gilliam and Skaggs 1988). On the other hand, channelized and culverted reaches facilitate delivery to a stream network by eliminating the riparian buffer and surface friction that might otherwise filter or reduce the amount of sediment delivered. The contributing variables work together in SPCW to produce a range of filtering capabilities. A section of one tributary with high sediment filtering capacity is shown in Figure 33.

In addition to acting as a sediment trap, root cohesion from vegetation stabilizes banks and hillslopes (Petersen *et al.* 1992). The overall benefits of vegetation in reducing sediment and stabilizing banks and hillslopes are significant. However, large trees can also expose soil to erosion when tree throw occurs (Figure 34). Tree throw is the upheaval of the root system that can be caused by bank incision from fluvial erosion undercutting the roots. When the underlying stability is removed, the roots cannot support the trunk causing it to fall also overturning and exposing the roots to sediment generating erosional processes. While tree throw increases short-term sediment supply it can mitigate long-term sediment supply by stabilizing hillslopes and providing barriers to sediments dislodged and transported by geomorphic processes (Budd *et al.* 1987).



Figure 33: Riparian corridor along Pedro Point I channel. Most of the vegetation is growing directly in the channel in this intermittent stream while in other parts of the watershed it is mainly concentrated adjacent to the channel.



Figure 34: Tree throw from an overturned blue gum eucalyptus creating mound $\sim 3 \frac{1}{2}$ feet tall adjacent to the tributary channel Pedro Point II subwatershed.

3.4 Summary

Sources in SPCW were characterized by the obvious processes generating the sediment. All sources were distinguished into one of five categories: debris flows, slumps, surface erosion (including creep), gullies, or fluvial erosion. Slumps and debris flows tend to be large mass wasting processes easily identified relative to sources influenced by creep alone. Surface erosion was modified to include creep processes whereas gullies and fluvial erosion were distinguished from areas only influenced by rainsplash erosion, sheetwash, and overland flow. Efforts to estimate quantities of sediment derived from sources influenced by only sheetwash, overland flow, and creep processes would require a long-term monitoring study. As a result, quantities of sediment produced from these sources were not estimated and were only designated as possible sources.

4. Methodology

Sediment sources can be complex and difficult to accurately recognize. Studies identifying these sources utilize a multitude of field, laboratory, and computer modeling techniques. Traditional methods include aerial photograph analysis supported by field observations and data collection (Collins *et al.* 2001; WFPB 1997a) and implementation of profilometers and erosion pins (Hooke 1979; Couper and Maddock 2001; Prosser *et al.* 2000). More technical studies frequently employ quantitative analyses incorporated into a Geographic Information System (GIS) model (DeRose *et al.* 1998; Millward and Mersey 1999; Dai and Lee 2001; Parsons and Abrahams 1993; Finco and Hepner 1998) or analyzed in conjunction with aerial photography and field data (Aniya 1985). More complex technologies have enabled the origin and dating of sediments based on floodplain cores by analyzing element content relative to source composition (Magilligan 1985; Pasternack *et al.* 2001; Owens and Walling 2002) and “fingerprinting” derived from sediment size and composition to identify sources (Clapp *et al.* 2002; Collins and Walling 2002).

Using aerial photographs, field data collection, and information from local land managers, sediment sources can be identified (WFPB 1997a). The methods used in this study incorporated these techniques and supplemented them with qualitative values derived from GIS modeling. Through these methods, sediment production from mass wasting, surface erosion, and some fluvial erosion processes were identified and assessed. While these are naturally occurring processes, urbanization in the form of development, roads, and trails, which is prevalent throughout the watershed, exacerbates sediment production enhancing the amount of sediment that is delivered to a drainage network. Natural and anthropogenic sources were distinguished by “triggers” and amounts of material delivered to the stream network quantified where possible.

Aerial photographic interpretation, GIS analyses, and field data collection were the main methods used to identify sediment sources throughout the upper watershed. Landslides and large gullies were observed from an aerial photographic survey and digitized into a GIS. Field survey data used in conjunction with GIS identified additional site-specific source areas. Volume of erosion was calculated where the general erosion was severe and localized enough to make an accurate estimate. A complete quantitative assessment of surface erosion processes including soil creep, sheetwash, and rainsplash erosion could not be quantitatively considered without a long-term monitoring study employing techniques, such as erosion pins.

The findings for this study were collected and analyzed in multiple steps. A trail and road assessment was conducted with the simultaneous collection, modification, and modeling of GIS data, including the Soil Erodibility Model (SEM), perennial flow points, effective drainage density, connectivity, and land use change. Select landslides and gullies were subsequently mapped in the field and from stereo aerial photographs. A shallow slope stability model, SHALSTAB, was used to estimate relative landslide susceptibility throughout the watershed. Finally, source areas were identified with the synthesis of findings, and prioritizations for management were made.

4.1 Aerial Photographic Interpretation

Aerial photographic interpretation provides valuable and accurate assessments of geomorphic and land use changes. It is a commonly used technique to assess mass wasting using a visual history of change. By evaluating sequential historical photographs, large areas with barren soil, mainly gullies, and those where past and recent mass wasting events have occurred can be readily identified and can be related to land use changes over time, such as urban development, farming, and ranching.

The U.S. Geological Survey (USGS) has created and compiled a wealth of data on landslides in San Mateo County, California using aerial photographic interpretation. Maps were originally created to evaluate geology, existing landslide deposits, and slope (Nilsen 1986). These findings were then analyzed to create a relative slope-stability map (Figure 35) (Brabb *et al.* 1972) that has since been updated and is now available in GIS format (Ellen *et al.* 1997). While these maps provide a foundation for determining landslide potential, and hence sediment sources, on a regional scale, a significantly more detailed map was generated in a portion of the South and Sanchez subwatersheds in SPCW as a result of numerous slides throughout the San Francisco Bay area, including 475 in the greater Pacifica area alone, during the January 1982 storm event (Figures 36a, b, and c) (Smith 1988). The previous landslide maps mainly identify large, deep-seated slides until the storm revealed the prevalence and potential of smaller, shallow slides (Ellen *et al.* 1988). The storm prompted extensive research on these smaller, fast moving debris flows predominantly using aerial photographs throughout the SF Bay region.

Washington State Department of Natural Resources Forest Practice Board (WFPB) has developed a commonly utilized method to categorize areas for landslide potential (Dietrich *et al.* 1998). This method uses aerial photography to conduct an inventory of disturbed areas followed by field inspections to validate these findings. These results are then extrapolated to areas with similar characteristics including geology and topography. The likelihood of future mass wasting events can then be spatially predicted based on these results (WFPB 1997a).

A method similar to that developed by the WFPB was used for an extensive study conducted on a San Francisco Bay area watershed, Wildcat Creek. This method utilized stereo aerial photographs to identify active and inactive landslides as well as the headward extension of tributaries (Collins *et al.* 2001). Coupled with field assessment, sediment input from these slides was estimated and field observations identified additional slides in heavily vegetated areas not visible in aerial photographs.

Methods similar to those developed by WFPB were employed to identify mass wasting and select surface erosion occurrences in SPCW in this study. Through aerial photographic interpretation landslides were identified and the scar area, track, date of occurrence, and possible triggers of mass wasting events in SPCW was revealed. The volume of debris flows was calculated based on the surface area obtained from the aerial photographs times the average depth between the deepest and shallowest depths of large landslides occurring in the

area. The average of these landslide depths was generated from a literature review. The total volume displaced from mass wasting events was

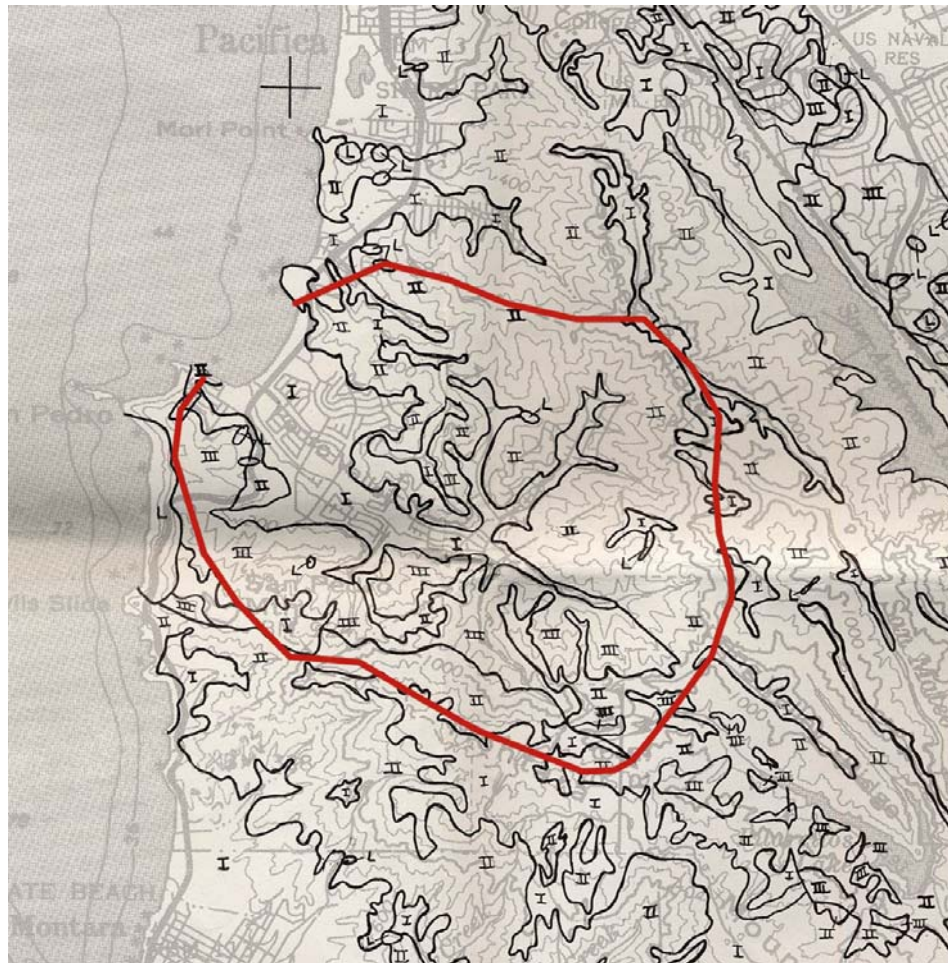


Figure 35: Generalized relative slope susceptibility map of SPCW (shown in red) at 1:62,500. Ranges on a scale of most stable at I to least stable at III (Brabb *et al.* 1972).



Figure 36a: Pre-1982 debris flow scars and tracks mapped from aerial photographs. Originally mapped at 12K, large portions of the Sanchez, South, and Middle Subwatersheds are covered (Smith 1988).

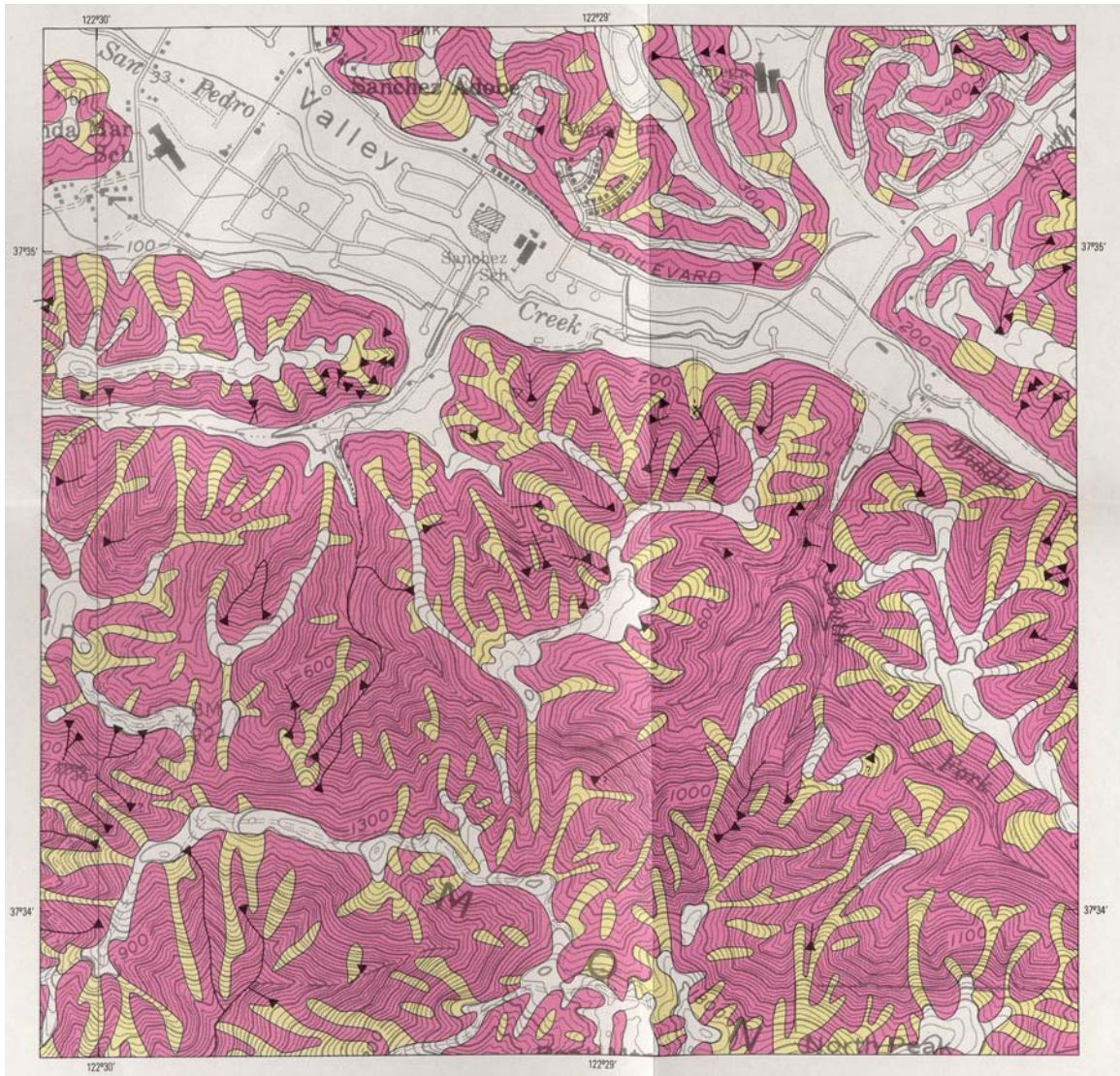


Figure 36b: Landslides and tracks from the 1982 storm event superimposed on a 1977 susceptibility map previously created by the author. The pink areas are the most susceptible, the yellow are intermediate, and white are the least (Smith 1988).



Figure 36c: Debris flow susceptibility map updated from the 1977 version with likely debris flow runout paths (Smith 1988).

calculated and the amount delivered was based on the proximity of deposition to the stream network. Gullies were also mapped from the aerial photographs but volume estimates were not estimated.

The number of landslides identified using the aerial photographic interpretation techniques depends mainly on the year the photography was taken relative to the occurrence of a landslide (Dietrich *et al.* 1998). For this reason, photographs from six different years with reference to corresponding ancillary data were analyzed: 1941 at a scale of 1:24,000, 1955 at 1:10,000, and 1975, 1983, 1991, and 1997 at 1:12,000. Gullies, landslide scarps, and obvious landslide tracks digitized into ArcMap 8.2 where they were analyzed in conjunction with existing layers, such as slope, geology, and soil. Land uses and trails were also digitized into a GIS from each of these years while landslides and gullies were mapped from all but 1991. The land uses were divided into three groups: developed, farmland/rangeland, and other, which includes natural and as of yet undeveloped lands. Approximate dates of land conversion, based on the year of the photograph where a change was observed, were also documented with the progression of development. Trails were attributed with dates of construction, levels of use, and levels of maintenance, and roads were coded with dates of construction. A few of the pre-existing trails that have since overgrown and been decommissioned were not included on the maps. Ancillary photographs at various scales supplemented the stereo photos with additional information including dates of trail and road construction, but were not directly mapped (see Appendix A for a complete list of photographs used).

4.2 Field Surveys

In sediment source analysis studies, field surveys are still the predominant method to accurately identify localized areas contributing to water quality deterioration and associated watershed degradation. They are particularly useful for total maximum daily load studies to determine sediment yield and sometimes the entire sediment budget of a watershed (Stillwater Sciences 1999; PWA 2003).

Field surveys of hillslopes help verify the findings of aerial photographic interpretation and GIS models. Detailed surveys identify specific areas of sediment delivery to the drainage network mainly from anthropogenic sources as these trails and roads provide access to the watersheds. Surveying these anthropogenic areas in great detail biases the results, as the natural sources are more difficult to access and can't be as readily identified in the field.

Site-specific land use impacts are revealed through field surveys. Direct correlations between mass wasting events and the physical trigger mechanisms that caused the incidents, including concentrated flow from a culvert or drainage ditch, are readily identified (WFPB 1997b; Bullard *et al.* 2002). These features are apparent on a small scale and can often be attributed to the spatial proximity of the associated trigger mechanism.

Findings from the aerial photographs and GIS analyses were considered in the field while evaluating local geomorphic variations. Volume from several sizeable and readily accessible gullies was estimated from cross-sectional area and depth. Anthropogenic sources triggering

surface erosion and landslides were identified and volumes of smaller sources visually estimated through a trail and road assessment. Most of the trails and some of the roads likely to be producing sediment with connectivity to the stream network were surveyed.

4.3 GIS Models

A GIS provides a valuable method of displaying and analyzing spatial data. Correlations between the multiple factors involved in sediment production can be investigated. These models make predictions based on underlying variables and visually display spatial relationships that would otherwise not be seen. Equations such as the Universal Soil Loss Equation (USLE) are often inputs for empirical models with each factor of the equation acting as a layer that spatially represents a known value. The USLE can be used to derive a layer of predicted soil loss based on inputs, such as sediment yield measurements. Deterministic models, such as the Shallow Slope Stability Model (SHALSTAB) are often based on known physical processes or relationships but require data on all contributing inputs. As a result, these models can only be applied to landscapes for which all contributing geomorphic processes are well represented by the model.

4.3.1 SHALSTAB

Landslide susceptibility models have been created mostly for safety reasons as they present a significant hazard to human inhabitants of steep-sloped hill and mountain areas. Since shallow landslides are an important source of sediment (Dietrich *et al.* 1998) and are often a direct result of land use, these models also apply to sediment source analysis studies. The Shallow Slope Stability Model (SHALSTAB) is one such deterministic model that the potential of shallow landslides across a study site, which frequently result in debris flows (Dietrich *et al.* 1998).

SHALSTAB is a deterministic GIS model based on research conducted by Montgomery and Dietrich used to analyze relative shallow landslide potential (Dietrich *et al.* 1998). Building on methods developed by the WFPB, this model shifts away from establishing geomorphologically similar mass wasting units to analyze areas of instability. This operator-interpreted method introduces a larger element of human error that SHALSTAB is able to minimize. Initial aerial photographic assessment integrated with field data collection generates a detailed landslide inventory, which can then be used to test the results of SHALSTAB. Analyzed with a digital elevation model data the relative slide susceptibility throughout the entire SPCW is determined and tested against known landslides.

SHALSTAB is a parameter free model that runs on the foundation of process driven elements of fluvial-induced geomorphic change. The model is based on the understanding of how fluvial processes interact with soil and underlying bedrock to generate landslides. Extensive field studies have been conducted in Oregon and multiple locations in northern California to modify and validate the results (Dietrich *et al.* 1998). Using digital elevation model data, the relative slope stability of a landscape is determined at which landslides may occur under steady state rainfall conditions (Dietrich and Montgomery 1998).

Slope stability and hydrologic flow models compose the foundation of SHALSTAB (Dietrich and Montgomery 1998). Slope stability is calculated using an infinite slope form of the Mohr-Coulomb equation as a function of the strength of resistance from cohesion and the frictional resistance on the failure plane. This equation was modified to remove the cohesion factor because of the difficulty in gathering such data as a result of the variability of its influence across multiple landscapes. Instead the friction angle was set to 45° to compensate for lack of root cohesion consideration. The modified equation

$$\frac{h}{z} = \frac{\rho_s}{\rho_w} \left(1 - \frac{\tan \nu}{\tan \phi} \right) \quad (1)$$

calculates the proportion of the soil column that is saturated at the point of instability, h/z , where h is the water level above the failure plane (m), z is the soil depth (m), ρ_s is the soil bulk density (1,200 kg m⁻³), ρ_w is the water density (1,000 kg m⁻³), ν is the slope angle (°), and ϕ is the angle of internal friction in the soil (45°) (Dietrich *et al.* 1998). The model was initially run with the soil bulk density of 1,700 kg m⁻³ with disappointing results. Subsequent iterations were conducted with the soil bulk density of 1,010 kg m⁻³, 1,200 kg m⁻³, and 1,500 kg m⁻³. As the soil bulk density for the study area and the various soil types is unknown, the model run with the value of 1,200 kg m⁻³ was analyzed with the best results.

The hydrologic flow model calculates steady-state subsurface flow based on soil transmissivity, the ability of subsurface flow to transmit water downslope, and Darcy's Law (Dietrich and Montgomery 1998), which determines the flow-through rate as a function of hydraulic conductivity, hydraulic gradient, and the cross-sectional area through which the subsurface water flows (Ahnert 1996). In the modified hydrologic flow model runoff is understood to be generated by shallow subsurface flow and saturation overland flow:

$$\frac{h}{z} = \frac{q}{T} \frac{a}{b \sin \nu} \quad (2)$$

q is the effective rainfall (rainfall minus evapotranspiration in mm/day), T is the soil transmissivity (m²/day), b is the hillslope width (m), a is the subsurface flow drainage area (m²), and ν is the degrees slope (Dietrich *et al.* 1998). The variables a , b , and ν were calculated from contributing area and slope grids generated as one of the steps in the model. Finally, both the slope stability and the hydrologic flow models are integrated in SHALSTAB to predict the magnitude of relative slope stability:

$$\frac{q}{T} = \frac{\rho_s}{\rho_w} \left(1 - \frac{\tan \nu}{\tan \phi} \right) \frac{b}{a} \sin \nu \quad (3)$$

This combined equation is expressed as the hydrologic ratio of the effective rainfall to soil transmissivity, which designates slope stability (Dietrich and Montgomery 1998).

The final product indicating shallow slope stability, q/T is best displayed in logarithmic form as the results range over multiple orders of magnitude (Dietrich *et al.* 1998). The slope stability value is expressed in negative values and the lower the value, the more unstable the slope. Slopes are chronically unstable below -3.1 as it is not likely that a rainfall event of the intensity needed to cause slopes to fail with this ranking will occur in nature. The results can also be displayed in ordinal classification as threshold values created by Dietrich and Montgomery ranging from low to high slope instability, or chronically stable to chronically unstable (Dietrich and Montgomery 1998). Anthropogenic influences such as roads and trails were not considered in the model were analyzed with the final results to identify more localized areas of potential instability.

Creating a SHALSTAB model for SPCW followed the general outline proposed by Dietrich and Montgomery (1998). The only initial data needs were digital elevation model from which various layers were derived and landslide data which was used to validate the accuracy of the calculated q/T values. As the available digital elevation model is based on the most recent hillslope topography, landslides that occurred in areas that have since been at least partially leveled and subsequently developed were removed from consideration in the model. SHALSTAB can be run with digital elevation data alone but within the constraints of this model were tested against the known landslide distribution. The model was very applicable to SPCW as it has similar topographic and geologic characteristics for which SHALSTAB has previously been modified and tested. In addition, the visible landslides were mapped and provided a good test against which to analyze the results.

4.3.2 Soil Erodibility Model

While not as significant as landslides in generating sediment, surface erosion does occur in SPCW. A simple soil erodibility model, the SEM, incorporates empirical data from % slope and a physical soil property, the K-factor, to generate a rating system (WFPB 1997b). As land uses significantly enhance and deliver surface erosion to the drainage network, this model can be readily compared to urbanization practices in SPCW. In contrast, vegetation acts as a buffer abating sediment delivery to the drainage network and was incorporated to the surface erosion analysis.

The most commonly used soil erodibility model is the Universal Soil Loss Equation (USLE), which is integrated into a GIS to calculate empirical data to derive long-term average soil losses (Battad 1993). Best used for predicting surface erosion primarily in agricultural lands (Ahnert 1996), the utility of the equation on forests

and rangelands is questionable (Battad 1993). While the model is not generally applicable to areas influenced by mass wasting, the dominant process in SPCW, Equation 4 presents the interrelatedness of the variables influencing soil erosion (Selby 1993).

The USLE has since been modified to the Revised Universal Soil Loss Equation (RUSLE), which maintains the original values, but incorporates more parameters to improve the effectiveness of the model (Battad 1993). The average annual soil loss, A ($t\ ha^{-1}\ yr^{-1}$), is calculated with the equation:

$$A = LS * R * K * C * P \quad (4)$$

where LS = combined slope steepness and slope length measurements (unitless), R = the rainfall erosivity factor ($\text{MJ mm ha}^{-1} \text{h}^{-1} \text{yr}^{-1}$), K = soil erodibility factor or the soil loss per rainfall erosion index unit as measured on a unit plot ($\text{t ha h MJ}^{-1} \text{mm}^{-1} \text{ha}^{-1}$), C = land cover and management factor, including land use and surface cover and roughness, which estimates the soil loss ratio (unitless), and P = the soil loss ratio of specific support practice factors including terracing and contouring (unitless) (Millward and Mersey 1999; Battad 1993; Marsh 1998; Simanton and Renard 1993). With these modifications RUSLE is able to be adapted to watersheds with varying geomorphology. For example, Millward and Mersey (1999) successfully applied RUSLE to a watershed after further modification of the LS variable to account for steep relief within their study area.

A very basic equation derived from RUSLE, the soil erodibility model (SEM), considers only the K -factor and slope values, or $A = K * S$, where K = the K -factor designated by the Soil Conservation Service (unitless) (Kashiwagi and Hokholt 1991) and S = % slope (WFPB 1997b). This model was modified slightly to better represent the range of k -factor values occurring in SPCW. The model output is classified into a range of low to high erodibility ratings (Table 1). This rating overlaid with land uses identifies anthropogenic sources of sediment. As surface erosion is secondary in the effectiveness of generating sediment to mass wasting within SPCW, it is not expected to be significant except where heavily affected by land use practices. Urbanization in the form of roads, trails, and development on the fringe of hillslopes are the predominant and most influential land use variables in terms of surface erosion production and sediment delivery to the drainage network. This model provided a simple, yet effective measure against which these land uses were then field surveyed to determine the most significant, localized sediment sources produced from surface erosion.

Slope Class (Percent)	$K < 0.25$ Not easily detached	$0.25 < K < 0.40$ Moderately detachable	$K > 0.40$ Easily detached
< 30	Low	Low	Moderate
30 – 65	Low	Moderate	High
> 65	Moderate	High	High

Table 1: Modified soil erodibility ratings derived from the K - factor and slope (WFPB 1997b).

4.3.3 Other GIS

Other GIS models and raster layers generated include the level of connectivity, effective drainage density, and perennial flow initiation. Connectivity, the likelihood of sediment delivery to the stream network, was used to determine the volume of sediment delivered to the tributaries from landslides and gullies. Delivery of sediment from potential sources to the drainage network was considered in all steps of the assessment. Because not all sediment from landslides becomes entrained in the streams (WFPB 1997a), recognizing the connectivity of sources to the drainage network is imperative when analyzing input. While this is also true for surface erosion, only surface erosion in relatively close proximity to the drainage network was considered. Estimates of connectivity compared with the SEM and

SHALSTAB models also revealed contributing areas susceptible to surface erosion and unstable slopes. The total sum of the lengths of drainages including roads, trails, hillslope drainage channels, and tributaries were compiled per subwatershed to determine the effective drainage density. Known pour points along the tributaries where surface perennial flow initiates were also modeled into a layer revealing drainage surface area required to maintain year-round flow. These models are examined in more detail in the Results section.

GIS is integrated with field data throughout the assessment. Ancillary data layers supplemented and supported the findings derived from the raster GIS models SHALSTAB and the SEM. Digitized landslide data derived from the aerial photography and 10-m DEMs were used to run the ArcView 3.2 extension, SHALSTAB, from which the relative slope stability was extrapolated across the entire study area. These results were compared with roads, trails, and land uses to identify additional areas of potential site-specific sources that are not evaluated within the context of this model. Field mapped landslides and gullies were analyzed in ArcMap 8.2 to calculate the volume of displaced sediment. The SEM was also generated using ArcMap 8.2. Again, current roads, trails, and land uses were compared with the final model to determine areas that were delivering enhanced levels of sediment as a result of anthropogenic influence. In contrast, the presence of vegetation and low gradient slopes were considered to determine areas where connectivity was abated.

Most layers are in both vector and raster format and analyzed in ArcView 3.2, ArcMap 8.2, and ArcInfo 4.0. All GIS layers are projected in UTM zone 10N using North American Datum 1983 and a complete list of those used is available in Appendix B.

4.4 Previous Work in SPCW

Several studies have been conducted in SPCW to assess properties of the channel and surrounding hillslopes. Collins *et al.* (2001) provided invaluable data on past and current main channel conditions and found that many stream channel alterations are explained by patterns of land use change. The USGS has repeatedly mapped geologic

properties, landslides deposits, and hillslope stability within SPCW on regional scales (Brabb and Pampeyan 1972; Brabb *et al.* 1972) and highly localized scales (Smith 1988). These studies have contributed to an improved understanding of processes triggering

debris flows, the types of landslides that are most significant in delivering sediment to the drainage network. In addition, detailed and readily accessible GIS data provided by the SPCWC and federal agencies were utilized throughout.

4.5 Synthesis

Compiling the findings generated a comprehensive analysis of sediment source assessment. Site-specific points of erosion identified from aerial photographic interpretation were integrated into a GIS to determine level of connectivity and if possible quantities of delivery. Sources were classified into erosion types and collectively considered as triggered by either natural or anthropogenic activity. Based on this assimilation and levels of connectivity, predictions about the amount of sediment generated for specific drainage areas were made.

Extremely thick and impenetrable vegetative cover dominates the undeveloped hillslopes and tributaries of SPCW, significantly hampering access to the majority of the watershed. Recent fire suppression practices enhance the vegetation density compounding the problem. Aerial photographs and GIS models provide sediment source information without direct access to the watershed. These methods produced both quantitative and qualitative data, which were supplemented with field data collection from relatively accessible portions of the watershed. Ancillary GIS layers including land use, vegetation, and geology facilitated the overall analysis. Finally, based on these findings, areas were prioritized for implementation of sediment abatement measures and management recommendations proposed for adoption.

5. Results

5.1 General patterns

Numerous assessments were used to identify contributing factors to sediment production. By examining aerial photographs a GIS inventory of current and past landslides and gullies as well as land use change over time was produced. Tracing land use change isolates landslides and gullies triggered by anthropogenic sources. Roads, trails, the stream network, and urban development data were used to calculate the effective drainage, or total areas of the watersheds contributing to channels. Known perennial flow points reveals elevated groundwater where flow may be intensified creating more erosion problems relative to the remainder of SPCW. The Sediment Erosion Model (SEM) identifies areas highly susceptible to surface erosion and SHALSTAB determines relative slope stability. Finally, the connectivity of the potential sources to the stream network is used to identify sources that contribute sediment to the stream network. These assessments outlined in general patterns are broken down in site-specific detail later in this chapter in section 5.2.

5.1.1 Landslide and gully distribution

Landslides and gullies identified on aerial photographs were classified as caused by either natural or anthropogenic influences (Table 2). Natural designation was given to slides and gullies where the occurrence could not be directly connected to human activity. Anthropogenic classification was given only to slides and gullies with considerable evidence of a human-influenced trigger.

Sources of landslides and gullies were predominantly classified as natural. Overall 500 slides and gullies were attributed to natural sources whereas only 146 were assigned to anthropogenic origins. Over $\frac{3}{4}$ of landslides and $\frac{2}{3}$ of the gullies were classified as natural (Table 2). While historic accounts indicate grazing on many of the hillslopes in SPCW, specific hillslopes that were formerly used for grazing are unknown and consequently this anthropogenic influence on sediment production cannot be separated from natural sources. As a result, landslides and gullies triggered by natural sources are likely overestimates. The same is true for landslides and gullies where farming occurred along toe slopes. While likely triggered by this land use, many were not classified as an anthropogenic because this direct cause and effect is difficult to accurately confirm.

Most gullies already existed in the 1941 photographs when farming had long since been rooted in the valley. Consequently, a direct correlation cannot be made because some of the gullying may have previously existed. As a result many of the gullies classified as natural may also actually be anthropogenic.

	Natural		Anthropogenic		Total
	#	%	#	%	
Gullies	33	69%	15	31%	46
Landslides	469	78%	131	22%	600

Table 2: Landslide and gully sources in SPCW categorized by number of events and % of total.

Anthropogenic sources were given only to slides and gullies that appeared to be closely correlated to human influence. Of the 604 total landslides, 22% can be attributed to anthropogenic sources whereas 31% of the 48 gullies can be designated as such. Anthropogenic influences were further categorized into trails, roads, and urban development, which include past urban construction and concrete drainage channels on terraced hillslopes (Table 3). Overall, 103 landslide and gullies were attributed to trails, 36 to roads, and 9 to drainage channels and urban construction.

	Trails		Roads		Drainage channels, urban construction		Total
	#	%	#	%	#	%	
Gullies	8	8%	7	19%	0	0%	15
Landslides	93	92%	29	81%	9	100%	133

Table 3: Break down of anthropogenic landslide and gully sources categorized by number of events and % of total.

Trails were the predominant anthropogenic source. This includes private roads not accessible by the general public, many of which are on the upper hillslopes. Many of the slides occurred high on hillslopes and the diverted and/or channelized flow created by trails often concentrates drainage, creating problem areas.

Roads include only those still in use and accessible to the general public. Most roads are located on the valley floor and lower hillslopes along the bases of tributaries in highly developed areas covered primarily by pavement. As a result the influence of these roads on landslides and gullies overall is generally smaller than trails because of lower slope gradients and fewer erodible surfaces. Near the creek where there are many erodible surfaces along terraces and channel banks, riparian vegetation often obscures gullies, slides, and even surface erosion from view on aerial photographs. As a result, the influence of roads on gullies and landslides is expected to be much higher than that found, increasing the overall anthropogenic influence.

A few landslides were triggered adjacent to artificially terraced hillslopes. The ditches constructed to drain water on the main slope face concentrates flow along the peripheral slopes either in culverts or by natural channels entrenched by the intensified flow. While this directed flow provides a more stable face slope, it often creates instability at the

points where it is diverted. As these structures are relatively new, no gullies have yet formed but nine new landslides have occurred.

Landslides and gullies were also classified by first year of visibility on the aerial photographs (Table 4). Most landslides were identified in 1941, the first year of review, and 1983, after the severe rainfall event that triggered a large number of slides. A large number of slides were also visible in 1975 after a few severe rainfall events that occurred in the 20-year span between observing photos in 1955 and 1975. Nearly all gullies were identified in 1941 when farming and grazing were the predominant land use. Gullies that have since formed are probably too small to be observed on aerial photographs and were therefore not included in the total.

	1941		1955		1975		1983		1997	
	#	%	#	%	#	%	#	%	#	%
Gullies	41	21%	0	0%	5	3%	1	0%	1	9%
Landslides	156	79%	39	100%	142	97%	253	100%	10	91%
Total	197		39		147		254		11	

Table 4: Years landslides and gullies were first visible on aerial photographs categorized by number of events and % of total.

Landslides were further dated into categories based on vegetation cover when first visible on the aerial photographs (Table 5). Fresh slides with no or minimal vegetation constitute 74% of the total, mature or partially revegetated slides constitute 18%, and old or mostly revegetated slides comprise 8%. Most landslides were visible for a few subsequent dates after first observed with recurring slides in some areas.

Landslide age	1941		1955		1975		1983		1997		Total
	#	%	#	%	#	%	#	%	#	%	
fresh	86	19.3%	31	7.0%	104	23.4%	217	48.8%	7	1.6%	445
mature	43	39.4%	6	5.5%	30	27.5%	27	24.8%	3	2.8%	109
old	27	58.7%	2	4.3%	8	17.4%	9	19.6%	0	0.0%	46

Table 5: Landslide “age” at first visible year on aerial photographs categorized by number of events and % of total.

5.1.2 Impacts of land use change on sediment production

Land use changes have direct implications on sediment production. Land use was traced for select years from 1941 to 1997 and compared for relative changes. A land use assessment of the entire watershed reveals potential historic sources of sediment and traces where these sources have shifted over time as well as the anthropogenic triggers influencing that change. General land use changes are

outlined below but a more detailed review of land use cover per subwatershed per year is provided in Appendix C.

Recent land use in SPCW has shifted from mainly farmland and grazing to predominately residential and urban development while maintaining a large portion of undeveloped, or “other”, land (Table 6). The land use “other” includes natural or otherwise undeveloped lands. Dramatic increases in residential development occurred between 1955 and 1975 simultaneously displacing farmland. Land use change after 1975 is slight, as most area available for development and farmland had already been utilized. “Other” has changed in area the least since 1941.

	1941		1955		1975		1983		1991		1997	
	total ha	%										
Developed	26.7	1.3%	199.3	9.4%	574.2	27.0%	578.4	27.2%	581.5	27.4%	581.5	27.4%
Farmland	304.8	14.3%	125.5	5.9%	18.5	0.9%	15.2	0.7%	13.5	0.6%	13.4	0.6%
Other	1793.0	84.4%	1800.0	84.7%	1532.0	72.1%	1531.2	72.1%	1529.8	72.0%	1529.8	72.0%
Total watershed ha	2125.0											

Table 6: General land use patterns per year observed for the entire SPCW in hectares and percent.

In 1941 land use in SPCW consisted primarily of farming and grazing with very little urban and residential development (Figure 37a). Areas classified as “other” were undeveloped and possibly used for grazing, comprised 84% of the total area (Table 6). The majority of the valley floor was farmland comprising 14% of SPCW and extending along all major tributaries near the confluences with the main channel. Development comprised only 1% existing as the initial stages of tract residential development in Pedro Point I subwatershed and scattered farmhouses and barns. Few trails and roads were established along ridge tops and the valley floor adjacent to the creek.

A total of 41 gullies were well established in SPCW in 1941 (Table 4). Most significant gullies were evident adjacent to the valley floor. Most of these gullies were upslope of farmland along the main stem and in the North, Crespi, Shamrock, and Pedro Point I subwatersheds. This implies an anthropogenic influence for example, gullies are often initiated by landslides that may have occurred with the removal of support from the toe slope for crop cultivation. Regular grazing on hillslopes may also have been significant (Culp 2002) but specific areas of grazing are unknown, therefore this influence cannot be directly accounted for. Gullies occurred mostly in artificial fill, mélange, slopewash, ravine fill, and colluvium deposits but either crossed or extended along most surficial geology.

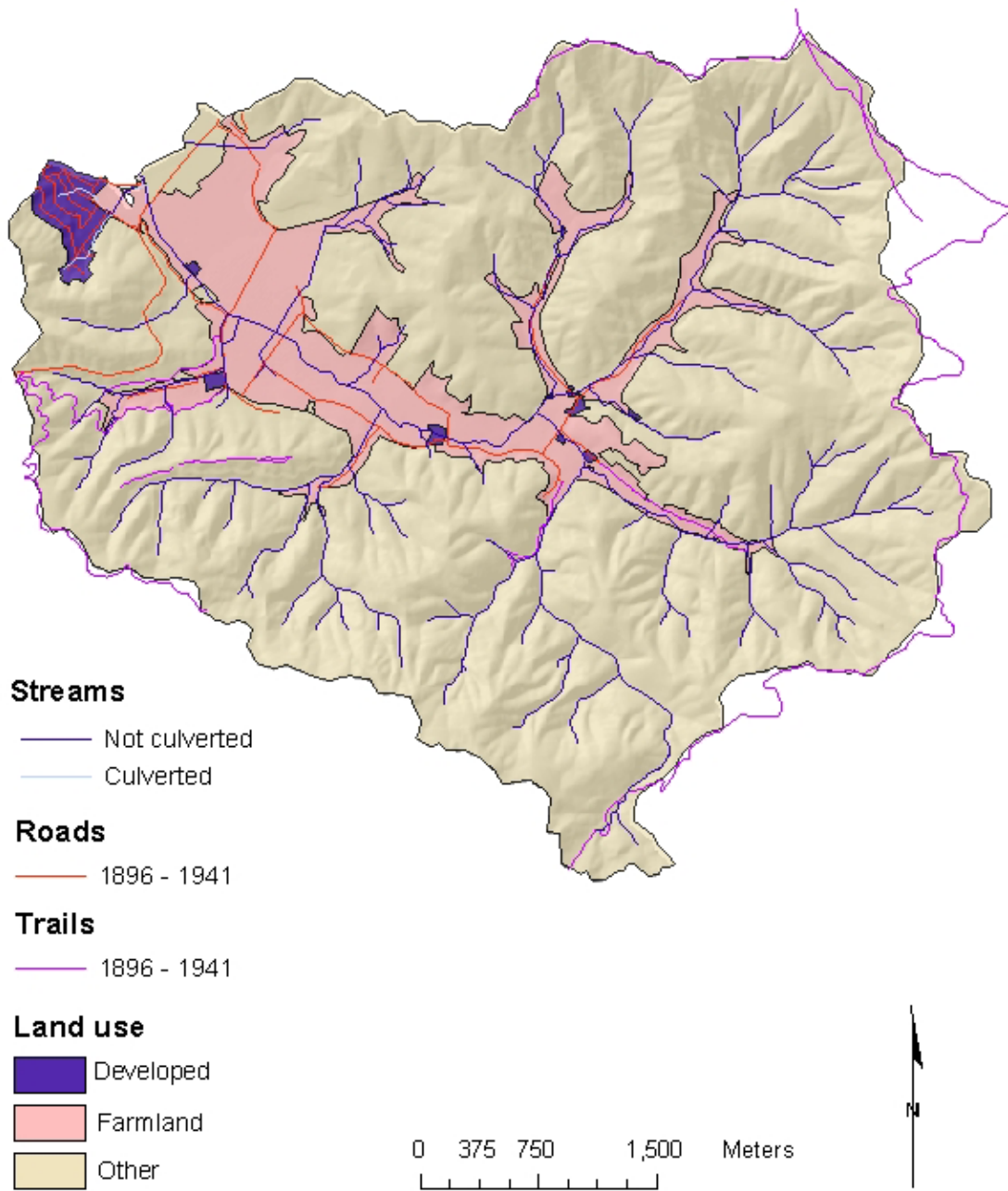


Figure 37a: Land use in 1941 with existing roads and trails.

Gullies present in the lower valley provide a broad area susceptible to surface erosion. As many gullies were observed in the 1941 photos, surface erosion was likely very significant before this time and continued to be significant unless mitigation measures were implemented.

The amount of sediment generated from surface erosion except in the gullies is presumed to be relatively high from farming and grazing practices and construction from development. Additionally, the upper slopes within the South subwatershed were sparsely vegetated where underlain by Montara mountain granite and in some areas with sandstone, shale, and conglomerate. Upper hillslope surface erosion was probably limited to these areas on some of the steepest slopes and underlain by the Scarper-Miramar complex that also has the highest surface erosion (k-value) potential of all soils within SPCW.

Landslides scattered throughout SPCW totaled 156 (Table 4). Small concentrations of slides occurred in the Crespi subwatershed and the western portion of the North subwatershed. The slides in Crespi subwatershed occurred in similar settings as gullies, where land use at the base slopes was used for farming. Most of the slides in the Crespi subwatershed occurred on slopewash, ravine fill, and colluvium deposits. Slides in the North subwatershed don't appear to follow any pattern and occur in slopewash, ravine fill, and colluvium deposits as well as *mélange*, graywacke, and along the peripheral of artificial fill.

Land use along the valley floor changed significantly from 1941 to 1955 (Table 5 and Figure 37b). Development increased nearly 10 times displacing farmland, which decreased by over 50% from 300 ha in 1941 to 125 ha in 1955. This residential development began to encroach on tributaries and expand further upslope in Crespi subwatershed. Other land use actually increased slightly, possibly from the decommissioning of farmland. New roads followed the expansion of urban development while new trails were created in the South and North subwatersheds.

Only 39 new landslides were observed on the aerial photographs between 1941 and 1955. All of the new landslides occurred on hillslopes away from the peripheral of urban development on the valley floor. Many new slides were near well-established trails formerly used as roads in Sanchez and Shamrock subwatersheds. Most of the landslides occurred in Shamrock and North subwatersheds primarily on slope wash, ravine fill, and colluvium substrate.

No new large gullies were formed between 1941 and 1955. However, all gullies visible in 1941 were still apparent in 1955. Previously existing gullies most likely expanded in depth and area but the precise extent of change was not measurable from the air photos due to the 1:10K scale of the aerial photographs.

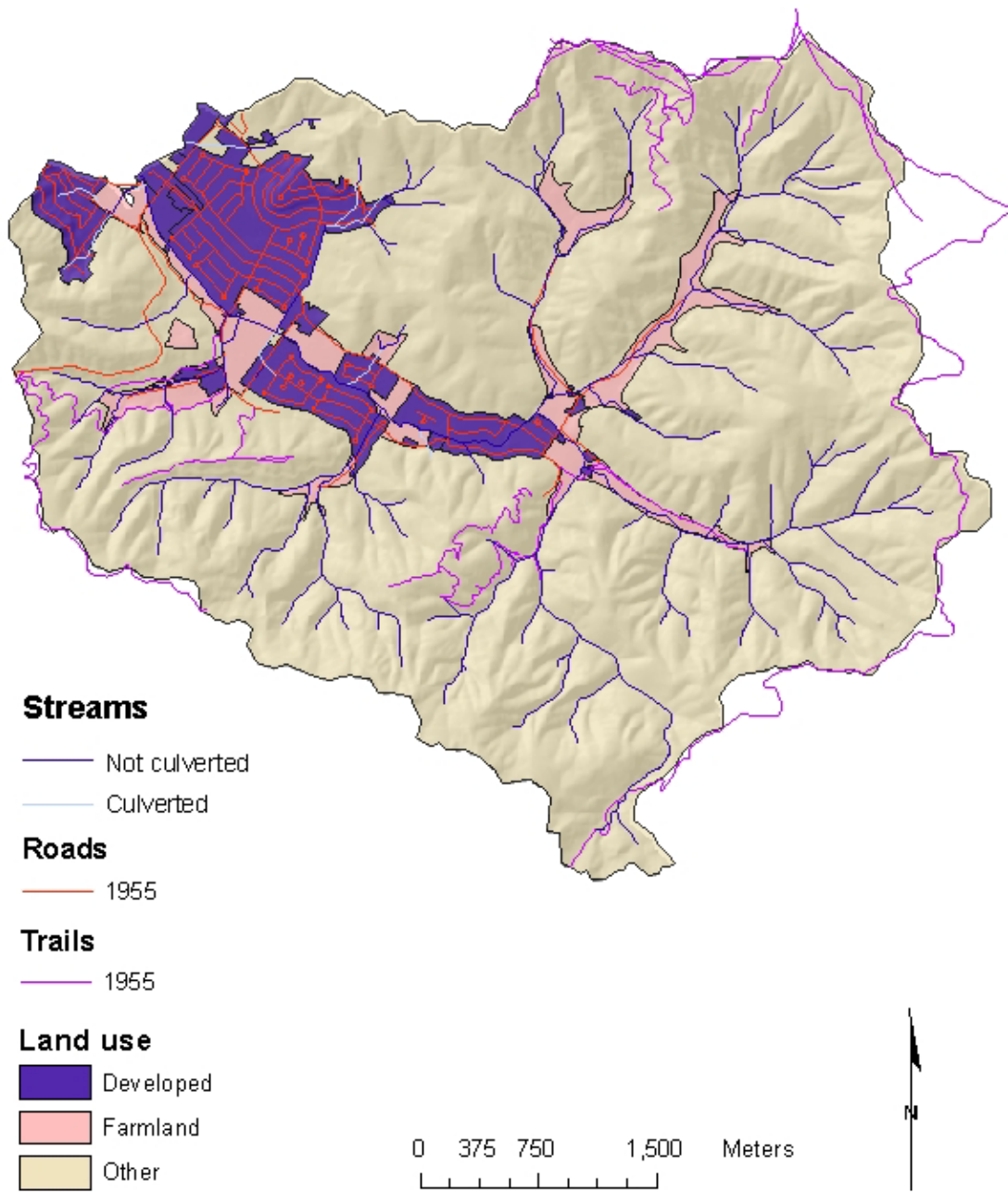


Figure 37b: Land use in 1955 with existing roads and trails.

Surface erosion likely occurred with the expanding urban development and road and trail construction. A network of roads covered the developed areas of the valley floor and extended along some of the tributaries. Along the peripheral of these developed areas construction practices probably generated loose soils highly susceptible to erosion during rainfall in the winter months. This would have increased short-term sediment supply to San Pedro Creek. Increased impervious surfaces of development concentrate flow and expedite the runoff rate to adjacent surfaces highly susceptible to erosion. These localized sites are likely becoming entrenched over time with the increasing development. New trails formed in the South and North subwatersheds also concentrated flow and during the heavy rainfall months, created source areas.

The most significant land use change in SPCW occurred in 1975 (Table 6 and Figure 37c). Between 1955 and 1975 developed land tripled while farmland drastically decreased seven times and other land use dropped 15%. Most of the previous farmland along the valley floor was converted to residential tract housing, and expansion in 1975 created the boundaries of most of the present-day development. Only a few farmland areas remained and have since been converted to ranches, such as the Shamrock Ranch, which still maintains one of the largest areas of contiguous, non-developed land along the valley floor (.1km²). The previously undeveloped hillslopes in the North subwatershed were also converted to residential housing while previous farmlands along the Middle subwatershed floor was decommissioned possibly for use as the present day San Pedro Valley County Park. The John Gay Trout Farm was operating on the valley floor of the South subwatershed and was washed out during a flood event in 1956. Extensive road networks followed the new development on the valley floor and many adjacent hillslopes. A trail network was extensively developed upslope of what is now the Picardo Ranch in the North subwatershed and upslope of the present Park Pacifica Stables in the Middle subwatershed. These trail networks were more extensive in aerial photographs from 1963 than 1975 and have since overgrown even more.

Between 1955 and 1975, 142 new landslides were observed on the aerial photographs (Table 4). This high incidence of slide events can at least partially be attributed to storm events in 1958 (VanderWerf 1994) and 1962 (Culp 2002). Photos from 1963 show very large slides in the South and Sanchez subwatersheds and large slides in the Middle and North subwatersheds from the 1962 intense rainfall event. Landslides found in 1975 were scattered evenly in SPCW predominately over the upper hillslopes in most substrates.

Between 1955 and 1975 many of the gullies were removed or leveled as a result of residential development. The new development lowered hillslope gradients and paved over pre-existing gullies mainly on the valley floor and the North subwatershed. A few new gullies were observed along the Middle subwatershed on the slopewash, ravine fill, and colluvium of the lower hillslopes. New smaller gullies not obvious on aerial photographs may be beginning to form on the peripheral of impervious surfaces in the urbanized areas.

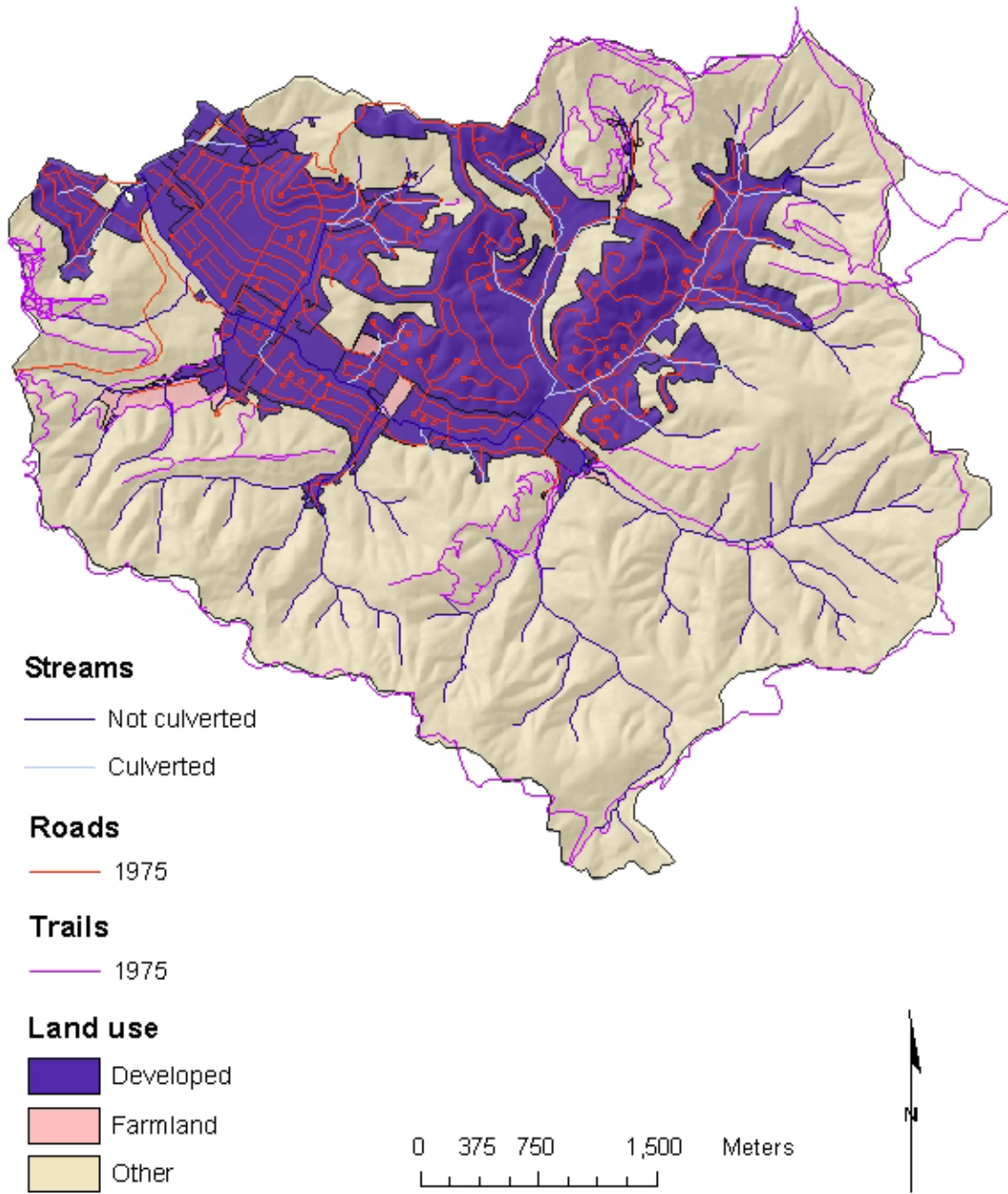


Figure 37c: Land use in 1975 with existing roads and trails.

Surface erosion probably increased along trails, roads, and the periphery of urban development. Many of the upper hillslopes with previously sparse cover have a thick vegetation layer in 1975 but many new trails cross these areas directing flow and creating localized sources. The new trail network in Pedro Point II along the coast was also likely becoming a significant source of surface erosion with increasing soil exposure from fresh landslides as a result of intensified recreational use. Extremely large landslide tracks obvious in 1963 photographs exposed a large surface area susceptible to surface erosion. This short-term erosion probably only occurred on fresh scars and deposits until vegetation was reestablished. Additionally, residential development and roads expanded significantly likely creating short-term sources on areas of exposed and displaced soil.

Land use changed very little between 1975 and 1983 (Table 6 and Figure 37d). Urban development increased slightly in the North subwatershed and on the valley floor while farmland decreased again by the new development. Other lands dropped only 0.8 ha also from this development. There was no new road development after 1975 while a few new trails were established in the South and Sanchez subwatersheds.

Between 1975 and 1983, 253 new landslides were observed (Table 4). Most were fresh from the January 1982 storm event that triggered 475 slides in the greater Pacifica area delivering 150 – 200 mm of precipitation to the area within less than 30 hours with an average intensity of 5.0 to 6.6 mm/hr (Monteverdi in Howard *et al.* 1988). While generally the slides are evenly dispersed throughout SPCW, a large number of slides occurred on the undeveloped hillslopes of the Middle and Sanchez subwatersheds and the upper North subwatershed. Landslides occurred on nearly every type of substrate within SPCW appearing to show no proclivity for any one type or location as was also found by Howard *et al.* (1988).

In 1983 only one new gully was observed within the Middle subwatershed, in slope wash, ravine fill, and colluvium substrate (Table 4). The remaining gullies in SPCW presumably deepened and expanded-- especially those bordering impervious surfaces-- unless mitigation measures were implemented.

Surface erosion in 1983 was probably most significant on fresh landslide scars and deposits and within gullies. The new landslides provided a large area of barren, unconsolidated materials susceptible to short-term surface erosion until revegetated. Surface erosion in the upper South subwatershed was probably less than in 1975 as the thin soils of the Scarper-Miramar complex were mostly revegetated by 1983. Erosion along roads and trails was probably also enhanced from the storm event and continued to develop significant source areas.

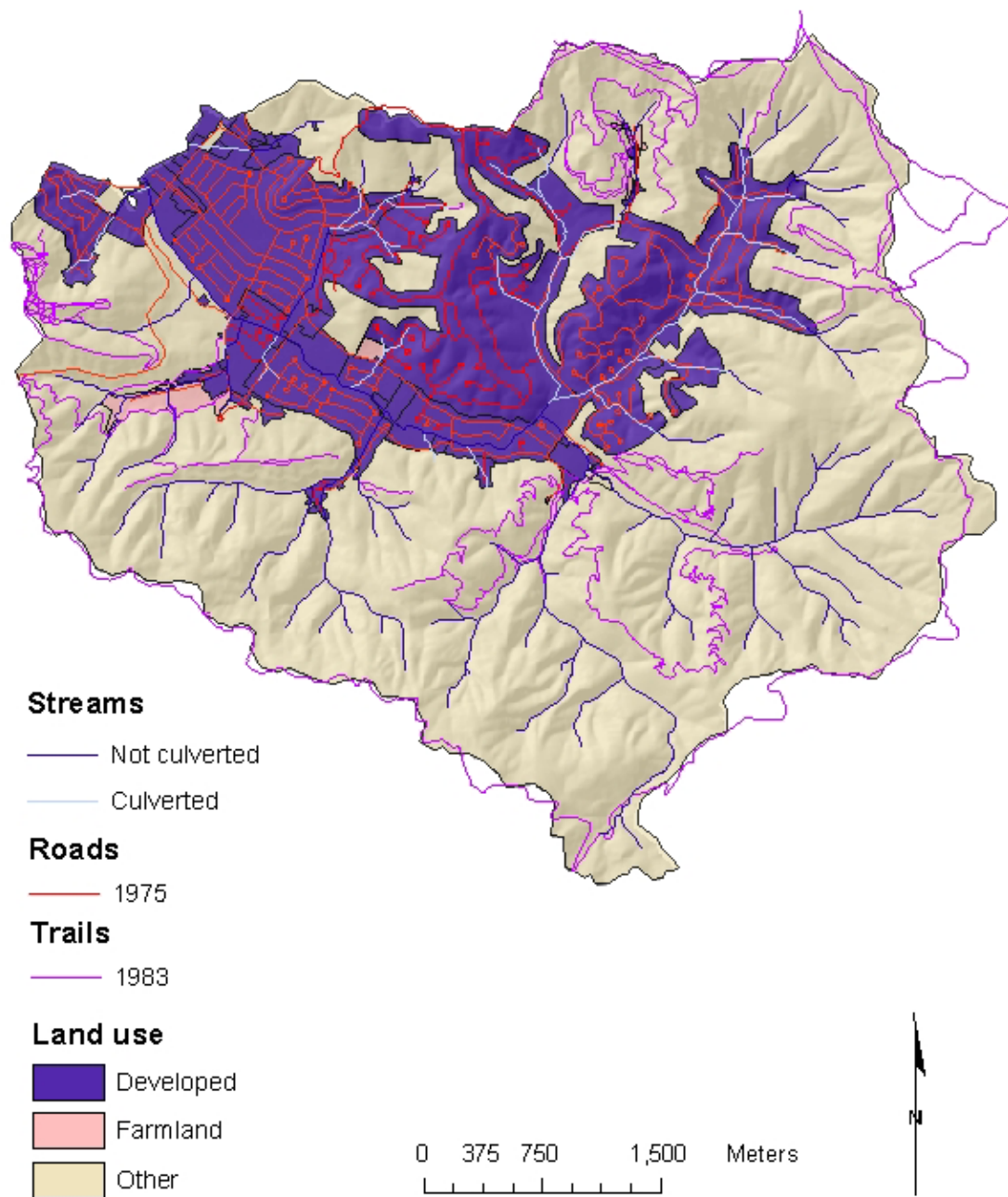


Figure 37d: Land use in 1983 with existing roads and trails.

Between 1983 and 1997, very little land use changed in SPCW (Table 6 and Figure 37e). Since the change between 1991 and 1997 was also so slight, only the map of the latter is displayed (Figure 37e). Developed areas increased by only 3.1 ha mainly in Shamrock and Sanchez subwatersheds. Farmland and other land uses decreased slightly by 1.8 ha and 1.4 ha respectively. All major roads currently existing in SPCW were constructed by 1975 and all major trails by 1983.

There were only 10 new landslides in SPCW observed on 1997 aerial photographs (Table 5). These slides were mainly distributed throughout the upper North, Middle, and South subwatersheds. This lack of a significant number of observable slides over a 13 year period indicates that there were not likely any severe storm events since 1983. The few new landslides occurred mainly on slope wash, ravine fill, and colluvium and sandstone, shale, and conglomerate.

Only one new gully was observed in Pedro Point II subwatershed on heavily impacted land between sandstone, shale, and conglomerate and slope wash, ravine fill, and colluvium substrate (Table 5). The gully is smaller than others identified on aerial photographs and was heavily obscured by vegetation. The dimensions of the gully were confirmed only by field identification. The difficulty in identifying this moderately-sized gully reveals that many smaller gullies are not included in this inventory, as they were not visible on aerial photographs. As a result the total number of gullies identified is biased toward large gullies and is an underestimate of the total number existing in SPCW.

Again, surface erosion most likely occurred in gullies and along the periphery of urban development, roads, and trails. Since the trails and roads had been established for many years, adjacent sites susceptible to erosion have had a longer time to become more significant sediment sources. The Scarper-Miramar complex of the upper South subwatershed is highly susceptible to surface erosion and has significantly more vegetation cover than in 1983. This would lessen the entrainment of sediment if the vegetation cover at ground level is sufficient to act as a filter. However chaparral and deciduous scrub, currently the predominant land cover type on these slopes, often have very little understory increasing the potential of sediment generation and delivery to the stream network.

Overall, landslide distribution did not appear to significantly favor any one geologic substrate over another. Most of the gullies occurred either entirely on or partially on slopewash, ravine fill, and colluvium deposits. This correlation is likely because gullies tend to occur at hillslope bases where this material tends to accumulate. Short-term surface erosion likely followed development. Long-term surface erosion occurred on landslide deposits, tracks, scars, gullies, and along the peripheral of roads, trails, and impervious surfaces of urban development.

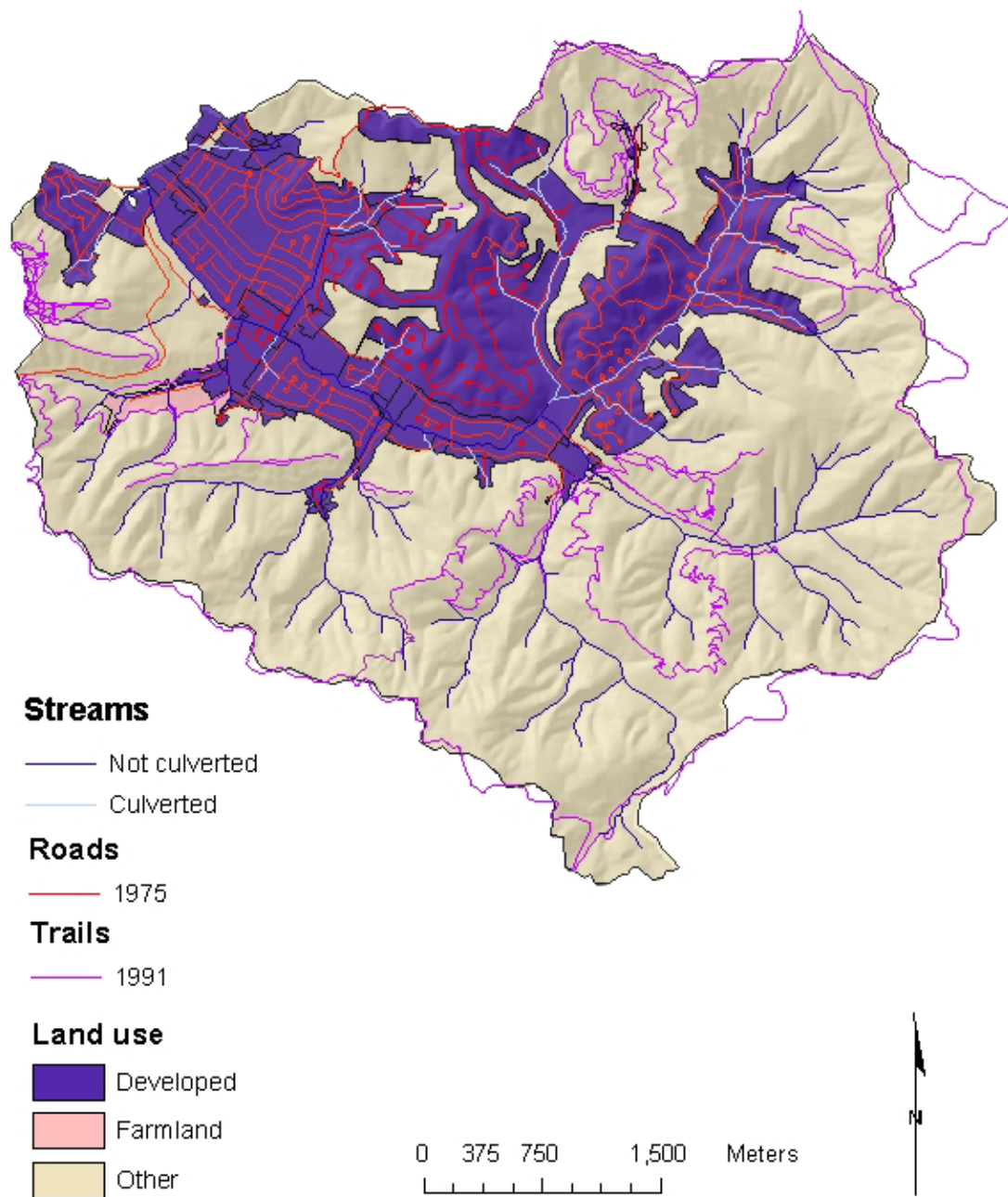


Figure 37e: Land use in 1997 with existing roads and trails.

5.1.3 Effective Drainage

The effective drainage, or total above-ground “channels” precipitation takes to drain a landscape (Montgomery 1994), was calculated for the study area in SPCW. These channels include the stream network, trails, roads, and concrete drainage channels on terraced hillslopes. Effective drainage is important to sediment production because areas with a larger total length of channels acting as drainages are more susceptible to concentrated flow and hence, erosion. Impervious surfaces especially along the peripheral of paved areas, such as parking lots, also contribute to the total effective drainage but were not included in this assessment. The total sum of these routes per subwatershed is displayed below (Table 7 and Figure 38) while a breakdown of the more detailed findings can be found in Appendix D. Collectively the hillslopes of SPCW contain 165,702 m of effective drainage.

Effective drainage ranges from the lowest of 410 m in the unnamed 4 subwatershed up to 68,080 m in the North subwatershed. The unnamed subwatersheds are the smallest in area and generally have the least development and drainage due to the severity of slope with no established valley floors like those of the

Subwatershed	m	% of total lengths
North	68,080	41.1%
Middle	19,635	11.8%
Middle/South	1,514	0.9%
South	16,735	10.1%
Sanchez	17,610	10.6%
Shamrock	15,032	9.1%
Crespi	6,277	3.8%
Pedro Point I	7,116	4.3%
Pedro Point II	5,593	3.4%
unnamed 1	565	0.3%
unnamed 2	670	0.4%
unnamed 3	721	0.4%
unnamed 4	410	0.2%
unnamed 5	5,744	3.5%
Total effective drainage (m)	165,702	
Total effective drainage (km)	165.7	

Table 7: Total sum of all streams, roads, trails, and drainage channels per subwatershed.

larger tributaries. The North subwatershed is the largest and most developed with a large portion of the area covered by impervious surfaces from roads, driveways, and large parking lots near schools and shopping centers. Lower slopes within the North subwatershed are therefore highly susceptible to surface erosion where concentrated flow drains across barren or slightly vegetated landscapes, especially channel banks with steep slopes. Landslides triggered by trails, some of which are used as roads by the land managers of the Picardo Ranch, on the upper hillslopes are common. The least developed of the major subwatersheds, the Middle, South, and Sanchez subwatersheds, have moderate effective drainage mainly from streams and trails.

The effective drainage density, the effective drainage divided by the total drainage area, was calculated per subwatershed (Table 8 & Figure 39). The effective drainage density offers a more complete perspective than the effective drainage alone as it considers the total area over which the effective drainage acts. Again, a more detailed list of the factors composing the total effective drainage density is displayed in Appendix D.

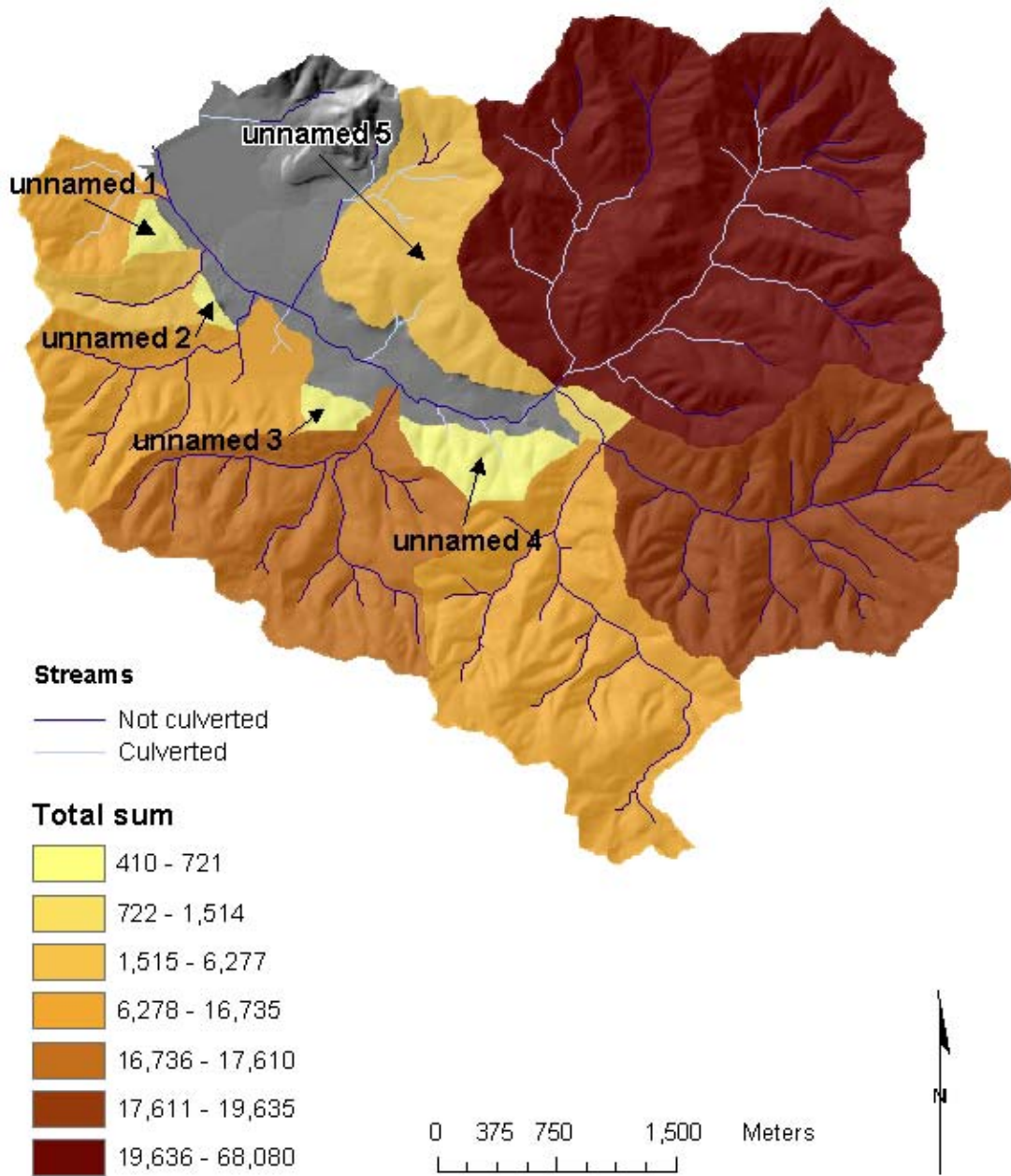


Figure 38: Total sum of the stream network, roads, trails, and urban drainage channels per subwatershed displayed in meters.

Subwatershed	Total drainage density (km/km ²)
North	11.1
Middle	6.0
Middle/South	15.1
South	5.9
Sanchez	7.5
Shamrock	10.4
Crespi	9.7
Pedro Point I	16.8
Pedro Point II	15.5
unnamed 1	7.1
unnamed 2	16.8
unnamed 3	8.0
unnamed 4	1.2
unnamed 5	9.1
Average	10.0

Table 8: Total effective drainage density per subwatershed.

The effective drainage density ranges from 1.2 km/km² in the unnamed 4 subwatershed to 16.8 km/km² in both Pedro Point I and the unnamed 2 subwatersheds. The overall average in SPCW falls at 10.0 km/km².

The smaller subwatersheds such as both Pedro Points and unnamed 2 have a higher density due to the small surface area with a large length of effective drainage. Rainfall does not infiltrate on impervious surfaces and instead concentrates and saturates adjacent land creating rapid runoff and often simultaneous erosion. During intense rainfall events, anthropogenic erosion is expected to be the highest in these small subwatersheds because the high numbers of effective channels relative to total surface area increases the speed at which sheetwash drains. While the North subwatershed has the highest effective drainage, its large surface area somewhat moderates the density, and therefore the overall impact on anthropogenic surface erosion.

Conversely, the South and Middle are large subwatersheds with a very low effective drainage density and the least developed area. As a result, sediment sources in these subwatersheds are largely a factor of natural processes such as landslides as collectively, less anthropogenic pressure is exerted.

Analysis of turbidity data collected in San Pedro Creek during three storm events over a four-day period in February 2000 found the average turbidity to be 10 times greater in the Middle and South forks than that of the North fork (Amato 2003). This implies that during this storm event, natural sediment producing processes, such as landslides and channel erosion, predominated the amount of sediment generated within these subwatersheds.

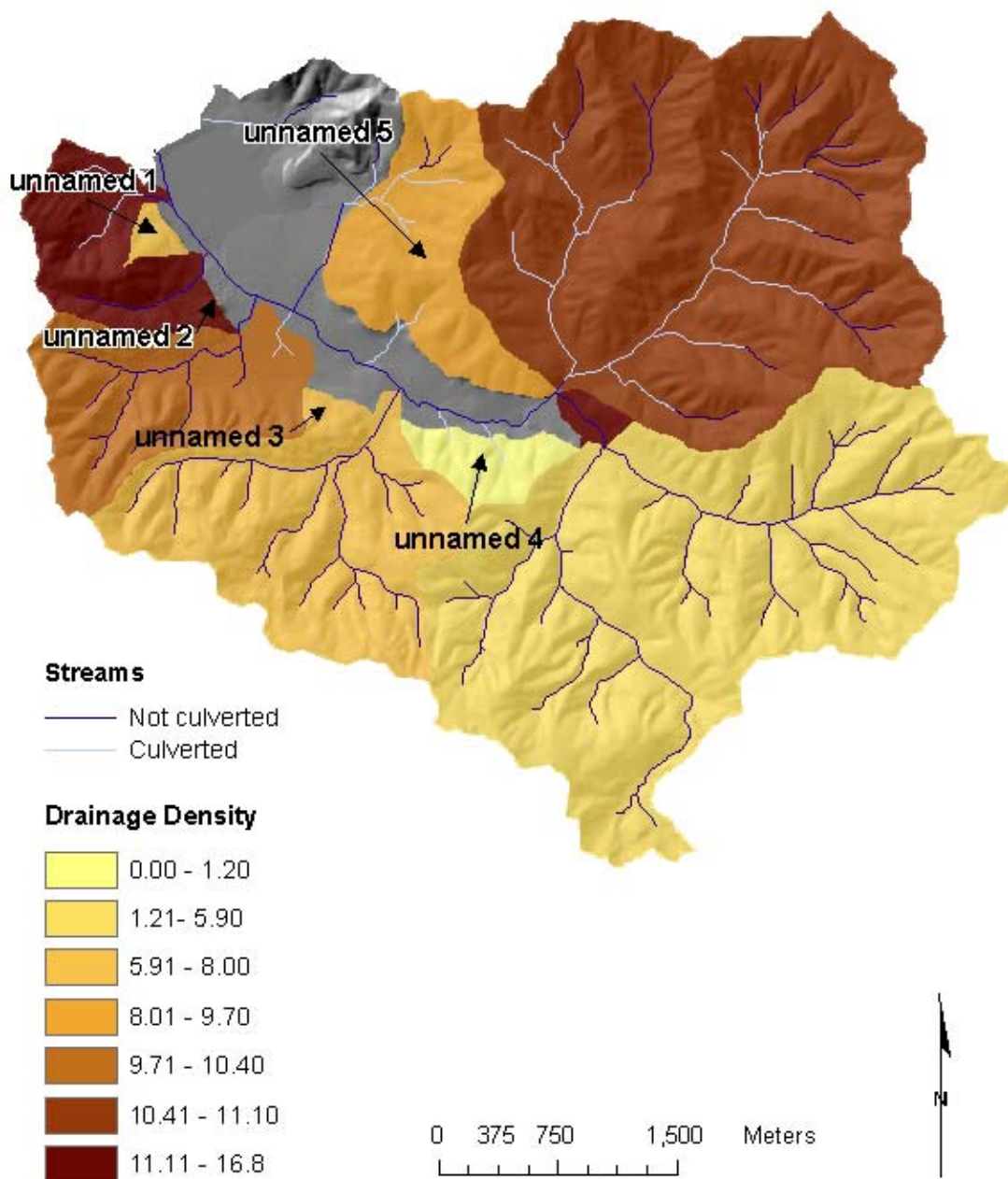


Figure 39: Effective drainage density of the individual subwatersheds displayed in km/km^2 .

5.1.4 *Perennial Flow*

The point at which perennial flow begins is important to sediment because during the rainy season, much of the sediment initially generated is from ephemeral and intermittent channels located upslope of the perennial flow point. Initial rainfalls flush this sediment from the upper channels into the stream network.

Select tributaries were surveyed in Fall 2002 to identify points where perennial flow began. A few tributaries were not included due to accessibility difficulties. The point at which flow began was found on eight tributaries with an average contributing upslope drainage area of 583,650 m². Along another eight tributaries the precise spot of perennial flow could not be determined because access was hampered by thick vegetation. Pour points were determined the farthest upstream as possible and therefore the perennial point is known to be within the contributing drainage area upslope from these locations. The average contributing area of these points is 702,838 m². Overall, these findings are consistent with the eight known perennial points and the average can be assumed to be similar to the average of the known points.

Most of the unknown points of perennial flow fall along the southern boundary of SPCW. Some of these drainages, such as 3, 6, 8, and 9 (see Table 9 and Figure 40), have little contributing area relative to the average of the known perennial points. This implies that the water table might be higher along the southern border in the Montara mountain granitics of the upper South, Middle, and Sanchez subwatersheds. Perched water tables could also be present along this southern edge of the watershed ensuring higher flow levels downslope than the remainder of the watershed and a higher initial point of perennial flow. If this is the case, the elevated levels of contributing water implies that these areas are more susceptible to landslides with higher levels of subsurface saturation, a primary cause of slope failure. However, the granitic bedrock of the far upper slopes of the South subwatershed is highly weathered and generally forms deep aquifers (Davis 2003) counter to these findings indicating a higher water table.

The point at which perennial flow begins implies that channel initiation begins somewhere upslope. Channel initiation, the transition point from overland and subsurface flow to channelized flow, may be represented by an ephemeral or intermittent channel. While the precise points of channel initiation were not found, it can be inferred to be somewhere upstream from the perennial flow points.

	Known perennial initiation areas	Perennial initiation areas upstream from this point	Predominant geology
Tributaries	km ²	Km ²	
1		1.0582	sandstone, shale, and conglomerate
2	0.6701		sandstone, shale, and conglomerate
3		0.3329	sandstone, shale, and conglomerate
4		0.6819	granite, slope wash, ravine fill, and colluvium
5	0.3381		slope wash, ravine fill, and colluvium
6		0.2394	granite
7		1.7261	granite, slope wash, ravine fill, and colluvium
8		0.4402	slope wash, ravine fill, and colluvium
9		0.3432	slope wash, ravine fill, and colluvium
10		0.8008	slope wash, ravine fill, and colluvium
11	0.5311		greenstone, slope wash, ravine fill, and colluvium
12		0.5906	greenstone, slope wash, ravine fill, and colluvium
13	0.4909		greenstone and sandstone
14	0.8035		greenstone, slope wash, ravine fill, and colluvium
15	0.5934		greenstone, slope wash, ravine fill, and colluvium
16	0.6515		sheared rock, slope wash, ravine fill, and colluvium, and artificial fill
Average area required for flow	0.6		
Average lesser area required for flow		0.7	

Table 9: Known areas of perennial flow initiation along tributary branches. Tributary numbers correspond with those displayed on Figure 38.

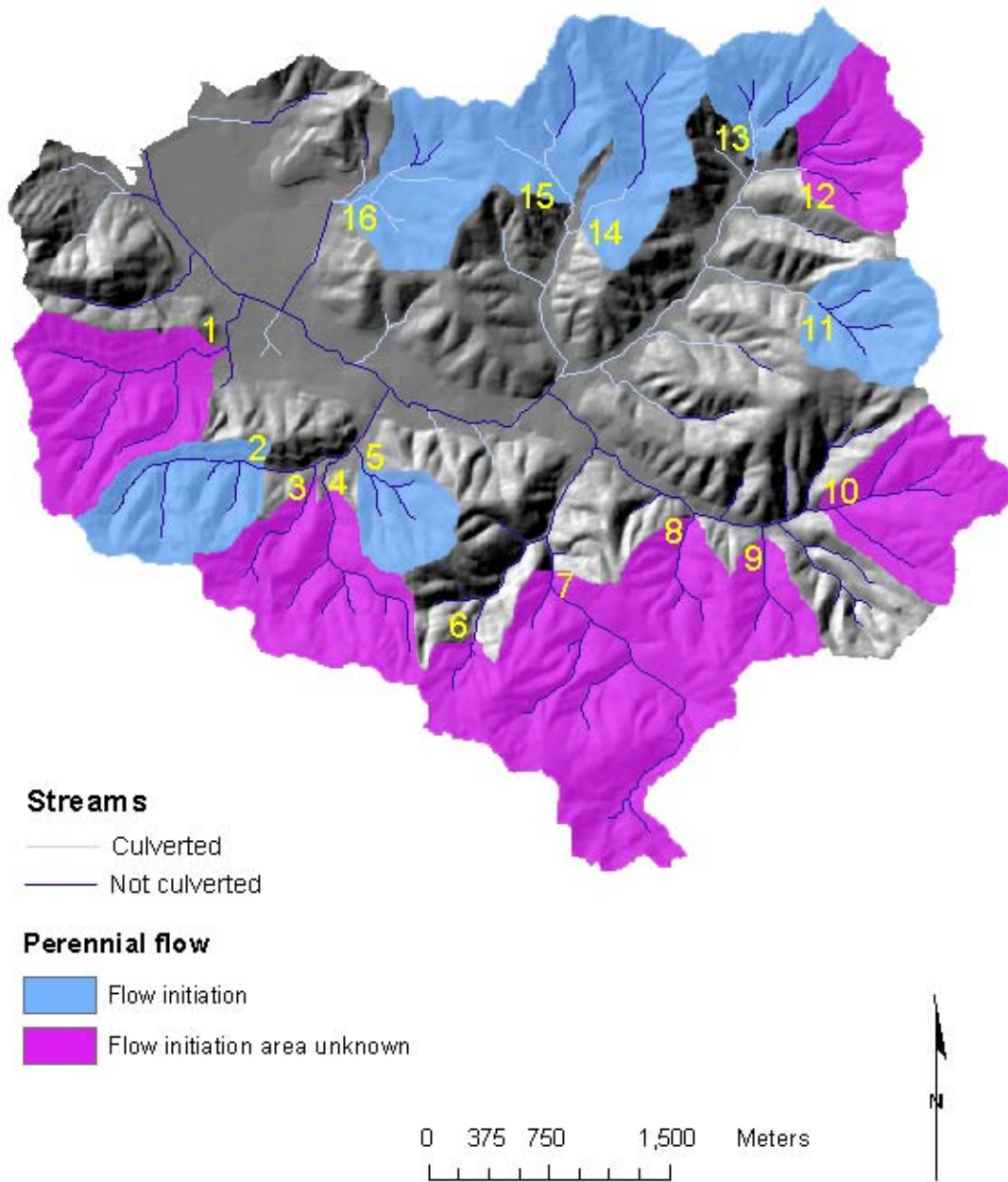


Figure 40: Sample tributaries surveyed to determine the area required to maintain perennial flow. Numbers on map correspond to Table 9.

5.1.5 SEM

The modified version of the Sediment Erosion Model (SEM) identifies areas susceptible to surface erosion based on percent slope and the k-factor, a soil property ranking the ability of sediment to be detached from soil (Section 4.3.2). The values are ranked from low to high (Figure 41). The k factor values in the soils of SPCW are moderately low and not very prone to surface erosion except where near anthropogenic influences such as trails and roads.

The model was not applied to the unnamed subwatersheds because they were not included as part of the study area in the initial assessment. Additionally, the k-factors for much of these subwatersheds were unavailable from the soil survey because of the large percentage of urbanization obscuring this property of the underlying soils. As a result many of the urban areas were not included in the SEM.

Surface erosion is highest on the upper slopes of the North and the South subwatersheds. The effectiveness of surface erosion is likely the highest in the North subwatershed along the network of trails following the ridgeline with relatively high-use. The grassland vegetation along the ridgetops is prone to piping and subsequent gullyng, which has occurred in a few locations. Hillslopes are criss-crossed with trails focusing flow and creating landslide problems with subsequent surface erosion as well. The aerial photographs indicate that the ridgetops in the South subwatershed historically had very thin vegetation with barren or sparsely vegetated soils, which have since been revegetated mainly by manzanita. The manzanita in the South subwatershed appears from field observation to have no significant vegetation understory, which would facilitate delivery of sediment to the stream network.

The relatively high water table determined from known perennial flow points along the southern boundary of SPCW likely contributes to increased levels of surface erosion higher on the hillslopes. The combination of these factors combined with the lack of trails and significant use supports natural processes as the predominant supplier of sediment from the South subwatershed.

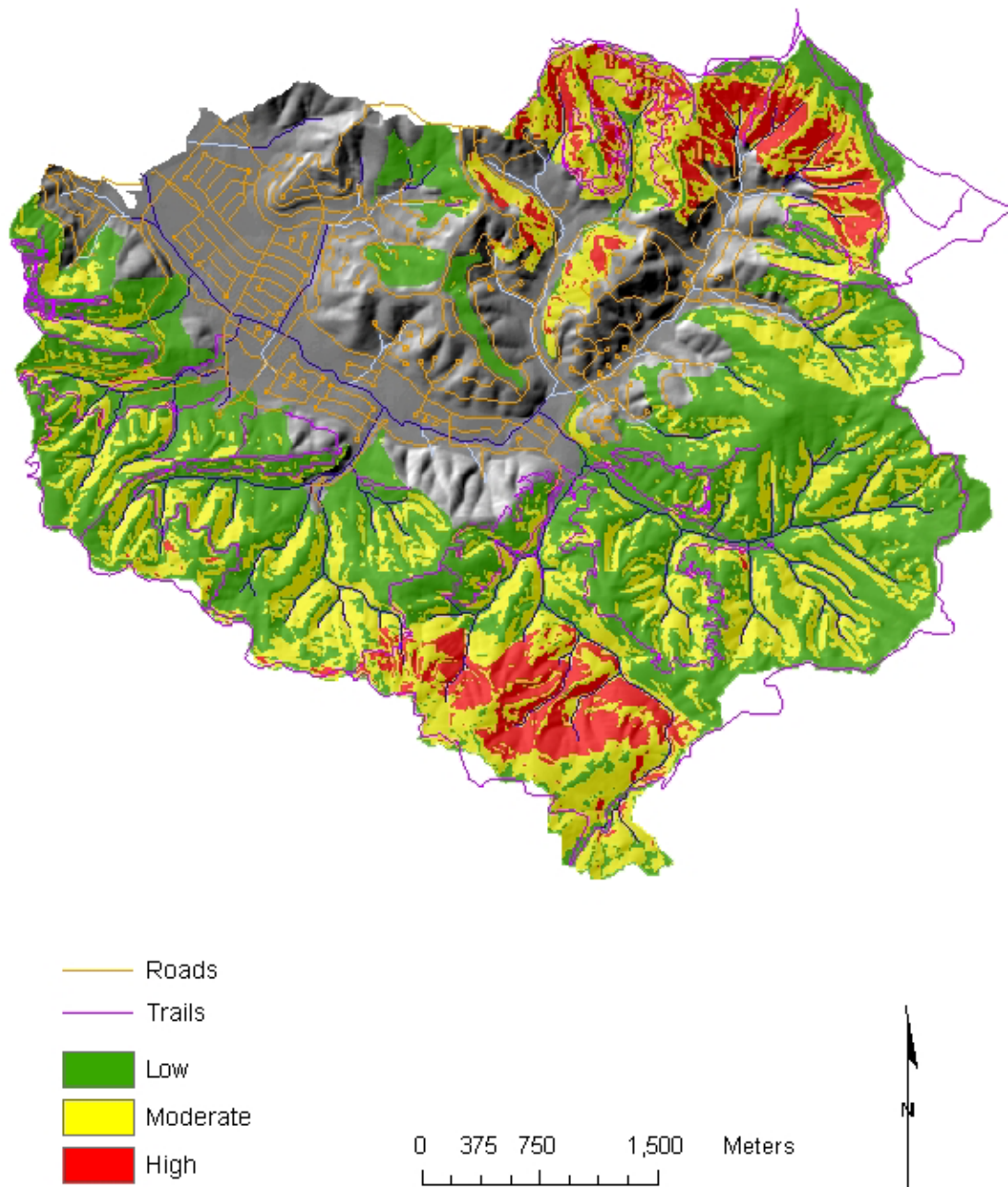


Figure 41: Sediment erosion model of SPCW showing high soil detachment in the upper watersheds of the South and North forks

5.1.6 SHALSTAB

The SHALSTAB model generated with known landslides and DEM data was run for SPCW predicting the relative slope stability under multiple rainfall scenarios (Figure 42). Using 10-meter digital elevation data, the model is considered successful if the majority of the landslides fall below the $\log(q/T)$ value of -2.8 (Dietrich *et al.* 1998). When calculated with the soil bulk density parameter at $1,700 \text{ kg m}^{-3}$, the q/T value indicated that only 31% of the mapped landslides fell within this range. This is slightly over half of the average 60% found in multiple watersheds from a validation study (Dietrich *et al.* 1998). The soil bulk density modified to $1,200 \text{ kg m}^{-3}$ and the model was run again with 48% of the slides occurring below the $\log(q/T)$ value of -2.8 and 78% occurring below the $\log(q/T)$ value of -2.5 , the generally accepted threshold for larger digital elevation data. This discrepancy of 12% between the validation study findings and the findings of the model with soil bulk density of $1,200 \text{ kg m}^{-3}$ was possibly partially the result of accuracy errors in landslide mapping from the aerial photographs.

The model found mainly the upper drainages throughout SPCW to be highly unstable, particularly in the South subwatershed. The known landslide distribution extracted from aerial photograph interpretation indicates that few landslides occurred on the steep upper slopes of the South subwatershed, contradicting the findings from SHALSTAB. This may have occurred because the actual bulk density of the Scarper-Miramar complex of the South subwatershed may differ significantly from the constant of $1,200 \text{ kg m}^{-3}$ input into the model. The hillslopes within this area are also the steepest in SPCW for which SHALSTAB may have overestimated the relative occurrence of landslides based on the soil bulk density value. Additionally, the dense vegetation may have obscured a large number of landslides from visibility on the aerial photographs so more actually exist than were documented from this research.

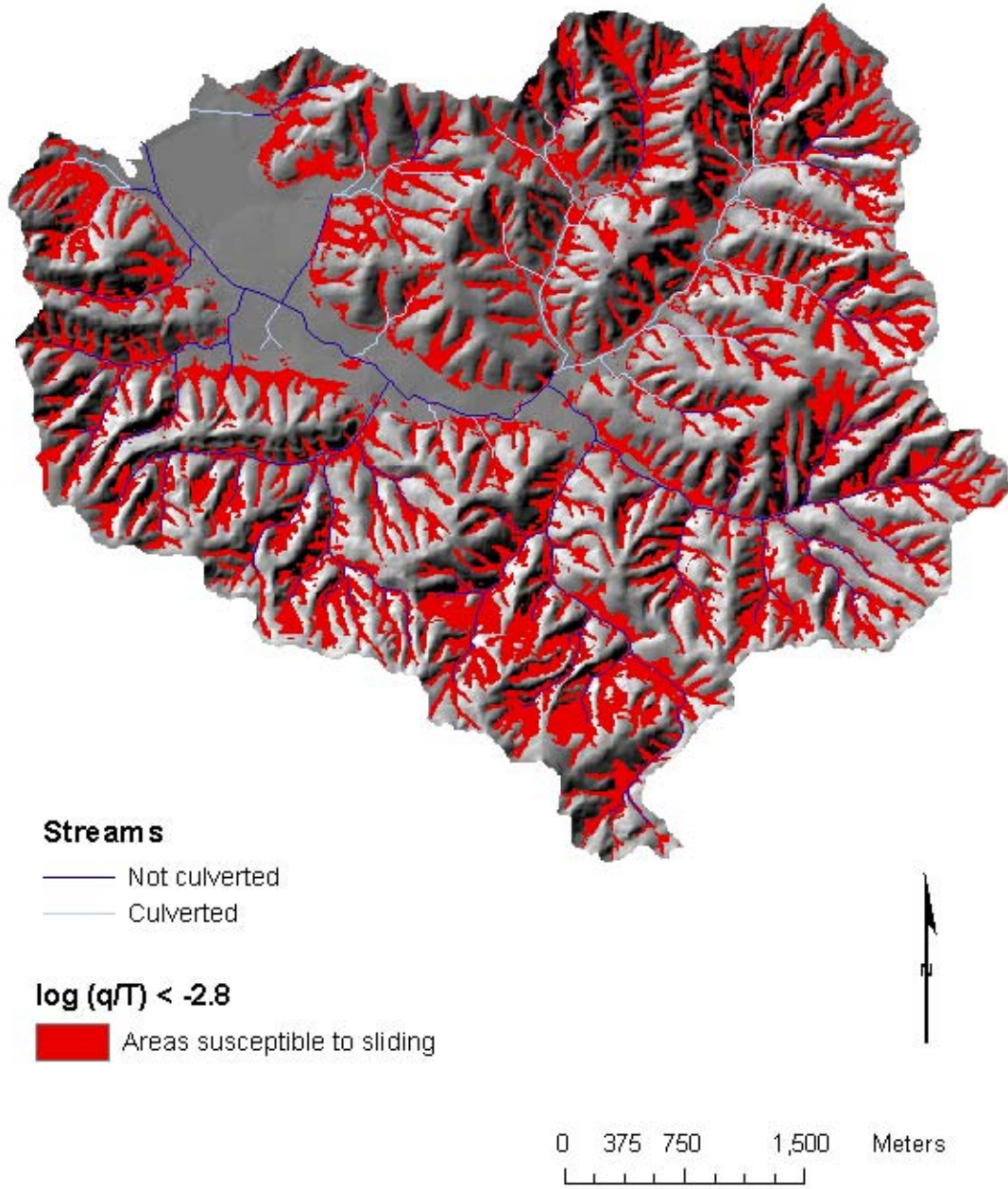


Figure 42: Relative shallow slope stability estimated from SHALSTAB where units are the ratio of effective precipitation/transmissivity (m^{-1}).

5.1.7 Connectivity

Detached soil only contributes to water quality deterioration where connectivity to the drainage network has been established. Many of the landslides that have occurred on the upper hillslopes of SPCW never reach the tributaries or do so at minute levels. Vegetation along hillslopes and especially in riparian corridors filters soil from sheetwash while it is being transported downslope. Low gradient slopes also act as settling areas to filter sediment before entering the drainage network. Connectivity buffers at multiple concentric distances from the drainage network were applied to the stream based on literature from previous studies (Riley 1998, Budd *et al.* 1987) (Figure 43). These buffers of 6.5 m, 50 m, and 100 m establish the level of sediment being delivered to the streams by the different sediment generating processes. Distance from the channels and the adjacent percent slope are combined to create a qualitative matrix ranging from moderate to very high potential for connectivity (Table 10). Clearly, the areas susceptible to the highest levels of erosion are directly adjacent to the stream network. These areas with very high connectivity are not visible on this map due to the scale but are examined in more detail in Section 5.2.

Distance from stream network (m)	Slope	
	< 40%	> 40%
6.5	High	Very High
50	Moderate	High
100	Moderate	Moderate

Table 10: Level of connectivity of possible sources to the stream network as a factor of buffer distance and percent hillslope.

The results of the SEM from Table 1 were combined with the level of connectivity from Table 10. Combining the vegetation buffer model with the SEM provides a more comprehensive assessment of connectivity at areas already prone to surface erosion (Table 11 and Figure 44).

The areas most susceptible to surface erosion are the upper North and South subwatersheds and those in close proximity to the stream. Just as with the SEM, the North subwatershed probably supplies a significant amount of sediment along trails in the areas that fall within the high to severe susceptibility levels. The South subwatershed is most prone to surface erosion along the very upper slopes, which are steep with little anthropogenic influence.

Areas of relative landslide potential generated from the SHALSTAB model can also be analyzed in conjunction with connectivity to the stream network (Figure 45). Like the SEM and connectivity, this model is only a prediction and the results of SHALSTAB are not as precise as expected. As slopes are generally unstable in drainages with relatively high delivery, the pattern of connectivity follows the areas highly susceptible to failure. Connectivity is likely increased outside of the displayed boundaries in the areas that are highly failure-prone as landslides can be mobilized for significant distances before

depositing, often in streambeds. Again, areas in the North and South subwatersheds are most susceptible to failure with the highest connectivity to the stream network. The results of the connectivity of this model are examined in more detail in the Subwatershed prioritizations section.

	Connectivity		
SEM results	<i>Moderate</i>	<i>Highb</i>	<i>Very high</i>
<i>Low</i>	Moderate	Moderately High	High
<i>Moderate</i>	Moderately High	High	Very High
<i>Highb</i>	High	Very High	Severe

Table 11: SEM model merged with connectivity values from Table 10 to determine the level of connectivity of the SEM.

Landslide and gully distribution was also analyzed by levels of connectivity, especially in relation to any landslide tracks. The general results are displayed in Figures 46a-e but the more detailed findings are laid out in Section 5.2. Overall, 65% of the landslides and 74% of the gullies identified on the aerial photographs are found to be connected to the stream network using this method. The amount delivered to the stream network was calculated as a factor of the connectivity buffer within which a landslide scar or track falls while also paying attention to the influence of local land use and vegetation. Delivery was calculated as a percentage of the total volume derived from the landslide scar. This percentage was determined by the slope and distance of the deposit from the stream network as is displayed in Table 10. A landslide following within the very high category, with a 6.5 m buffer and > 40% slope, was assumed to have 75% delivery while a landslide within the moderate category with a 100 m buffer and < 40% slope was determined to only have 25% delivery.

Surface area was calculated from landslide scars and gullies traced from the aerial photographs. The average landslide scar is 120 m² while the average gully is 969 m². Landslides scars and tracks were traced separately with the average track extending 45 m in length downslope from a landslide. Gullies that were obvious on aerial photographs are fairly large. Many of the smaller gullies were concealed by vegetation or were just too small to accurately be identified by air photos. Average landslide scar depths were estimated from literature. The average landslide scar depth between the deepest and shallowest depths for four large landslides in SPCW was 1.9 m (Howard *et al.* 1988). As the landslides surveyed in that report were large, and Wentworth (1986) found the depths of slide scars in SPCW to range from 1-3 m, a conservative depth of 1.2 m was used to estimate the average depth of a landslide scar to accommodate for smaller landslides.

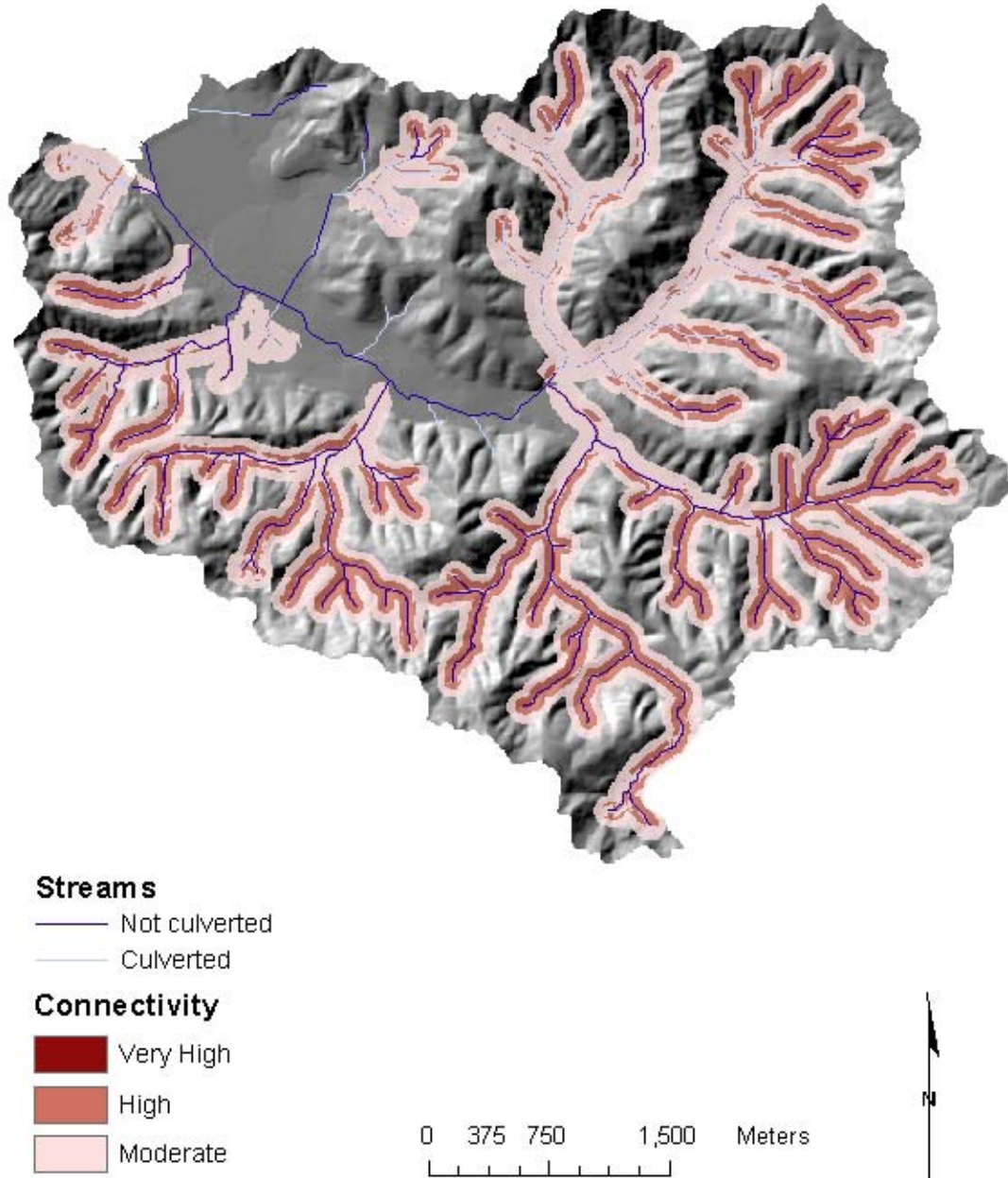


Figure 43: Connectivity at concentric distances in meters from the stream network.

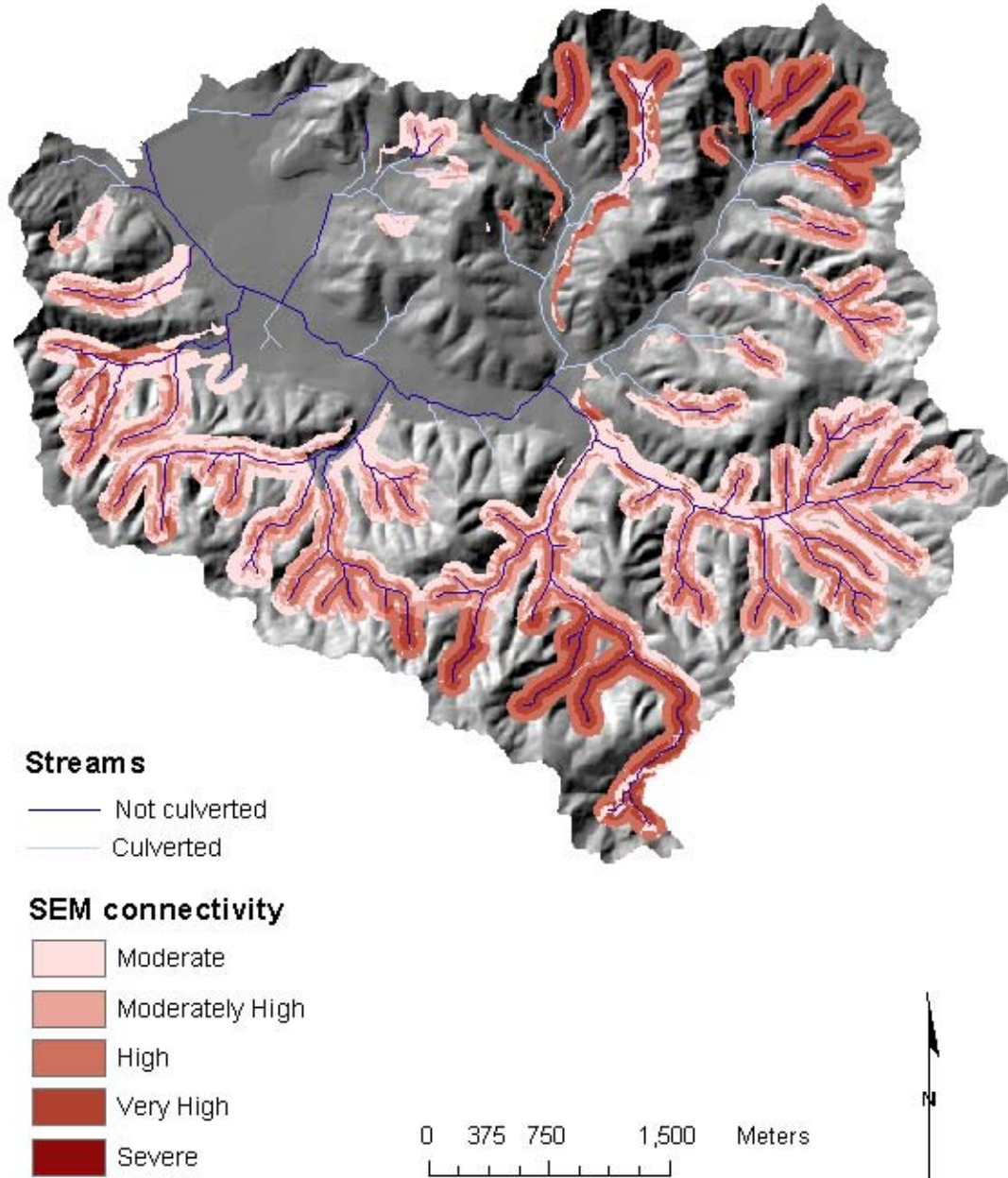


Figure 44: Results of Table 11 displaying areas significantly susceptible to surface erosion with direct potential connectivity to the drainage network.

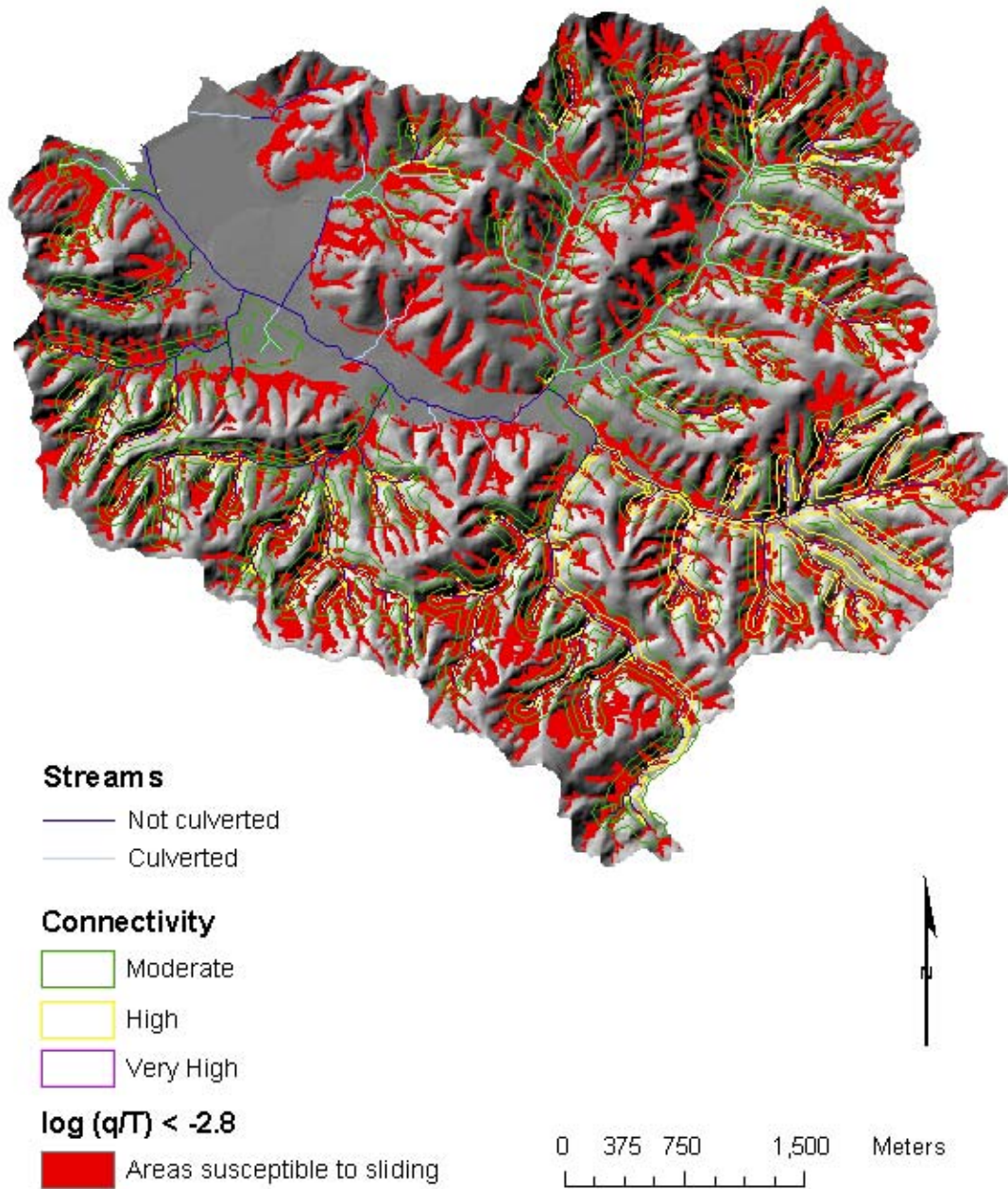


Figure 45: SHALSTAB displayed with results of Table 10 displaying relative landslide potential connectivity.

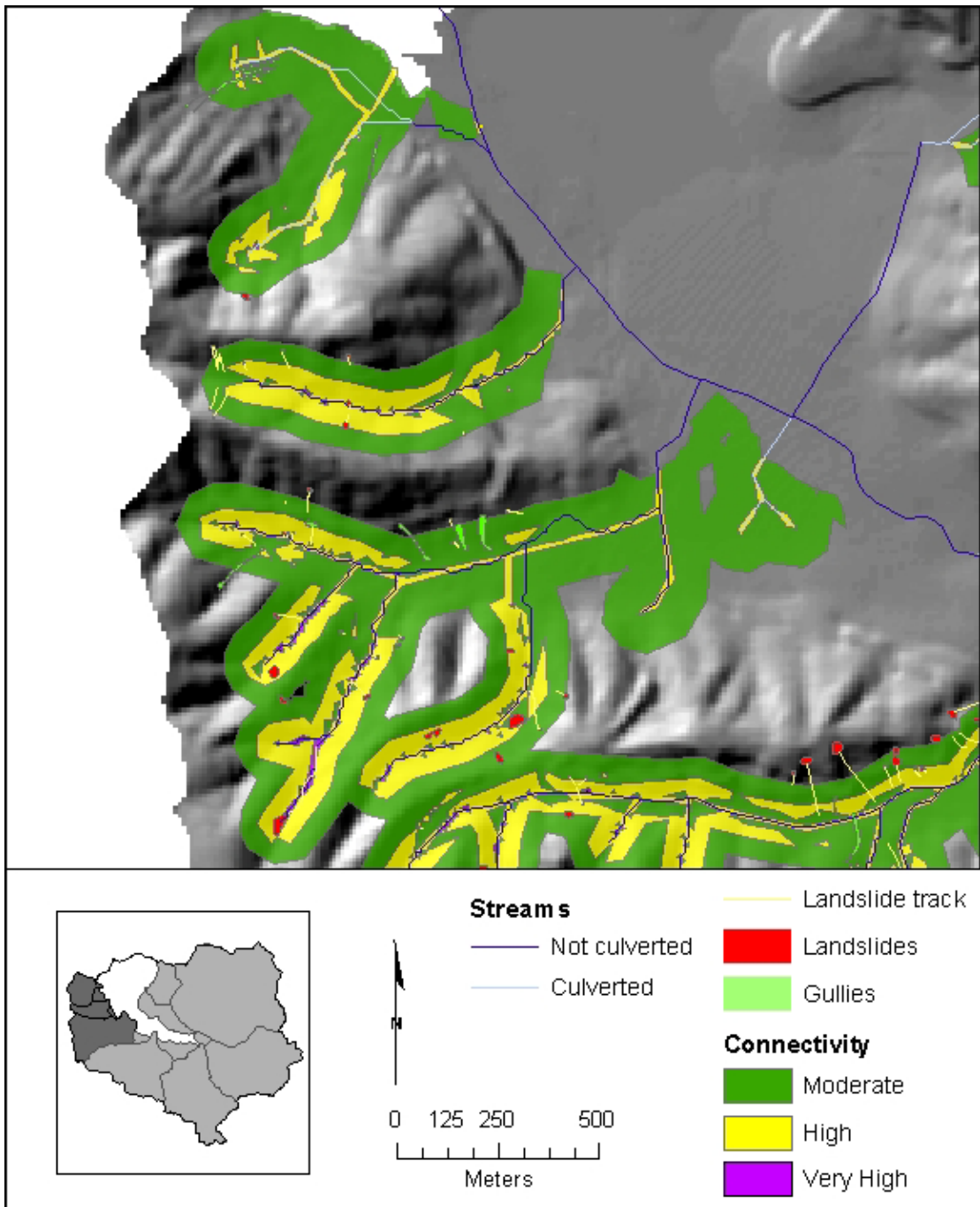


Figure 46a: Landslide and gully connectivity to the stream network in Crespi and Pedro Point I and II subwatersheds.

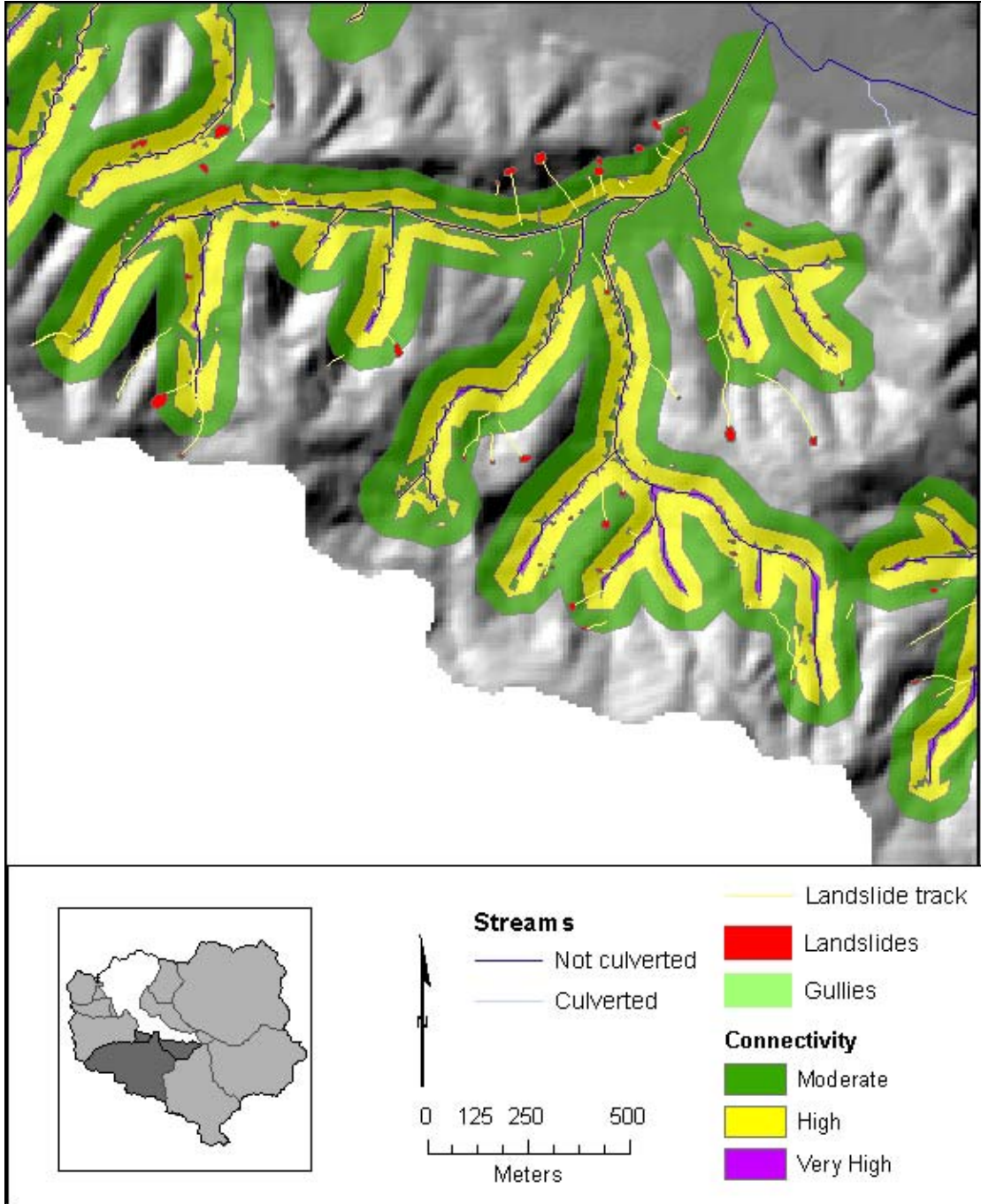


Figure 46b: Landslide and gully connectivity to the stream network in Sanchez subwatershed.

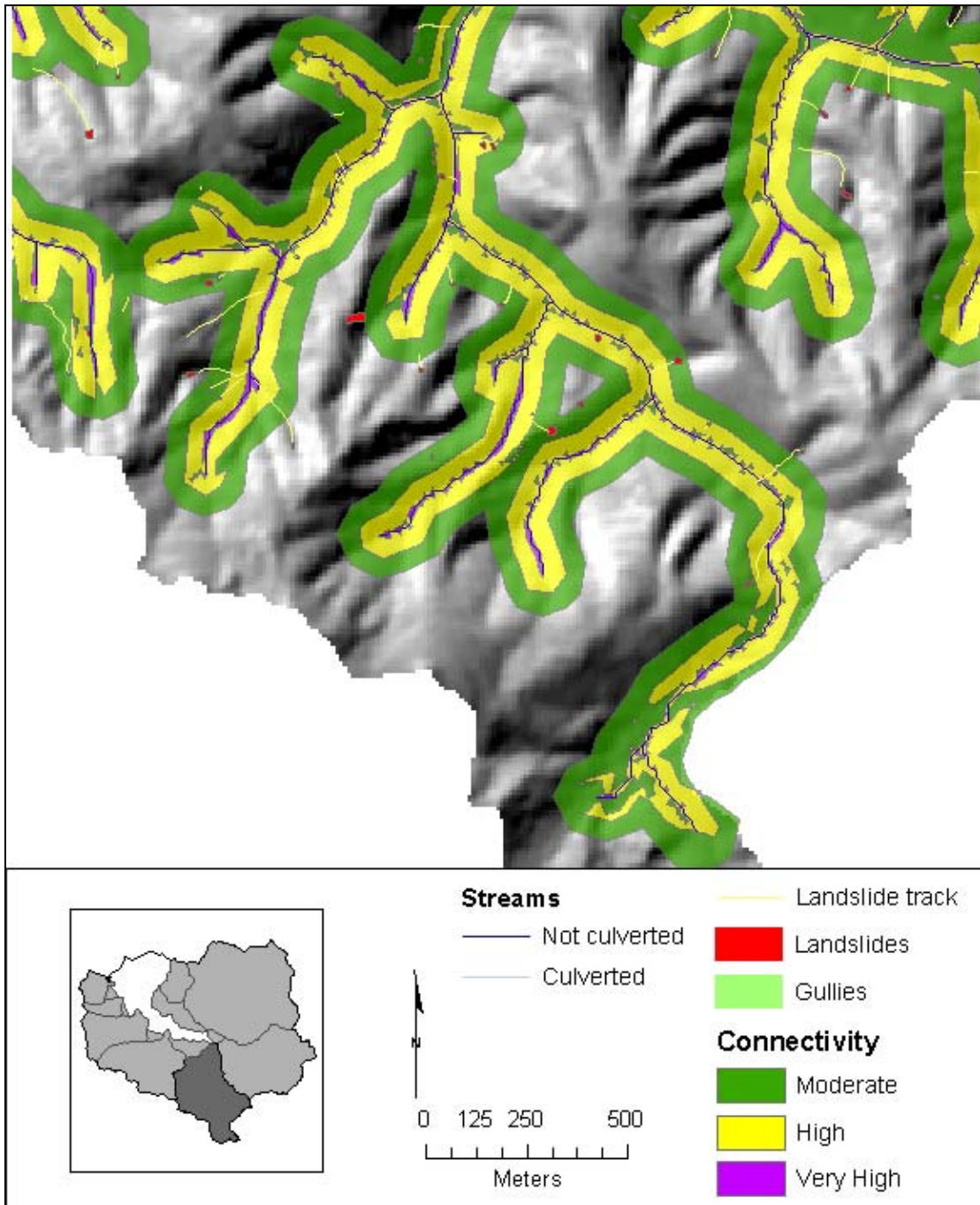


Figure 46c: Landslide and gully connectivity to the stream network in South subwatershed.

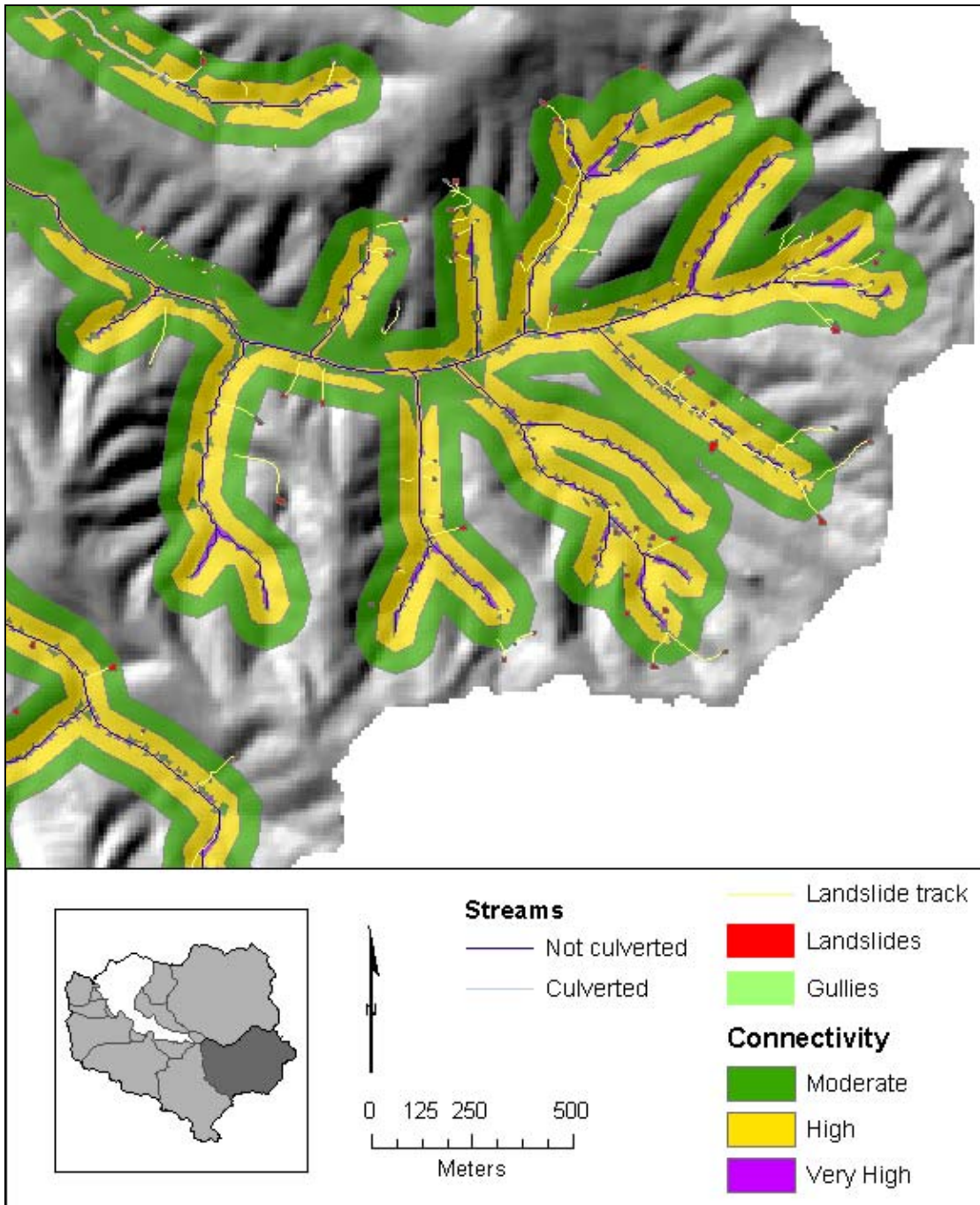


Figure 46d: Landslide and gully connectivity to the stream network in Middle subwatershed.

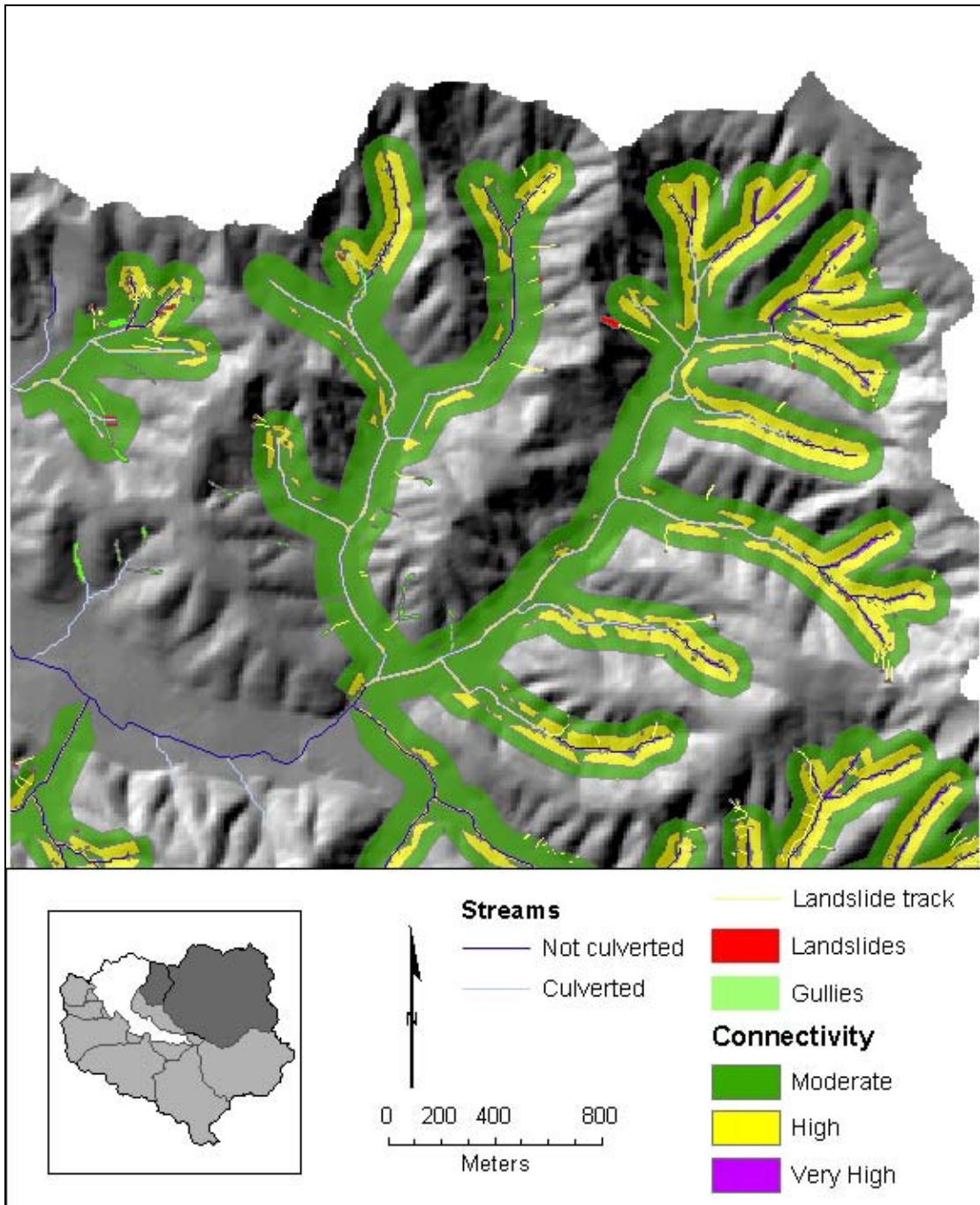


Figure 46e: Landslide and gully connectivity to the stream network in North and Crespi subwatersheds.

Volume estimates were then calculated as scar surface areas were obtained from aerial photographs. Gully and surface erosion volumes were evaluated on a site-specific basis only where estimated in the field. The depths of gullies observed in the field varied significantly so an average was not extrapolated to all gullies. Additionally, most gullies found on the aerial photographs no longer exist as they have since been replaced by urban development. At the average surface area of 120 m^2 and the average depth of 1.2 m, the average landslide volume is calculated to be 144 m^3 . The supporting literature provided adequate data to extrapolate the average depth to landslides across the entire landscape providing relative volume estimates. The landslide volumes derived from these calculations are crude. However, attaining precise values of sediment generated from all landslides was not feasible for this study. However, the estimates provided are useful to identify the relative sources of erosion while providing approximate sediment values.

Collectively these values and models are used to identify potential past, present, and future source areas across the landscape of SPCW. Section 5.2, Subwatershed Prioritizations, is a more complete breakdown of these values qualitatively revealing source areas with quantitative values where available. This section mainly focuses on anthropogenic sources as the findings were collected from the road and trail assessment.

5.2 Subwatershed prioritizations

This section breaks down the major site-specific sources within the individual subwatersheds with qualitative and if possible quantitative values derived from the techniques outlined in Section 5.1. The findings from the techniques used are analyzed individually and in conjunction on a much larger scale to find existing problem areas. A management prioritization is then designated for these specific sites for each subwatershed and finally in Section 6.0 sediment mitigation suggestions are offered.

While land use was covered in detail under Section 5.1, Table 12 shows the area and percentage of each type of land use within each subwatershed. This is effective to help determine the level of anthropogenic influence per subwatershed. The land use was not calculated for the unnamed subwatersheds. Nearly all of the first four unnamed subwatersheds is “other” land use and the fifth is predominantly developed.

Subwatersheds	Developed		Farmland/Rangeland		Other		Total ha
	ha	% of total	ha	% of total	ha	% of total	
North	232.2	37.8%	1.9	0.3%	379.9	61.9%	614
Middle	0.8	0.3%	0.0	0.0%	327.2	99.7%	329
Middle/South	8.3	79.7%	0.0	0.0%	2.1	20.3%	10
South	2.0	0.7%	0.0	0.0%	280.0	99.3%	284
Sanchez	8.9	3.8%	0.0	0.0%	223.7	96.2%	235
Shamrock	23.2	16.1%	11.6	8.0%	108.9	75.8%	145
Crespi	36.8	56.9%	0.0	0.0%	27.9	43.1%	65
Pedro Point I	24.8	49.5%	0.0	0.0%	25.3	50.5%	51
Pedro Point II	0.0	0.0%	0.0	0.0%	36.2	100.0%	36

Table 12: Current land use by subwatershed.

The number and locations of landslides and gullies are identified as found on aerial photographs (Table 13). Quantitative values were derived for select landslides based on surface area derived from air photos and a depth estimate based on existing literature and field measurements. Only existing gullies with predicted connectivity were considered as many have been replaced by urban development. All old and new landslides with connectivity were considered in the volume estimates.

Subwatershed	Total landslides	Landslides with connectivity	Landslides with high & very high connectivity	Total gullies	Gullies with connectivity
North	206	104	62	11	11
Middle	148	111	69	3	3
Middle/South	0	0	0	0	0
South	59	39	26	0	0
Sanchez	78	68	47	2	2
Shamrock	34	25	12	7	5
Crespi	21	21	10	5	5
Pedro Point I	10	1	0	7	4
Pedro Point II	16	11	5	1	0
Unnamed	33	1	0	13	5

Table 13: Total landslide and gully inventory from those identified on aerial photographs between 1941 and 1997.

The inventory considers past landslides and gullies. Table 14 further analyzes the number of landslides and gullies per subwatershed distinguishing those with predicted connectivity. Connectivity was determined based on distance and slope gradient of an identified potential source to the nearest tributary. Many of these lower order tributaries are intermittent or even ephemeral restricting the period of sediment delivery to the rainy season. Volumes of delivery were calculated as a percentage of the total based on the level of predicted connectivity as explained in Section 4.0.

Subwatershed	Volume of sediment with predicted connectivity (m ³)			Total
	25%	50%	75%	
North	1,580	2,230	730	4,540
Middle	1,290	3,240	1,420	5,950
Middle/South	0	0	0	0
South	570	1,460	570	2,600
Sanchez	1,180	2,240	2,560	5,980
Shamrock	300	1,440	940	2,680
Crespi	450	1,580	0	2,030
Pedro Point I	0	70	0	70
Pedro Point II	50	230	0	280
All unnamed	110	0	0	110

Table 14: Total landslide volume delivery estimates based on levels of predicted connectivity of landslide scars to the stream network.

The following sections are a detailed assessment of each subwatershed where site-specific sediment generating sources are identified. Surface erosion was described where it was obviously occurring from visual observations or the supporting data, such as obvious anthropogenic influences (trails, roads, culverts) or the SEM, suggested the intensity of occurrence. Quantitative estimates were made for severely eroded locations. Where there was no field data collected but the GIS data indicated potential sources, speculations of potential sources were made based on known sediment generating processes and the influential external factors. While both natural and anthropogenic sources were identified, this study mainly prioritizes only anthropogenic sources for management. Sediment production can be mitigated from human-influenced sources while little can be done to reduce naturally generated sediment without implementing large and/or extensive engineering structures like hillslope terraces. These terraces have proven not to be entirely effective as landslides triggered along the peripheries were found in the North subwatershed. Landslides and gullies with predicted connectivity are displayed on the maps associated with each subwatershed. Most of the gullies do not still exist but were still shown to display past sources. The values from Tables 12, 13, and 14 are integrated throughout the text in the following sections.

5.2.1 North subwatershed

The North subwatershed is the largest and one of the most urbanized with development extending up and over many of the lower hillslopes. Surface erosion is significant in the upper slopes where the Candlestick-Kron-Buriburi complex of soils is highly susceptible to detachment and a significant network of highly eroded trails exists. Landslides are evident throughout the upper slopes often near this trail network. This anthropogenic influence has increased the effectiveness of precipitation in generating sediment from surface erosion and concentrating flow to generate landslides. Most former gullies near the bases of the lower slopes have been replaced by the impervious surfaces of urban development. The effective drainage density, including streams, roads, trails, and urban drainage ditches on hillslopes of the North subwatershed is relatively high at 11.1 km/km².

Predicted connectivity within 100 m of the stream network has been predicted for 104 or 50% of the total 206 landslides identified in the upper slopes of the subwatershed. Of the total landslides, 49 delivered an approximate 2,230 m³ within the very high connectivity class and 10 with high connectivity delivered an estimated 730 m³. The remaining 45 slides delivered roughly 1,580 m³ of sediment. While landslides occur on most geologic substrates, many in the North subwatershed occur on slope wash, ravine fill, and colluvium and along the northeastern and eastern hillslopes that are the most susceptible to failure.

Predicted connectivity is complicated in the North subwatershed because most of the tributaries have been culverted even though the map displays the relatively accurate existing route of the culverted tributaries. However, nearly all of the identified landslides with high connectivity occurred on the upper hillslopes before the flow is culverted. For the few slides that don't connect directly with the channel, sediment is likely mobilized along roads and drained to the culverted network.

Only one major gully was found to still exist in the North subwatershed (Line 20 on Figure 47). It occurs on a hillslope within range of the nearest drainage and has established moderate connectivity. The gully empties to the backyard of a residence along a major street, Terra Nova Blvd. Vegetation in the yard likely filters most of the sediment and the nearby road probably captures the remainder, facilitating delivery to the stream network.

The hillslopes forming the northern boundary of the subwatershed are highly susceptible to surface erosion. The northeastern portion of these hillslopes is mostly free of trails within the range of predicted connectivity to the tributaries. Trails in the northwestern hillslopes near Picardo Ranch however are abundant over these highly erodible soils. Surface erosion and landslides occur downslope in multiple places from this trail network in the upper subwatershed (Points 1, 2, 3, 11, & 12 on Figure 47).

Select sections of trails are highly prone to surface erosion from readily detached soils and have established high connectivity with the stream network (Lines 16 – 19 on Figure 47; Figure 48). Many additional significant erosion sites along the upper hillslopes don't appear to have yet established connectivity but are likely to in the future. This includes the trails along the upper hillslopes from which small gullies have formed and appear to be routed downslope (Lines 14 & 15 and Points 13 on Figure 47; Figure 52).

Several large landslides occurring near the urban fringe displayed the need for slope stability as development in the valley expanded. As a result terraced channel drainages that were intended to stabilize landslide prone hillslopes actually triggered a few landslides adjacent to the channels (Points 4 & 6 and Line 7 on Figure 47) and an additional slide that appears to be the result of the terraced channels (Point 8 on Figure 47).

Surface erosion along trails upslope from these terraces is another contributor of sediment. The upper drainage ditch receives sediment from transport of loose soil, which is then culverted and delivered to the stream network (Line 5 on Figure 47; Figure 50). Rilling along the barren soils upslope of the ditch produces loose sediment contributing to the total amount delivered (Point 9 on Figure 47; Figure 51). The production of sediment is possible along any terraced hillslope with a somewhat active trail upslope (Point 10 on Figure 47).

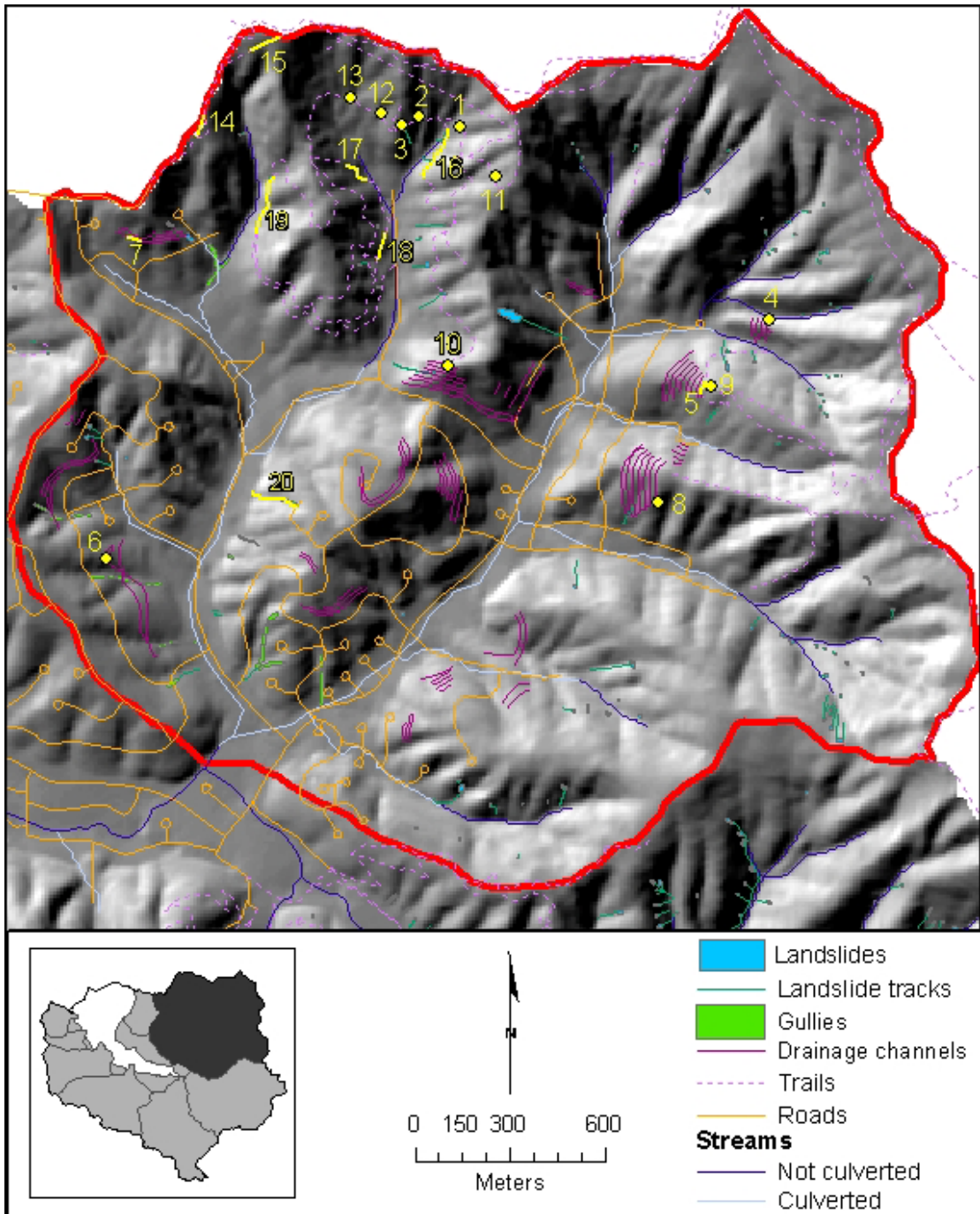


Figure 47: North subwatershed outlined in red indicating significant sediment sources in yellow. Also showing landslides and gullies with predicted connectivity.



Figure 48: Trail network along the upper slopes of the Picardo Ranch. Landslide scars are visible downslope from road at the arrows and in many other places along the trails (Points 1, 2, 3, 11, 12, & 13). Surface erosion is also significant on many of these trails (Lines 16 – 19 on Figure 47).



Figure 49: Landslide deposit downslope from trail on Picardo Ranch subjected to surface erosion (Point 3 on Figure 47).



Figure 50: Trail eroding into drainage culvert of terraced hillslopes (Line 5 on Figure 47).



Figure 51: Rilling upslope of trail on terraced hillslope contributing to the sediment delivered to the drainage ditch in Figure 50 (Point 9 on Figure 47).



Figure 52: Trail channeling flow and creating a moderate gully draining toward the North Fork (Line 15 on Figure 47).

5.2.2 *Middle subwatershed*

The Middle subwatershed is one of the largest yet least developed. Contrary to the North subwatershed, a minute level of development exists as San Mateo County Park facilities near the confluence of the Middle and South Forks. The remainder of the subwatershed is currently in a relatively natural state subjected to past farming and grazing practices.

There are significant lengths of effective drainages within the subwatershed. Most are trails on the valley floor connected to the upper hillslopes and the many lower order tributaries draining to the Middle Fork. Due to the large size of the subwatershed, the overall effective drainage density is relatively low at 6.0 km/km². However the trails drainage density have an effect. For instance, drainage density along the Hazelnut Trail has created interbasin transfer from the Middle Fork to the South Fork (Line 14 on Figure 53; Figure 58). Situations like this increase the effect of the drainage density. Many trails act as drainages that are extremely effective in generating sediment.

Surface erosion is most influential along these trails and gullies downslope, as generally the soils are not inherently easily detached throughout the subwatershed (Points 12 & 13 on Figure 53). Deep incision occurs along portions of the upper Valley View Trail and is routed further downslope generating past landslide and current gullying.

Most landslides are independent of obvious anthropogenic influences. Notable exceptions include those downslope of the trails north of the Pilarcitos fault, which the Middle Fork loosely follows. The past farming and possibly grazing practices along these slopes have created a compacted surface concentrating flow to the smaller drainages with slope wash, ravine fill, and colluvium substrate. This substrate is inherently prone to gullying compounding the effectiveness of surface erosion creating and propagating gullies.

Several landslides occurred upslope of the lower portion of the Hazelnut Trail crossing the trail in several places (Points 9, 10, & 11 on Figure 53). The colluvium deposited by these slides is in very close proximity to the stream and is likely to be a source of sediment. Hazelnut Trail may be focusing flow into these drainages creating incision further downslope. Further up the trail deep incision is occurring in colluvium along an ephemeral drainage that slid both in 1941 and 1983 (Point 8 on Figure 53; Figure 55).

Connectivity has been predicted for 75% or 111 of the total landslides occurring in the Middle subwatershed. Since 1941, a total of 14 slides with very high connectivity delivered 1,420 m³ while 55 slides with high connectivity delivered 3,240 m³ of material. The remaining 42 slides with moderate connectivity delivered 1,290 m³ of sediment. The high amount of sediment delivery relative to the North subwatershed has been supported by turbidity data collected by Amato (2003) that found turbidity

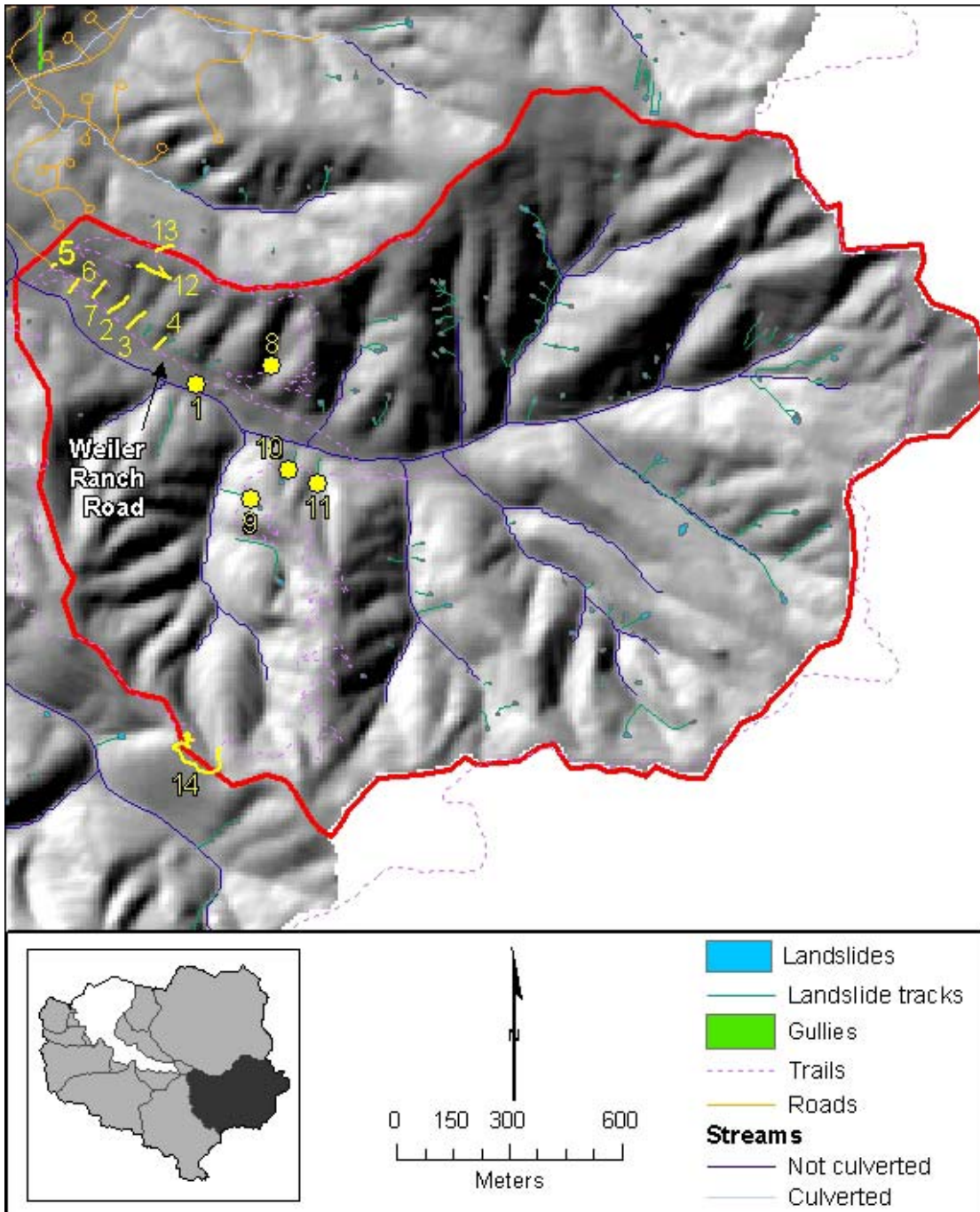


Figure 53: Middle subwatershed outlined in red indicating significant sediment sources in yellow. Also showing landslides and gullies with predicted connectivity.

to be ten times higher in the combined Middle and South Forks during three sequential storm events. Although relatively high, the estimates of the volume of sediment delivered to the stream network from landslides are likely underestimates for the Middle subwatershed because of the increased connectivity that the trail network provides. The landslide distribution pattern generally corresponds with the relative slope stability model with the highest susceptibility along the lower order drainages of the upper slopes.

Six gullies currently exist in the Middle subwatershed along the south facing hillslope north of Weiler Ranch Road. All gullies are within range of predicted connectivity to the Middle Fork but do not likely deliver much sediment across the long strip of very low gradient, non-native grasses near the base. This grassy area actively works to filter sediment while park management practices concurrently also minimize the amount of sediment delivered to the creek. A few of the gullies are culverted under the trail to this strip of land (Lines 4 & 6 on Figure 53; Figures 56 & 57). The gully along Line 4 incises through a landslide deposit and has removed an estimated 50 m³ of the material deposited by the landslide. Some of the flow is delivered to the culvert while a portion is diverted along the drainage ditch as is implied by the incision around the culverts.

Most sediment generated from these ephemeral drainages is intercepted before reaching this strip of non-native grass. Much of the flow is diverted along a drainage ditch paralleling the Valley View Trail flowing on a low gradient downslope toward the main channel (Lines 2, 3, 5 & 7 on Figure 53). While most sediment from the hillslope does not likely connect to the Middle Fork, it probably enters the stream from the culverts in the Middle/South subwatershed.

A series of slumps were found between Weiler Ranch Road and the Middle Fork (Point 1 on Figure 53; Figure 54). Two barren scars have an estimated surface area of 20 m² and total deposits of 60 m³. This upper bank of this terrace has slumped roughly 3 m depth from its previous position 10 years ago (Heisinger 2003). A third adjacent slump was significantly vegetated but was likely a previous source of significant sediment. Delivery of sediment from this source is nearly 100% because of the proximity of less than 3 meters from the base of the deposit to the stream.



Figure 54: Slump on terrace between Weiler Ranch Road and the Middle Fork (Point 1 on Figure 53).



Figure 55: Deeply incised drainage in colluvium with repeat history of landslides (Point 8 on Figure 53).

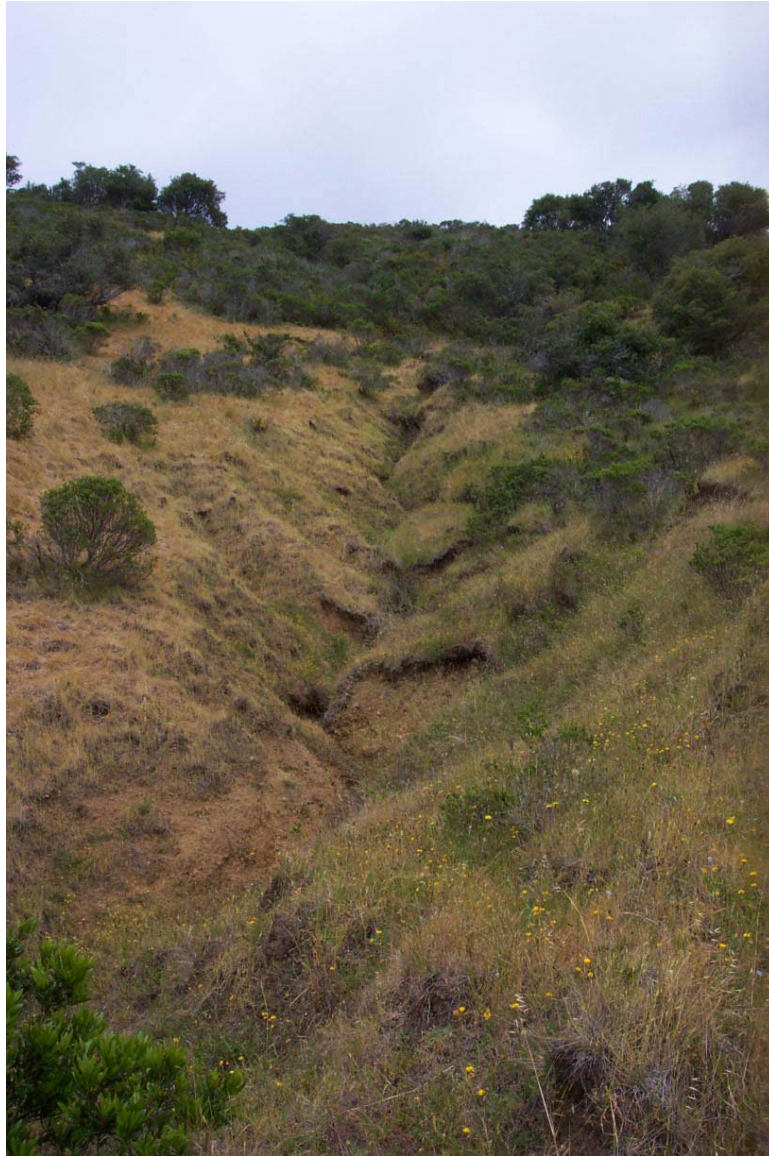


Figure 56: Gully incising through landslide deposit along Weiler Ranch Road (Line 4 on Figure 53).



Figure 57: Incision at culvert from uphill ephemeral drainages (Point 6 on Figure 53).

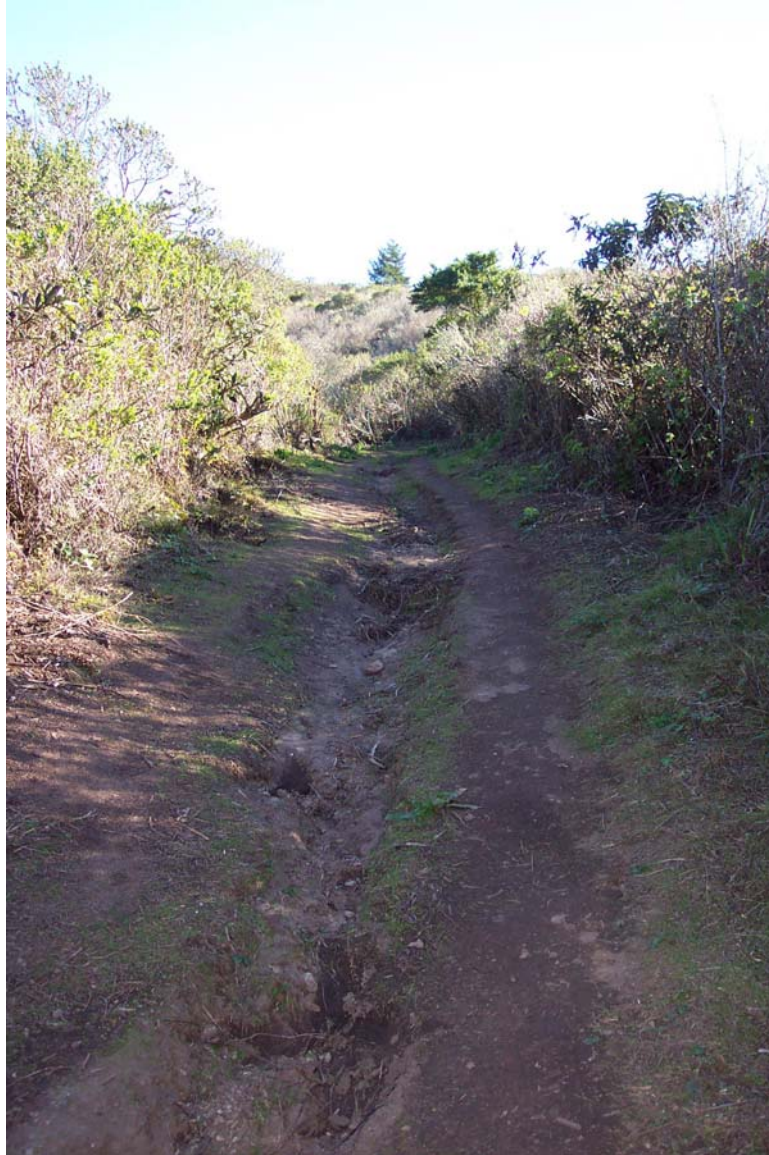


Figure 58: An ephemeral drainage along a portion of Hazelnut trail. Stream piracy is occurring along this stretch as flow is diverted from the South subwatershed to the Middle subwatershed (Line 14 on Figure 53).

5.2.3 *Middle/South subwatershed*

The Middle/South subwatershed is the small drainage that extends from the confluence of the Middle and South Forks to that with the North Fork. It is a very urbanized subwatershed with a very high effective drainage density of 15.1 km/km² and the many impervious surfaces make sediment production mainly a factor of anthropogenic influence.

As there are no sizeable landslides or gullies in the Middle/South subwatershed, surface erosion is the predominant sediment producing process. There is evidence of substantial surface erosion along the upper slopes of roadcuts following the north side of the main channel. The Candlestick variant loam soil complex in this area bordering the road is highly susceptible to detachment. Detached soil is culverted under the road and directly upslope from the channel in multiple places. Sediment routed from the gullies in the Middle subwatershed also drains into the Middle/South channel via this route.

Incised drainage ditches lead to incised culverts from east of Point 2 to 5 on Figure 59, the last significant culvert along the road. Points 2, 3, 4, and 5 are culverts that facilitate delivery of sediment within the ditch to the stream channel. The ditch adjacent to the nearly impervious Weiler Ranch Road runs along the base of the valley draining a large portion of the hillslope. Point 1 on Figure 59 is one of the many upslope surfaces stripped nearly to bedrock from surface erosion providing small amounts of sediment with nearly direct connectivity (Figure 60).

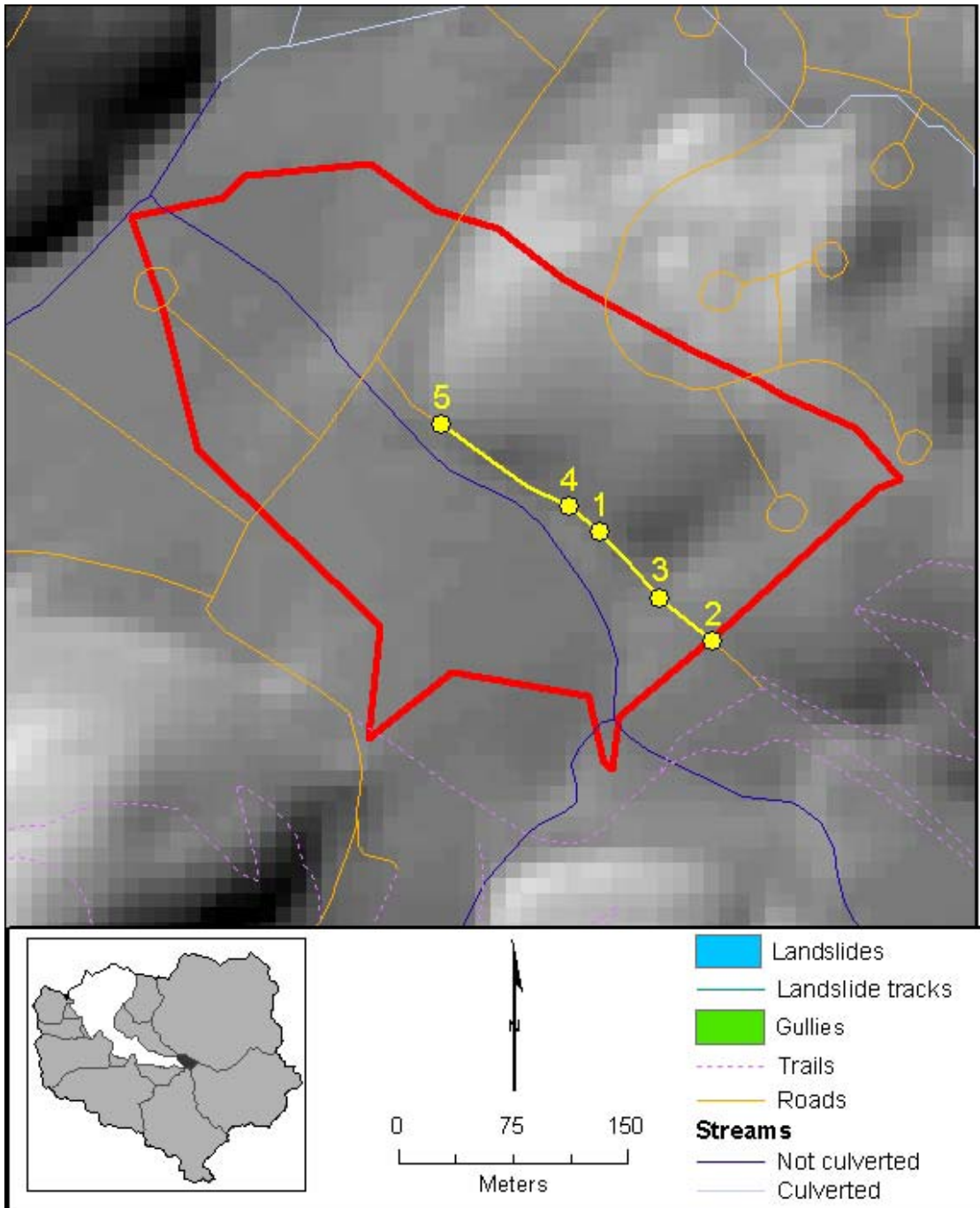


Figure 59: Middle/South subwatershed outlined in red indicating significant sediment sources in yellow. The yellow line indicates flow in drainage ditch that is diverted by culverts.



Figure 60: Surface erosion along an upslope roadcut draining to ditch and culverted under the road directly to the Middle/South fork (Point 1 on Figure 59).

5.2.4 *South subwatershed*

The South subwatershed like the Middle, has very little development and is predominately in a natural state. Again, the only development is the county park facilities comprising only 0.6% of the total land use. The effective drainage of the South subwatershed is relatively low consisting of only trails and the stream network. Because of the large size with little effective drainage, the effective drainage density of the South subwatershed is 5.9 km/km², nearly identical to that of the Middle subwatershed. Surface erosion is most significant along the upper slopes of the South subwatershed in the readily detachable Scarper- Miramar soil complex. Landslides predominately occurred independent of anthropogenic influence and there are no visible gullies in the South subwatershed.

There were a total of 59 landslides identified in the South subwatershed, 39 with predicted connectivity. Since 1941 four slides with very high connectivity delivering 570 m³ of sediment and 22 slides with high connectivity have delivered 1,460 m³. The remaining 13 slides with moderate connectivity have delivered 570 m³ of sediment. The slopes along the southern boundary of the subwatershed are the most susceptible to failure. However, relatively few slides occurred in these areas unlike the findings predicted by the SHALSTAB model. While there are not a large number of landslides in the South subwatershed, most have direct connectivity with the stream ensuring high levels of sediment input. This is consistent with Amato's (2003) findings of substantially higher turbidity from the combined Middle and South Forks than the North Fork during a three-day storm event.

Surface erosion connectivity is high throughout most of the upper subwatershed. The soil in close proximity to the stream network is easily detached with relatively steep slopes. There are no trails in this area however eliminating the anthropogenic impact. The chaparral is thick on the upper slopes and likely filters some of the sediment except where the gradient is too steep or where no understory has developed. For example, small channels have formed in gravelly barren soils draining to manzanita with little vegetative understory (Point 9 on Figure 61; Figure 68). With high connectivity to the stream network, this is a likely source although the end of the channel was not visible or accessible.

Flow concentration along the lower portion of the Hazelnut Trail has created deep incision on the uphill bends of the trail in several spots (Lines 1 & 5 on Figure 61; Figures 62 & 63). Incision along Line 1 has dislodged at least 20 m³ of sediment and likely delivered most of it to the stream only 17 m away down a relatively steep gradient. Along Line 5 at least 20 m³ of material has been removed and at least partially delivered to the stream 18 m away also down a relatively steep gradient. Concentration of flow was also found on the higher portion of the Brooks Creek Trail (Line 10 on Figure 61).

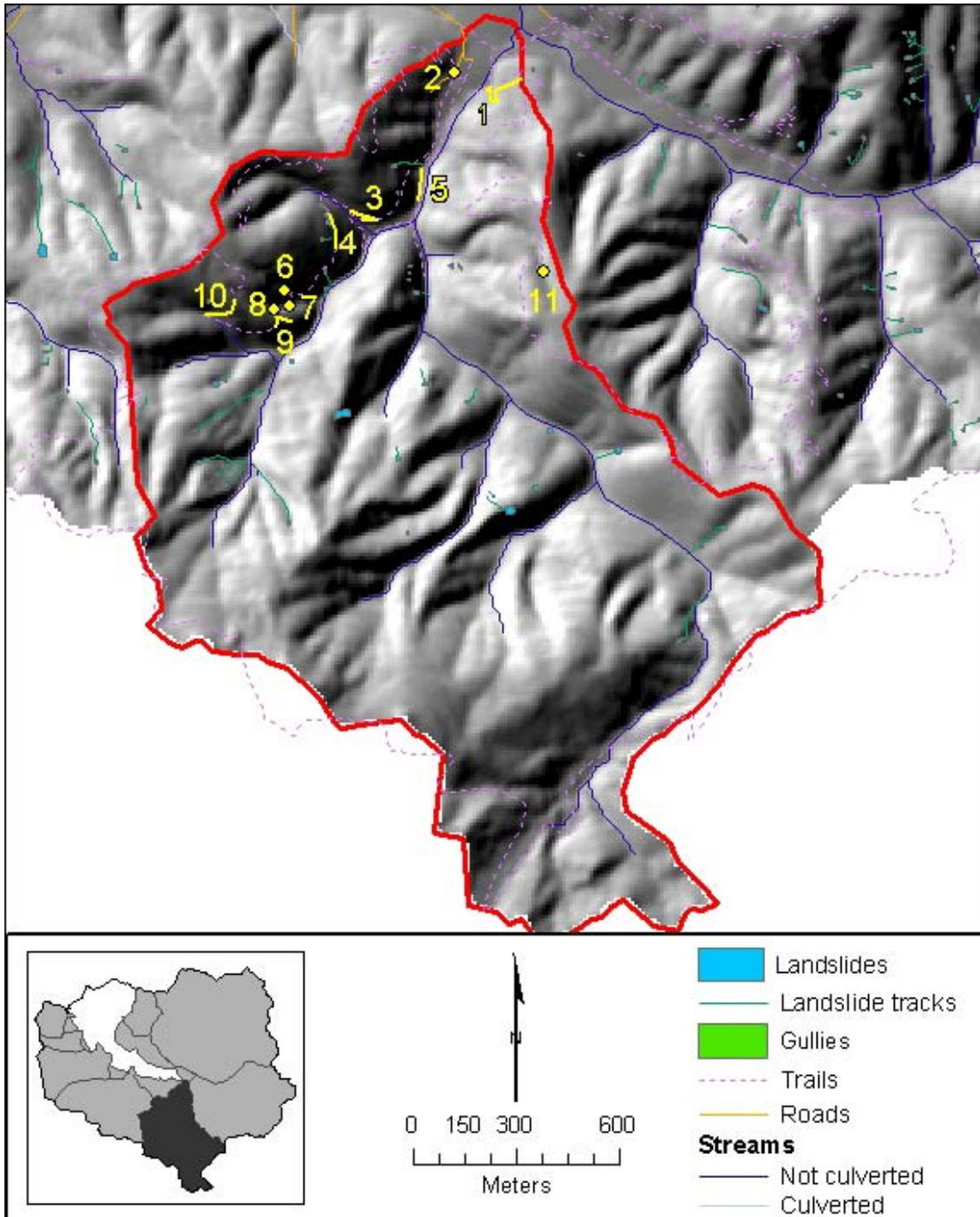


Figure 61: South subwatershed outlined in red indicating significant sediment sources in yellow. Also showing landslides with connectivity to the stream network.

Significant surface erosion with diffuse loose soils was found along trails that did not concentrate into a channel in several locations (Lines 3 & 4 on Figure 61; Figures 64 - 67). Some of this surface erosion is coming from a barren road cut upslope of point line 3 on Figure 61. While it doesn't appear that the road was ever fully established, sediment is being generated from the cut and being transported downslope to the trail. While flow does not appear to focus into a channel, the general surface erosion is significant and within moderate connectivity to the stream network. Landslides have occurred on the upper slopes along Line 4 creating unconsolidated material on which rilling has occurred draining sediment onto the trail but no deep incisions have yet formed on the hillslope or on the trail. Many control structures such as logs supporting the outer, downslope edge of trail, have been installed along the Brooks Creek Trail. This is likely because of the high incidence of uphill landslides and broad surface erosion along the trail. Control structures were also implemented along a colluvium-filled drainage on Hazelnut Trail (Point 11 on Figure 61; Figure 70). A landslide appears to have occurred in the drainage triggering the addition of retention walls and culverts to keep the area drained from potential future failures. Colluvium appears to be collecting just downslope from the trail though and has proven to be a source as connectivity was determined through field observations.

In many locations along the upper Brooks Creek Trail, high ephemeral channels have incised through colluvium from landslide deposits (Point 6, 7 & 8 on Figure 61). This has caused steep, highly incised drainages in several locations requiring bridges over which the trail crosses.

Finally, surface erosion is occurring at the road currently maintained from slumps along the hillslope (Point 2 on Figure 61; Figure 69). While the amount of sediment delivered from this site is not very high, the connectivity of the road network to the stream is direct since the road is on the floodplain.



Figure 62: Fluvial erosion along a ditch from ephemeral drainage along uphill section of lower Hazelnut Trail (end of Line 1 on Figure 61).



Figure 63: Surface erosion along uphill section of trail. Channel on inside where sediment deposits and in the middle of the trail (upper portion of Line 1 on Figure 61).



Figure 64: Surface erosion along on barren hillslope, which was a former road cut, along Brooks Creek Trail upslope of upper trail along Line 3 on Figure 61.



Figure 65: Barren loose soil from upper trail dumping onto lower trail and further downslope (Line 3 on Figure 61).



Figure 66: Surface erosion on Brooks Creek Trail with rilling in unconsolidated landslide deposits on the upper trail cut (Line 4 on Figure 61).



Figure 67: Surface erosion along Brooks Creek Trail (Line 4 on Figure 61).



Figure 68: Channel along Brooks Creek Trail draining on the upper slopes (Line 9 on Figure 61).



Figure 69: Surface erosion upslope from road eroding directly to drainage ditch (Point 2 on Figure 61).

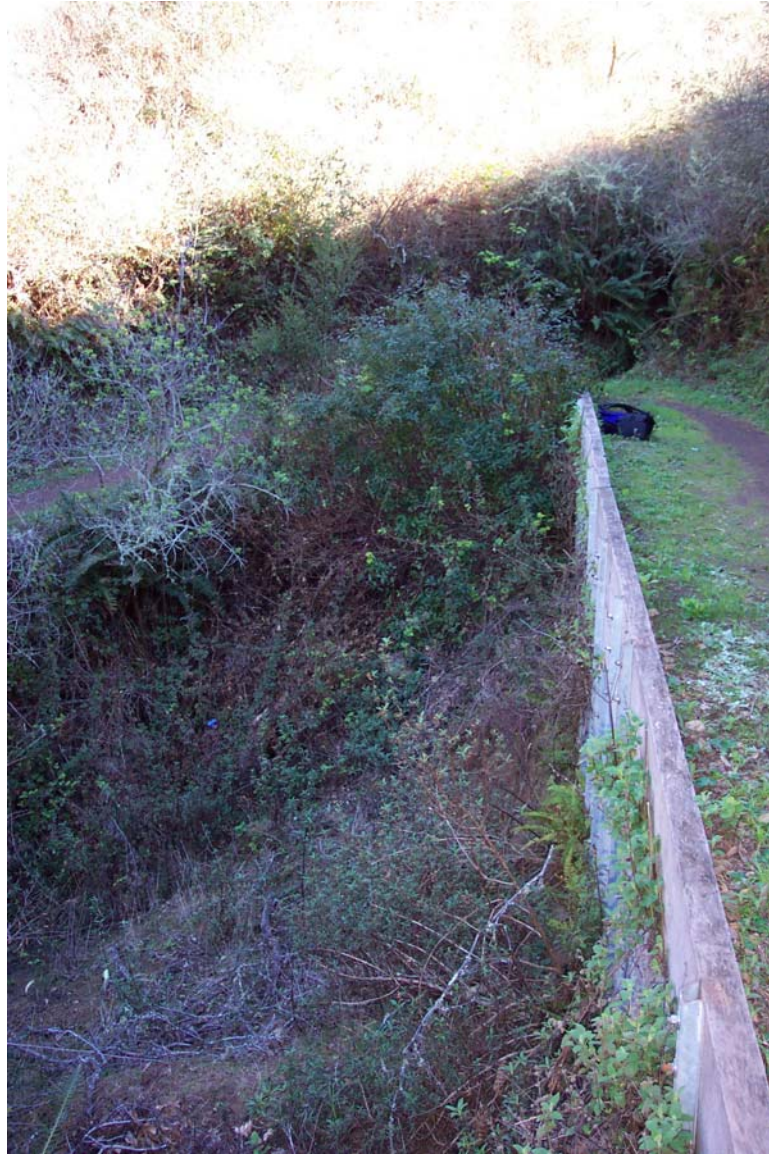


Figure 70: Control structures implemented after a slide. Colluvium is still collecting downslope in drainage with direct connectivity observed from field observations (Point 11 on Figure 61).

5.2.5 *Sanchez subwatershed*

Sanchez subwatershed is moderately sized with a small amount of urban development. One road extends up the valley along the tributary and a number of trails follow the surrounding ridgeline. Many landslides have been triggered by the former Coastside Boulevard running along the northwestern edge of the subwatershed. Two gullies were found in the 1941 aerial photographs, but both appear to have been revegetated in the most recent photographs. Surface erosion is severe in the far southeastern area of the upper watershed and along Coastside Boulevard. The effective drainage density of Sanchez subwatershed is relatively moderate at 7.5 km/km².

There were 78 landslides identified in Sanchez subwatershed. Many of the hillslopes in the upper subwatershed are prone to slope failure as is represented by the landslide distribution, particularly in the southern portion of the subwatershed. Connectivity was predicted for 68 of these slides with 69% or 47 within the high and very high classes. Twelve slides within the very high connectivity class delivered approximately 2,560 m³ and the 35 slides that fell within high connectivity delivered an estimated 2,240 m³ of sediment. The 21 moderately connected slides still delivered a substantial amount of sediment of 1,180 m³.

A large percentage of slides are connected to the stream network and erosion is substantial downslope of Coastside Boulevard. This road was constructed in 1915 as the highway between Pacifica and Half Moon Bay and was decommissioned from

vehicular traffic by the end of World War II (VanderWerf 1994). The trail is still partially paved creating an impervious surface since 1912. Landslides and surface erosion occur in several locations downslope from the trail (Points 1, 4 & 8 to 11 on Figure 71; Figures 72a-b & 78). Mountain biking, hiking, and equestrian use of upslope trails compounds the problems creating compacted, nearly impervious surfaces and concentrated flow (Lines 2 & 3 on Figure 71; Figures 73 & 74).

Surface erosion is also substantial on unmaintained but frequently used trails paralleling an intermittent branch of the main Sanchez Tributary. Heavy recreational and mountain bike use exposes large amounts of barren soil susceptible to erosion (Point 5 on Figure 71; Figures 75a-b). Extensive use of this area has caused the channel to be diverted to multiple intermittent and ephemeral channels, some of which have incised significantly through what appears to be a landslide deposit (Line 6 and Point 7 on Figure 71; Figures 76 & 77).

Surface erosion predicted connectivity is high in the upper hillslopes near the southeastern boundary of the subwatershed. Since there are a few trails in this area on steep slopes, it is probably a significant source of sediment within this subwatershed (Line 12 on Figure 71). Collectively, sediment derived from anthropogenic activity within Sanchez subwatershed is significant.

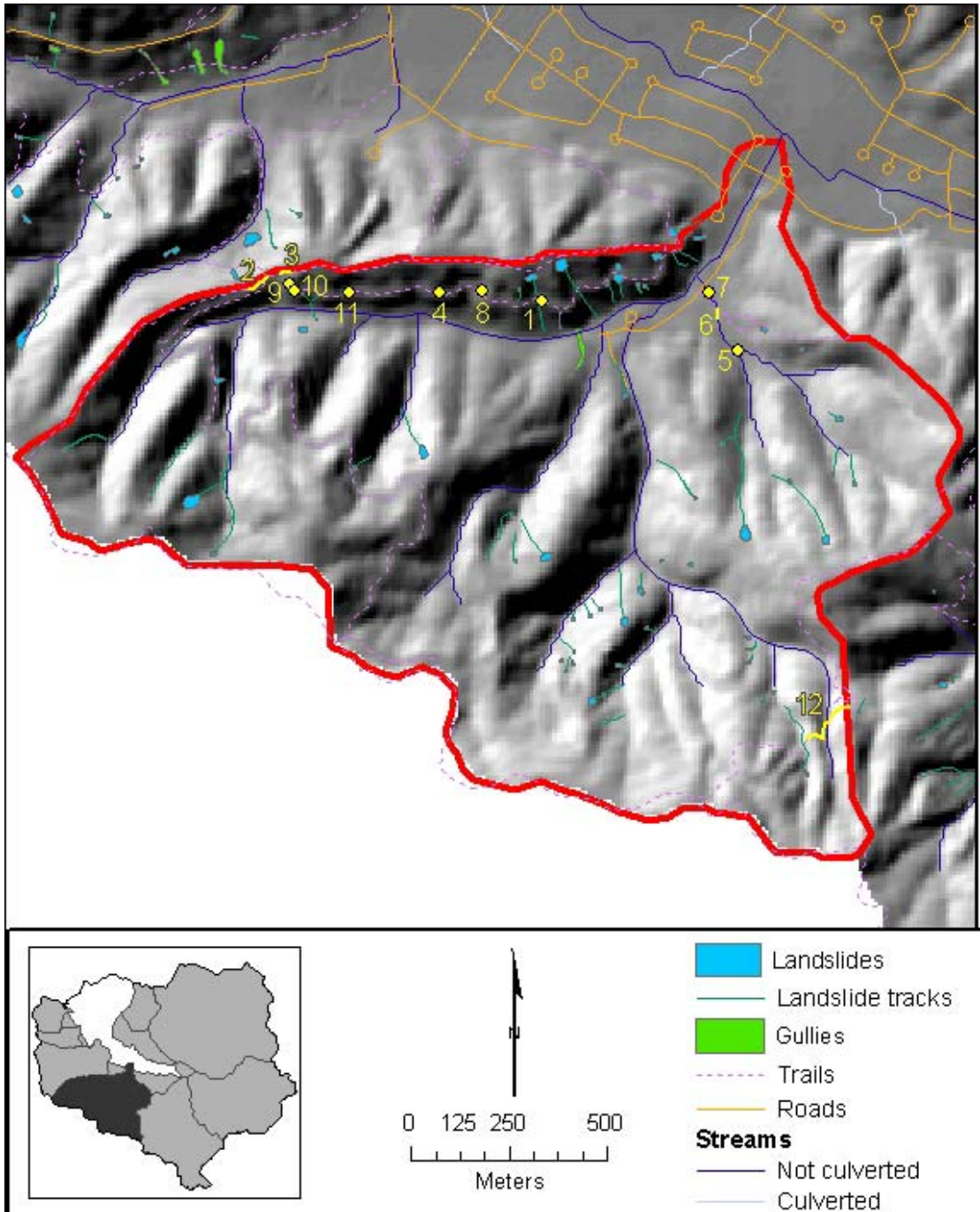


Figure 71: Sanchez subwatershed outlined in red indicating significant sediment sources in yellow. Also showing landslides with connectivity to the stream.



Figure 72a: Severe mass wasting and subsequent surface erosion downslope of Coastside Boulevard draining to Sanchez Fork (Point 1 on Figure 69).

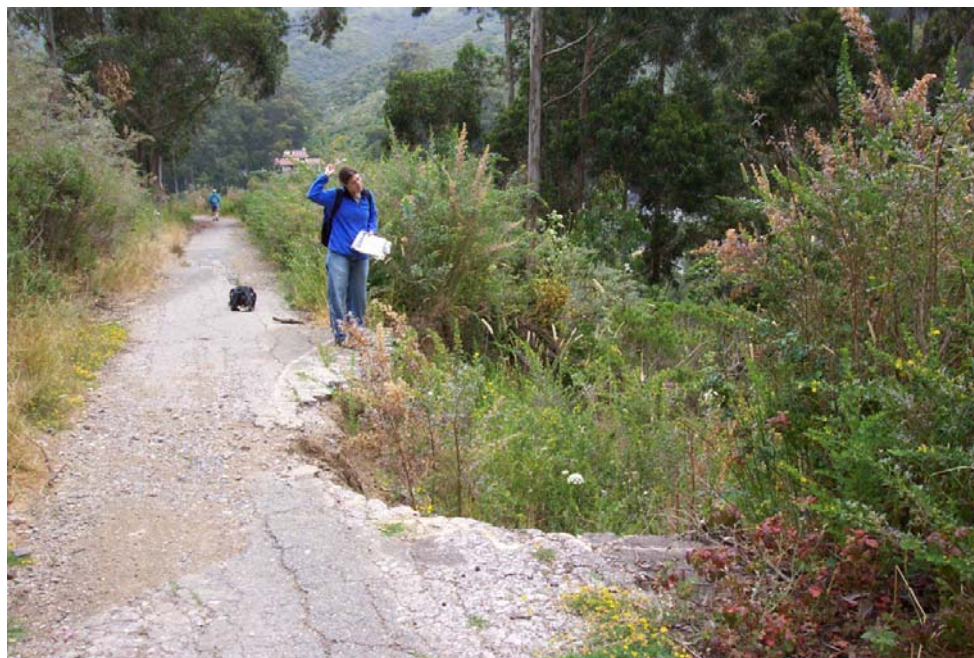


Figure 72b: Same source as shown in Figure 70a taken over 8 months later after one complete rainy season. Pavement has receded slightly more from trail as indicated by the paint markers.



Figure 73: Rutted trail heavily utilized by mountain bikers (Line 2 on Figure 71).



Figure 74: Surface erosion along compacted and gullied trail on the ridgeline between Sanchez and Shamrock subwatersheds (Line 2 on Figure 71).



Figure 75a: Loose unconsolidated soil exposed from significant recreational use (Point 5 on Figure 71).



Figure 75b: Loose unconsolidated soil exposed from significant recreational use (Point 5 on Figure 71).



Figure 76: Channel with significant incision and very exposed tree roots adjacent to heavily compacted trail (Line 6 on Figure 71).



Figure 77: Deep channel incision into landslide deposit (Point 7 on Figure 71).



Figure 78: Trail cut eroded to bedrock with sediment accumulation along the base from surface erosion along upslope soils (Point 8 on Figure 71).

5.2.6 *Shamrock subwatershed*

Shamrock subwatershed is moderately sized with a small amount of urban development, a moderate amount of ranchland, and a significant amount of undeveloped land. Roads sprawl throughout the developed areas and many trails accessed for equestrian use extend along the stream and hillslopes. Similar to Sanchez subwatershed, landslides occurred downslope of the paved highway (Highway 1) following the northern boundary of the subwatershed. Severe gullies have also occurred just downslope of this road from the concentrated runoff. Surface erosion is probably most significant on these gullies and other problem areas just downslope from the trails. The effective drainage density of Shamrock subwatershed is relatively high at 10.4 km/km².

There were a total of 34 landslides identified in Shamrock subwatershed. Of the total, 25 have predicted connectivity. Thirteen of the landslides have moderate connectivity delivered 300 m³ of sediment to the creek while the remaining twelve within the high and very high classes delivered 1,440 m³ and 940 m³ of sediment, respectively. A small number of slides are connected directly to the stream network relative to the larger subwatersheds. The landslides in this subwatershed appear to be influenced by the anthropogenic influences of the roads and trails along the upper hillslopes. Slope susceptibility to failure is the highest in the upper hillslopes of the subwatershed, particularly in the southwestern portion where at least one large slide has occurred.

There were seven gullies identified in Shamrock subwatershed of which four were concentrated just downslope of Highway 1. As of 1997, only three appear to still exist in the subwatershed (Points 1 to 3 on Figure 79; Figure 82) while the others were either graded for development or are obscured by vegetation and are not visible. These three gullies cover a total surface area of 2,840 m², have predicted connectivity with the stream network, and likely deliver substantial amounts of sediment.

Surface erosion is occurring along the gullies and trails. The Candlestick variant loam soil complex underlying the three gullies is especially susceptible to detachment. The gully at point 1 on Figure 77 drains most of Highway 1 through the culvert just uphill. Erosion occurring along the trail leading to the southern boundary is directly routed to the stream network through water bars and culverts (Points 4 to 7 on Figure 79; Figure 81). Concentrated flow along the trail creates incision directing sediment to the tributary (Lines 8 & 9 on Figure 79; Figure 83). The ranch at the base of this valley maintains horses and the trail appears to be frequented by equestrians. This use supplies loose soils that are readily entrained as sediment. In addition, surface erosion is also likely significant on the sparsely vegetated lands used at the base of the valley for horse grazing in Shamrock Ranch (Figure 80). Mountain bike trails, which are also accessed for equestrian use, switchback down the northern slope of the ridge forming the southern boundary of Shamrock subwatershed. Only a sample of these trails was mapped. The intensive use accompanied with these trails has created impervious surfaces with adjacent loose sediment that ultimately spills onto the road and directly into the stream network through the culverted storm drain system (Point 10 on Figure 79; Figure 84).

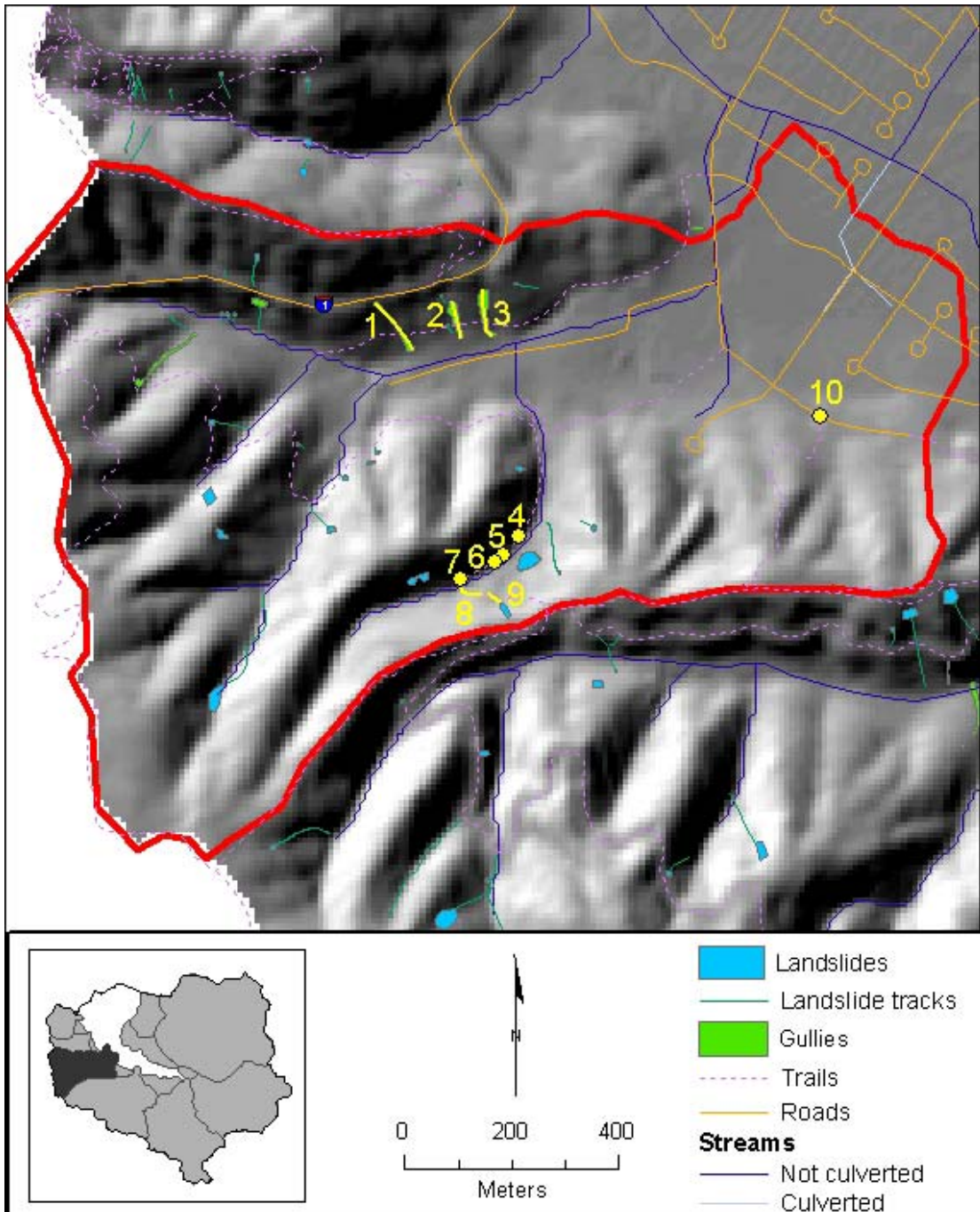


Figure 79: Shamrock subwatershed outlined in red indicating significant sediment sources in yellow. Also showing landslides and gullies with predicted connectivity to the stream network.



Figure 80: Shamrock Ranch in the base of the Shamrock valley with sparsely vegetated fields used for grazing.



Figure 81: Incision in trail routing sediment directly into stream (Point 5 on Figure 79).

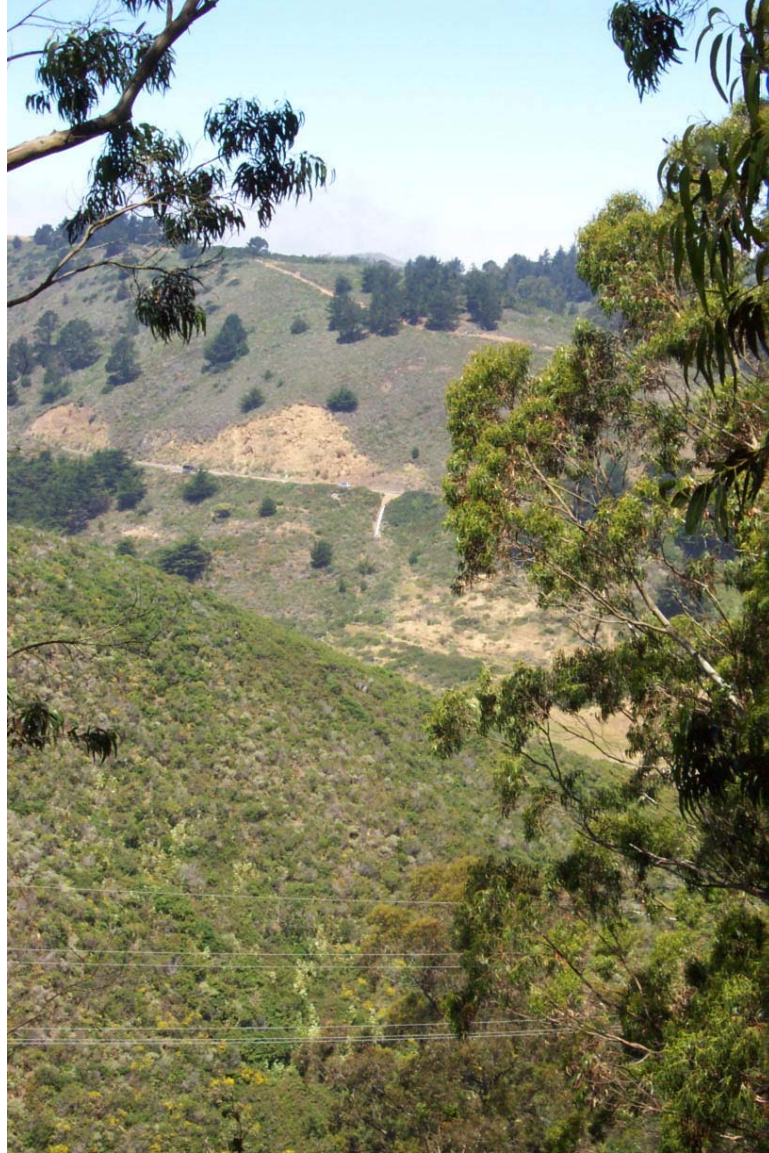


Figure 82: Gully formed from culverted flow downslope of Highway 1 (Point 1 on Figure 79).



Figure 83: Sediment in excavated culvert draining directly to stream along the trail upslope from the Shamrock Ranch (end of Line 8 on Figure 79).



Figure 84: Nearly impervious compacted trail used significantly by mountain bikers. The cumulative flow drains down the trail to the road at Point 10 on Figure 79.

5.2.7 *Pedro Point I subwatershed*

The Pedro Point boundary as classified by the SPCWC was divided into sections I and II, both of which are intermittent drainages. The subwatershed boundary for Pedro Point I covers the northern extent and consists of roughly 50% developed land and 50% undeveloped land. The channelized subtributaries of Pedro Point I Fork vary from the stream network established by the SPCWC. The channel was modified near the confluence with the main channel based on the actual route observed in the field. Consequently the actual subwatershed boundaries differ slightly from those shown in Figure 85 since the extents were generated from the former stream network. Roads extend throughout the developed area and trails cover the upper hillslopes along the southwestern boundary of the subwatershed. The few scattered landslides generally lie on the hillslopes between the trails and the developed areas. The developed lands were covered by gullies in 1941 but have since been graded and paved. The effective drainage density is relatively very high at 16.8 km/km².

The steep upper hillslopes between the trail network and residential development on the lower slopes are relatively prone to failure. Most of the area susceptible to landslides is covered by blue gum eucalyptus and residential development on the mid slopes. There were a total of 10 landslides identified in Pedro Point I subwatershed predominately in this slide-prone area. Only one of these slides has predicted connectivity. The tributary to which it is connected is culverted but the road that runs above it likely acts as a sufficient substitute for connectivity. An estimated 71 m³ of sediment was delivered to the stream network from this landslide.

There were four significant gullies in the subwatershed in 1941 that have since been displaced by urban development. The combined total surface area of the gullies covered 2,808 m². The only obvious gully still existing is among the trails in the upper hillslopes. While in the midst of a trail network and on steep hillslopes, connectivity has not yet likely been established. Surface erosion of these trails could potentially be significant in the future if connectivity is established (Figure 88).

Soil detachment is low to moderate in Pedro Point I subwatershed. Areas most susceptible to erosion are downslope where the flow from the impervious surfaces is concentrated as shown from the culverts on Figure 86 and 87. Points 1 and 2 in Figure 85, the outflows of culverts connected to the storm drain system of the upper slopes, were the only significant sediment source found with predicted connectivity to Pedro Point I tributary. The culvert draining the urbanized hillslope has created a significantly incised channel extending approximately 55 meters before dissipating into a thickly vegetated riparian corridor. The low gradient, thickly vegetated corridor probably filters the majority of the sediment.

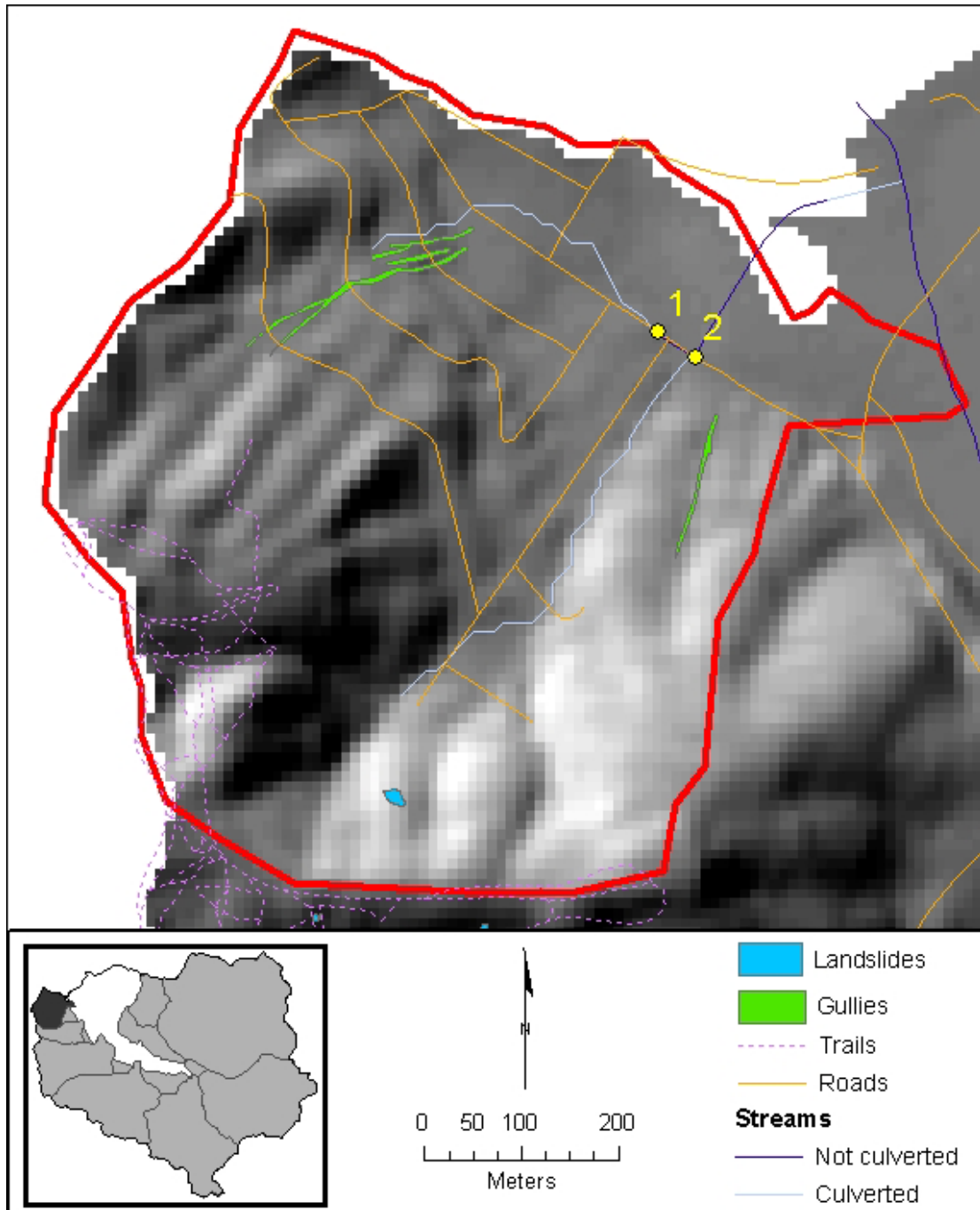


Figure 85: Pedro Point I subwatershed outlined in red indicating significant sediment sources in yellow. Also showing the only landslide and gullies with predicted connectivity.

The main channel of the Pedro Point I Fork is heavily vegetated filtering the majority of the sediment generated at the incised areas of the culvert outlet. Any sediment that is transported through the entire tributary has only 118 m distance in the main channel until the outlet at the ocean is reached. The actual sediment transportation and deposition at this point most likely fluctuates significantly from coastal currents and wave action. The discharge should be sufficient during high flows, the only periods when sediment would connect, to flush and/or keep the entering sediment suspended minimizing the total sediment accumulation within the watershed.



Figure 86: Channel incision from culvert draining the urbanized hillslope at Point 1 on Figure 85.



Figure 87: Channel incision from another culvert draining the urbanized hillside and accumulated flow from culvert at Point 2 on Figure 85.



Figure 88: Severe surface erosion on trails that have not yet established connectivity in the upper Pedro Point I subwatershed. The impervious nature of these trails slows infiltration of rainfall increasing the speed of runoff similar to urban land cover.

5.2.8 *Pedro Point II subwatershed*

Pedro Point II consists of entirely undeveloped land, although intensely used for recreation and far from natural. A network of trails throughout the upper hillslopes near the western boundary was partially created by landslides as observed from the aerial photographs and highly prone to surface erosion. These trails were used by off-road motorcyclists for many years and have created nearly impervious surfaces similar to those in urban environments. Only one gully was identified in the subwatershed of which connectivity may be established along the trail network during high rainfall events. Because of the extensive trails, the effective drainage density is relatively very high at 15.5 km/km².

There were a total of 16 landslides identified within Pedro Point II subwatershed. Connectivity was predicted for eleven of the slides but only five had a high level of connectivity. An estimated total 230 m³ of sediment was delivered to Pedro Point II Fork from the slides with high connectivity and 50 m³ from the slides with moderate connectivity. Most of the landslides were likely generated from former use by off-road motorcyclists.

The only gully in the subwatershed is upslope from the trail along the base of the valley (Point 5 on Figure 89). The downslope end of the gully is at least 200 m from the head of the intermittent tributary. While the distance is long and the gradient is low, trails connect the gully to the channel likely delivering sediment at least during periods of heavy rainfall. An estimated 30 m³ of material has been removed from the gully, some of which has been delivered to the stream.

Surface erosion is significant throughout the subwatershed. The soils most susceptible to detachment lie to the east and downslope of the trail network and the gully in the Barnabe-Candlestick complex. However, these soils are not inherently very susceptible and most erosion was likely induced by anthropogenic activity. Connectivity of these soils to the stream network has been established in this area and is likely influenced by the heavily impacted trails upslope delivering an estimated 820 m³ of sediment in the severely eroded areas (Points 1- 8 on Figure 89; Figures 90-92). Some of the values comprising the total surface erosion duplicate that already attributed to landslides as slides initiated most erosion along these trails. Sediment generated from surface erosion along the total 4,846 m of trails also likely connects to the stream network during heavy rainfall from the heavily compacted soils.

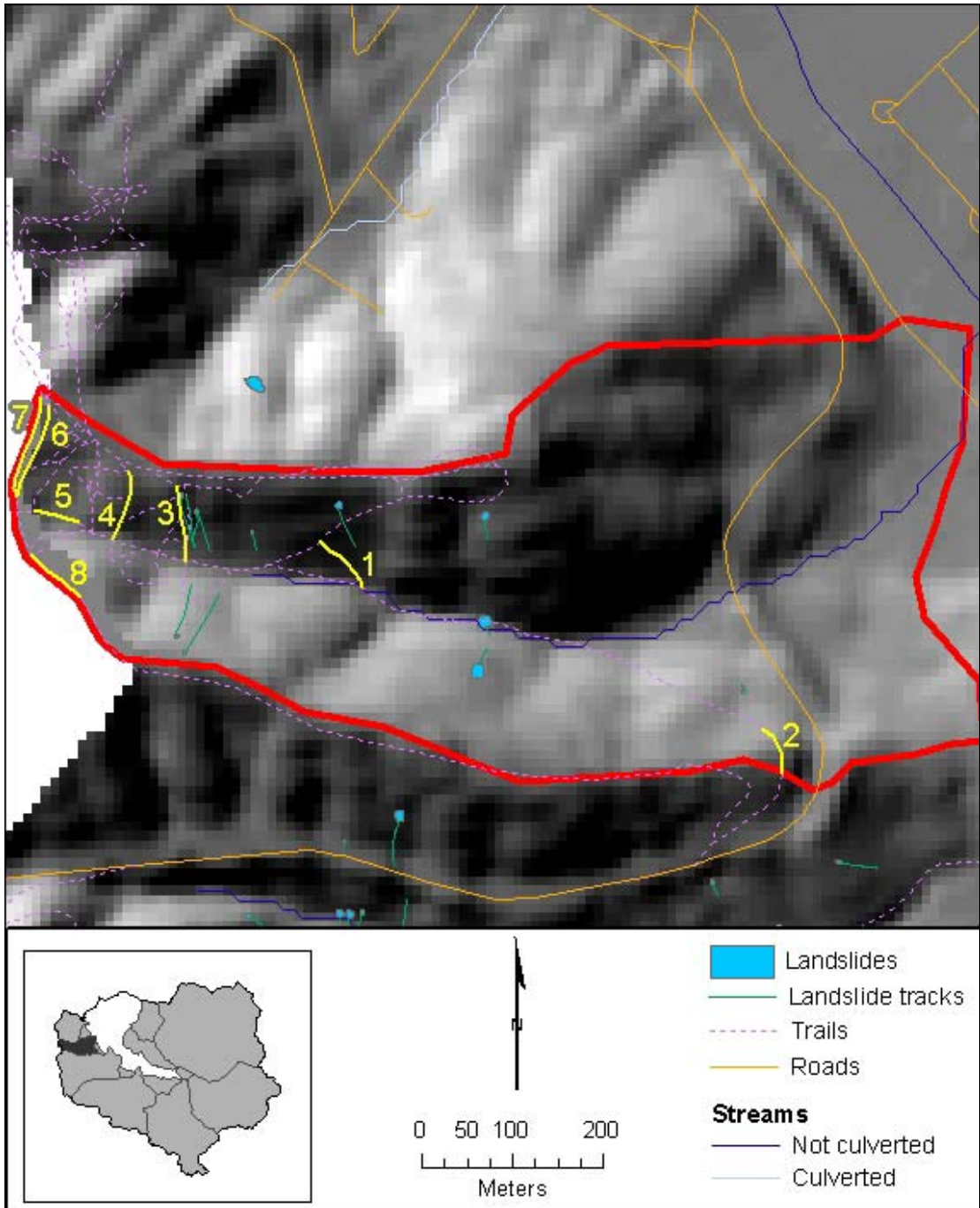


Figure 89: Pedro Point II subwatershed outlined in red indicating significant sediment sources in yellow. Also showing landslides with predicted connectivity.



Figure 90: Surface erosion along former trails (line 3 in Figure 89). An estimated 150 m³ of sediment has been removed from this portion of the trail network.

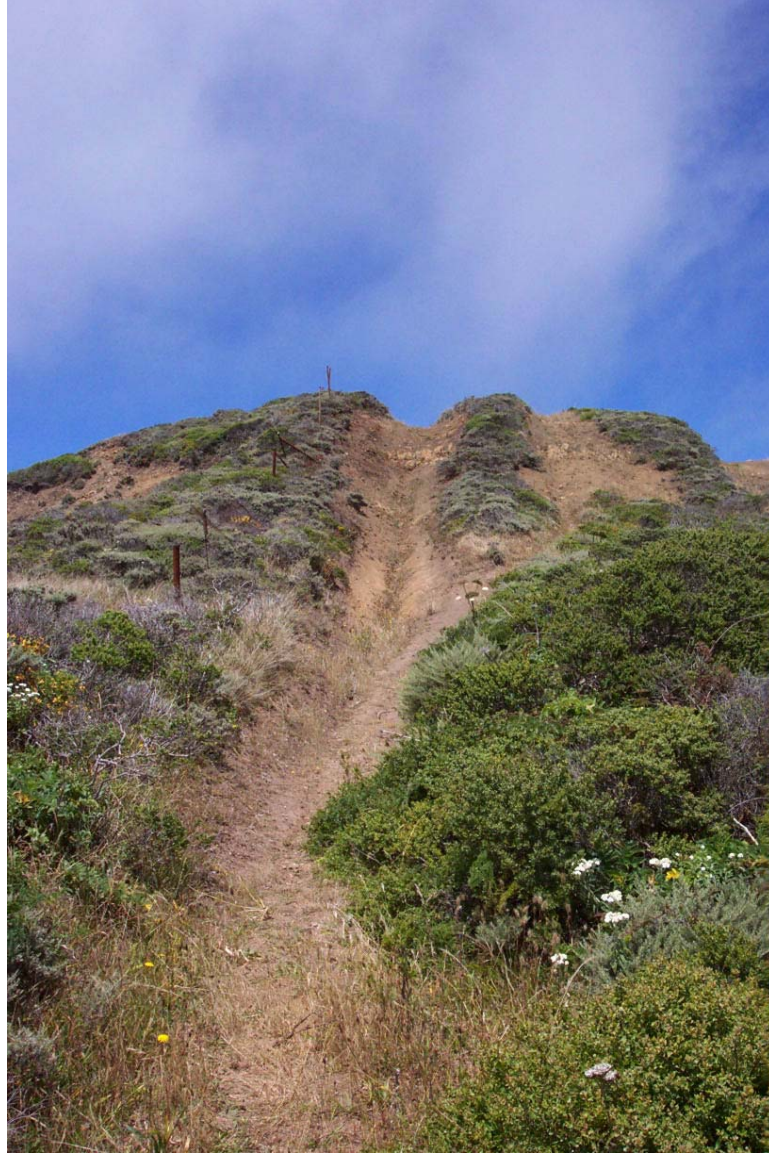


Figure 91: Surface erosion along former trails (line 7 in Figure 89). An estimated 160 m³ of sediment has been removed from this portion of the trail network.



Figure 92: Erosion to bedrock exposing tree roots along upper trail cut. Upslope from eroded trail at line 1 on Figure 89 increasing the effective drainage where incision is initiated.

5.2.9 *Crespi subwatershed*

Crespi subwatershed is mostly developed with a moderate amount of undeveloped lands. Roads follow the development and stream flow is culverted throughout the subwatershed. Every landslide has established connection to the drainage network. As all of the tributaries are culverted, the roads and storm drains act as drainages linking the sediment to the channel. The five gullies that were present in 1941 have since been graded for development and no longer exist. The effective drainage density is moderate at 9.7 km/km².

Hillslopes in Crespi subwatershed are only susceptible to failure along the northern and eastern hillslopes in areas predominately covered by blue gum eucalyptus. Of the total 21 landslides, all had predicted connectivity. The 10 with high connectivity delivered an estimated 1,580 m³ of sediment while the 11 with moderate connectivity delivered 450 m³ of sediment to the stream network. A few landslides are in areas that have since been developed and no longer exist and the remainder fall within the upper hillslopes of the northern portion of the subwatershed. There has only been one new landslide since 1975 in the Crespi subwatershed.

The soils in Crespi subwatershed are not inherently susceptible to detachment. In addition, most soils are covered by impervious surfaces partially negating their physical properties. Where drainage is concentrated erosion can be severe as was obvious with the extensive gullying visible on the 1941 aerial photographs. These gullies have since been graded and paved for development but once covered a total surface area of 8,980 m².

The only area found with surface erosion was upslope of a trail at Point 1 on Figure 93 shown in Figure 94. The total amount of sediment generated from this site is not very high but it is in close connectivity to the tributary.

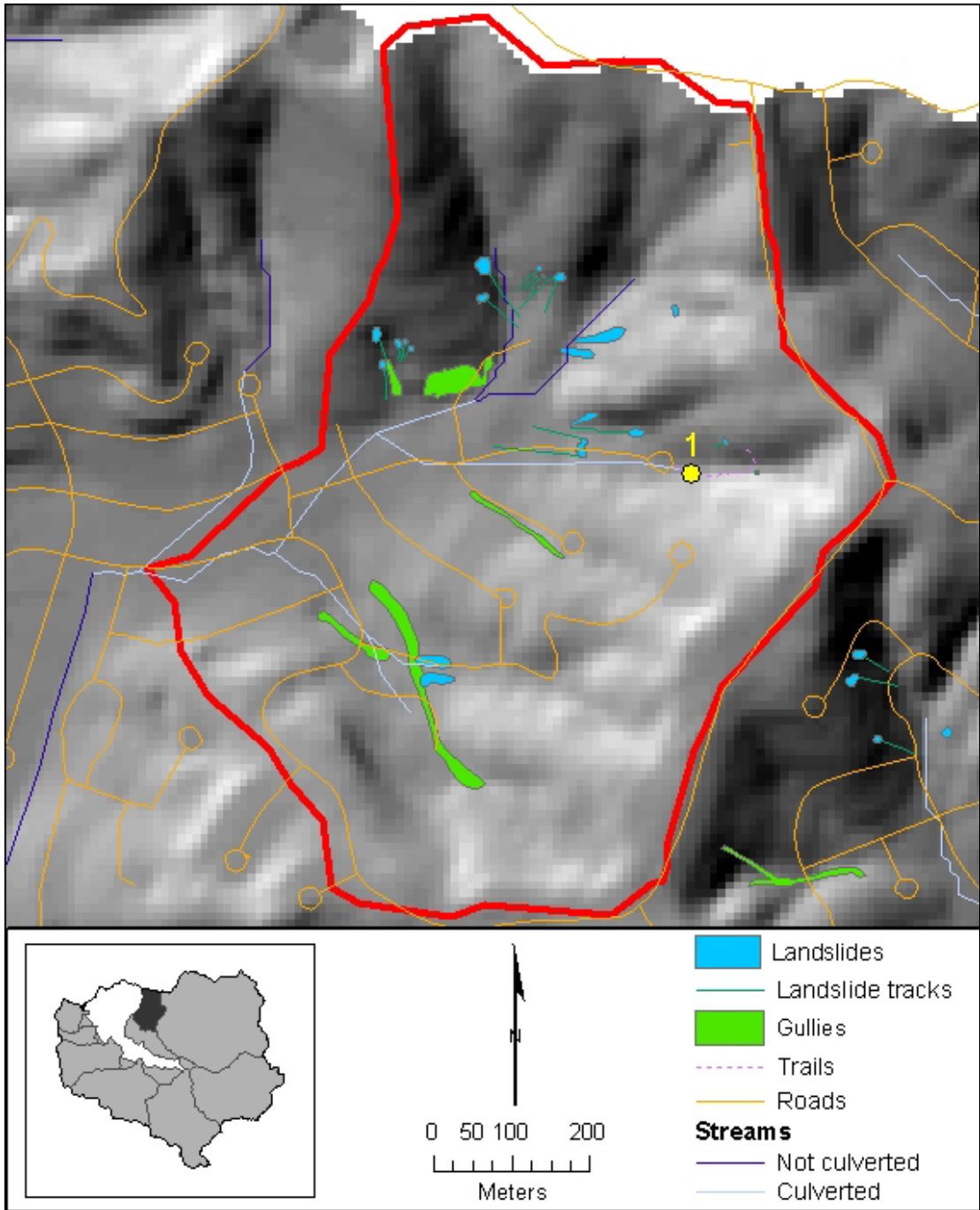


Figure 93: Crespi subwatershed outlined in red indicating significant sediment sources in yellow. Also showing landslides and gullies with predicted connectivity to the stream network.



Figure 94: Surface erosion over unconsolidated material delivering sediment to the downslope trail and adjacent drainage (Point 1 on Figure 93).

5.2.10 Unnamed subwatersheds

The unnamed subwatersheds collectively include hillslopes that generally do not drain directly to one of the tributaries previously assessed. Included are five main sections, unnamed subwatersheds 1 to 5, containing numerous smaller drainages bordering the main channel. Most have little or no roads and only ephemeral flow.

Of the 33 total landslides within the unnamed subwatersheds, only one has predicted connectivity to a tributary. This slide is near the Sanchez Fork and delivered an approximate 110 m³ to the tributary. Adjacent to this landslide is an area along the trail that appears to persistently fail requiring trail reinforcement to stabilize the hillslope (Point 4 in Figure 95; Figure 99). Some of the lower landslides are in close proximity to the road network and may contribute sediment. An estimated 3,860 m³ of material was displaced from these slides, some of which may have been delivered to the stream network via these roads. However, a large amount of the sediment is likely filtered out through residential yards and little probably connects to the stream network. The remainder of the landslides occurred in the upper parts of the subwatersheds.

There were a total of 13 gullies identified in the unnamed subwatersheds but most have since been displaced by residential growth. Only five gullies had predicted connectivity to the stream network, four that formerly covered a surface area of 5,540 m² have since been graded for development. Other gullies that likely have connectivity to the main channel through roads and culverts are still actively contributing sediment in unnamed 2 & 3 subwatersheds. A very significant gully in unnamed 3 subwatershed has been deeply incised with the removal an estimated 1,400 m³ of material (line 1 in Figure 95; Figures 96a,b & 97). This gully is possibly the highest source of sediment in SPCW and has shown significant signs of change over just one rainy season. The upslope sections of the trails that are highlighted are concentrating flow to the gully (Figure 97). The only existing gully is in the unnamed 2 subwatershed, was visible in 1975 and currently covers a surface area of 140 m². Another gully in the unnamed 1 subwatershed covered a surface area of 670 m² in 1941. The present status of the gully is unconfirmed as it is obscured by vegetation on the aerial photograph. The sediment generated from surface erosion in these gullies connects with the storm drain network through gutters and culverts.

The total amount of sediment connectivity from surface erosion for the unnamed subwatersheds is unknown. However, select stretches of significant erosion (lines 2, 3, and 6 in Figure 95; Figure 98) along trails, roads, and in gullies are estimated collectively at 80 m³. Line 5 in Figure 95 also acts as an ephemeral drainage generating sediment and effectively delivering it to the drainage network through a downslope culvert.

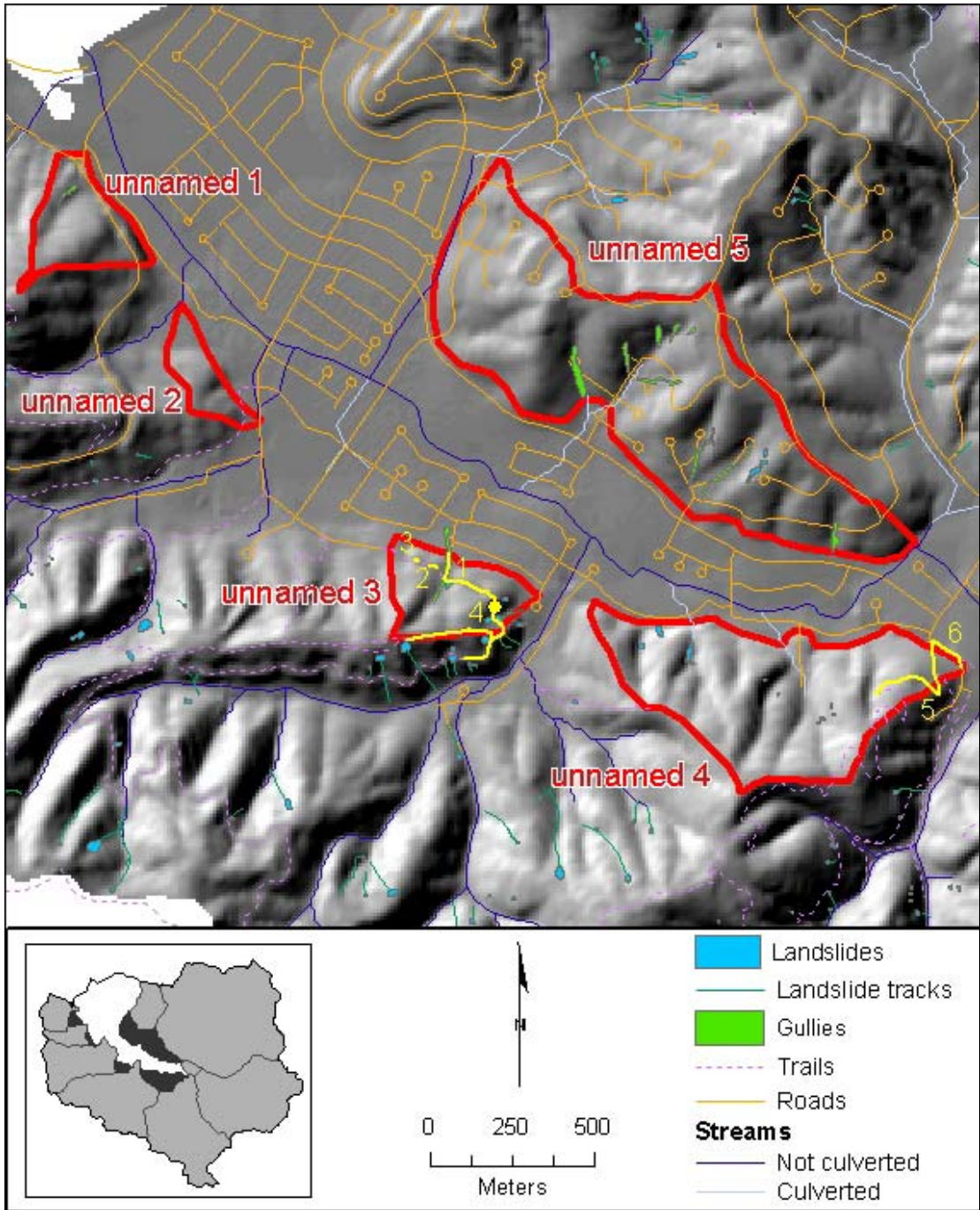


Figure 95: Unnamed subwatersheds outlined in red indicating significant sediment sources in yellow. Also showing landslides and gullies with predicted connectivity to the stream network.



Figure 96a: Severe gully in drainage downslope of paved Coastside Boulevard (Point 1 on Figure 95).



Figure 96b: Severe gully in drainage downslope of paved Coastside Boulevard. Same gully as shown in 96a taken 8 months later after one complete rainy season. Tarps have washed downslope and culvert has broken and moved partially downslope (Point 1 on Figure 95).



Figure 97: Convergence of flow from rutted upper trail and partially paved lower trail. Trails in Sanchez subwatershed draining to gully in unnamed 3 subwatershed contributing to the gully in Figure 96a & b.



Figure 98: Undercut vegetation and exposed tree roots on upper trail cut along Coastside Boulevard (Point 2 on Figure 95).



Figure 99: Erosion control tarps washed downslope of trail on landslide deposit. (Point 4 on Figure 95).



Figure 100: Ephemeral drainage from upslope switchbacks (line 5 in Figure 95).

6. Conclusions

Because of the nature of this thesis, many of the conclusions that were drawn have already been discussed in the Results section. The conclusions here will include the relative contribution of past, present, and future sediment within the respective influential subwatersheds. Recommendations are then proposed in order to mitigate sediment generated from sources that are triggered by anthropogenic influences. Finally, this chapter includes the limitations of this research, identifies possibilities for further research, and explains how this work has contributed to the general knowledge of sediment production processes and sources in the San Pedro Creek Watershed.

6.1 Changes in sediment sources

Past and present sediment production was most significant in Crespi, North, Middle, South, Sanchez, Shamrock, and unnamed 5 subwatersheds. Most of the total calculated sediment was generated from the Middle and Sanchez subwatersheds. This is largely because of an impervious road constructed along the slide-prone hillslopes of the Sanchez subwatershed (VanderWerf 1994) triggered many slides and subsequent gullying while past farming practices along the lower hillslopes generated the same response in the Middle subwatershed. Past farming and possibly grazing practices have also compacted hillslopes in Crespi, North, Middle, and unnamed 5 subwatersheds. As urban development expanded, new roads that triggered many gullies and subsequent surface erosion were created in Sanchez and Shamrock subwatersheds. Drainage terraces constructed in the North subwatershed to protect residential development from unstable hillslopes provide direct delivery of sediment from surface erosion and in some cases triggered landslides. Past storm events have generated many natural landslides, especially in the Middle, South, and Sanchez subwatersheds, effectively delivering short-term sediment to San Pedro Creek. Pedro Point II and Crespi are small intermittent drainages with only seasonal flow that have still generated a substantial amount of sediment from recreational and farming practices, respectively. These drainages have also delivered significant amounts of short-term sediment to the network during high flow events in the rainy season.

Future sediment production is most likely to be from many of the same subwatersheds including North, Middle, Sanchez, and unnamed 3. Hillslopes partially covered by urban development and paved roads will continue to erode into gullies where runoff from the impervious surface concentrates in the North, Sanchez, and unnamed 3 subwatersheds. The gullies in the Middle subwatershed will continue to incise while draining sediment into the ditch along the valley and into the main channel through culverts in the Middle/South subwatershed. However, some of the upslope runoff may be diverted as existing trails have been decommissioned along the ridgeline of the Middle subwatershed. Lack of use on these trails will promote new vegetation growth somewhat decreasing the amount of runoff contributed to the gullies. Future intense rainfall events will likely continue to trigger natural landslides especially in the South, Middle, and Sanchez subwatersheds guaranteeing sources of short-term sediment supply.

6.2 Proposed recommendations for sediment mitigation

Sediment was generated from both natural and anthropogenic sources. Little can be done to reduce sediment production from natural sources besides implementing large, labor intensive, and often impractical and expensive engineering structures. Some of these structures would include the terraced hillslopes that already exist on many slopes in the North subwatershed, concrete revetments, retention walls, and large culverts such as that draining Highway 1. Instead of stopping excessive sedimentation, these structures often merely displace the sources elsewhere. Additionally, such massive techniques are generally implemented where anthropogenic influence has already created a problem, often just exacerbating the issue as is exhibited on the hillslope terraces of the North subwatershed. Hillslopes in the upper South subwatershed have been and remain in fairly natural condition, minimizing the need to implement large-scale sediment reduction structures, as most sediment generated from this subwatershed is short-term.

Bioengineering techniques provide a simpler, pragmatic, inexpensive, and more environmentally friendly solution. Some of these methods have already been utilized in San Pedro Creek where a new bridge was constructed along the Middle Fork. One such method that is particularly applicable to the hillslopes is vegetation planting. Willows were planted to stabilize channel banks and reduce the effectiveness of surface erosion while simultaneously creating steelhead habitat and eventually contributing to water temperature regulation. Areas with little vegetation or barren soils could benefit from vegetation stabilizing hillslopes and providing a riparian buffer through which upslope sediment would be filtered. Previous restoration efforts in Pedro Point II subwatershed have already incorporated revegetation and other simple techniques including mesh retention over barren soils, water bars along trails to diffuse runoff (Figure 101), cut tree and shrub branches that provide stabilize and nutrients for new vegetation (Figure 102), and supply gravel on the roads still occasionally used to promote soil aeration for better infiltration of runoff (Figure 103). These techniques appear to be effective on the hillslopes in Pedro Point II subwatershed that have become nearly impervious from the former off- road motorcycle use. Some of these practices could also be implemented along the lower northern slopes of the Middle subwatershed where previous farming practices created nearly impervious lands and current gullies that extend to the base of the slope. Marsh (1998) identifies additional site-specific mitigation materials and techniques that are generally used for stream bank stabilization but may be applicable for some of the erosion along the lower hillslopes include straw bales, fiber nets (burlap), and constructing sedimentation basins.

Some of the simpler engineering structures already in place that have proven to be ineffective could be modified or removed. Tarps draped across problem areas to abate surface erosion prevent both evaporation of saturated soils and establishment of vegetation. In a few areas, these tarps have washed downslope and are now preventing new vegetation from growing where they have been displaced (Figures 104 & 105). The partially paved Coastside Boulevard (Figure 106) that was built in 1915 (VanderWerf 1994) concentrates runoff to a few sites on the lower slopes creating gullies. Erosion in one gully is so severe that sandbags, tarps, retention poles, and a failing culvert have been

installed to stabilize the trail and try to reduce further erosion (Figure 104). While delaying erosion, these props are proving to be ineffective in impeding long-term erosion. Removal of the pavement along the trail, aeration of the underlying soils, and installation of many more water bars would effectively diffuse runoff and reduce the erosion at this concentrated site. To effectively mitigate sediment generated from this gully and prevent further incision, large-scale modifications would likely need to be made to the gully due to the already extensive depth. General incision along many of the trails throughout the subwatershed is severe enough in places that grading followed by the installation of new water bars may be necessary.



Figure 101: Existing and apparently effective sediment control measures implemented in Pedro Point II subwatershed.



Figure 102: Tree and shrub cuttings (at arrow) placed along trail in an area with deep incision to reduce erosion and promote vegetation growth.



Figure 103: Large gravels spread onto the nearly impervious surface of the road. Over time the gravels will aerate the soils making the road more permeable to moisture.



Figure 104: Ineffective erosion control structures. Tarps have washed downslope over the sandbags supporting the trail in just one rainy season.



Figure 105: Tarps proving to be ineffective control measures have washed downslope of an area of an eroding area along the Coastside Boulevard.



Figure 106: The partially paved surface of the Coastside Boulevard.

6.3 Limitations

Throughout the course of this research multiple limitations regarding the accuracy of the data were recognized. These following limitations affect the application of the data to mitigate sediment:

- Smaller landslides may not have been observed when occurring between years of aerial photographs. Colluvium was discovered along upper trail cuts in several locations where no evidence of upslope landslides was found on the aerial photographs (Figure 107).
- The scale of the 1941 aerial photographs reviewed for landslides was relatively small at 1:24K. At this scale many smaller landslides were not visible.
- Thick vegetation on the hillslopes obscured many small landslides. A study conducted in a forested landscape of southwestern British Columbia found obscured landslides to make up to 85% of the total failures comprising 30% of the total mobilized debris (Brardinoni *et al.* 2002). SPCW is not heavily vegetated throughout and these values are likely too high for this landscape. However, the still significant lack of visibility may partially account for the relatively small number of slides found in the South subwatershed relative to others less vegetated. It is also possible that fewer slides were obvious because of the hillslope stability provided by the roots of the vegetation.
- Landslides were difficult to accurately digitize from the aerial photographs onto the georeferenced coordinate system. Most of the photographs had significant distortion that was adjusted while digitizing each individual landslide. The landslides were traced as precisely as possible, but there is likely an overall error in accuracy somewhat compromising the results.
- The quantitative values used are crude and represent the minimum levels of sediment entrained since 1941. Overall values for surface erosion could not be made throughout the entire watershed and many landslides, and possibly gullies, were not visible on the aerial photographs and consequently, not included in the total. However, comparisons of relative sediment contributions were identified and isolated to the distinct subwatersheds.
- Anthropogenic sources were assessed more fully than natural sources. The thick vegetation makes SPCW inaccessible by foot and difficult to visualize on aerial photographs limiting access to natural sediment sources. However, anthropogenic sources are more accessible and often more influential than natural sources in supplying long-term sediment. Since sediment mitigation efforts are most likely to be applied to anthropogenic sources, the overall objective of this study was still met.



Figure 107: Unconsolidated landslide material along the upper hillslope of the Valley View Trail in the Middle subwatershed. Landslides were not observed on aerial photographs but evidence of occurrence was found in the field.

6.4 Possibilities for future research

In order for a sediment source analysis of SPCW to be complete, a channel bank assessment is needed. While the hillslopes have proven to contribute a substantial amount of sediment to the stream network, the channels deliver sediment with the best connectivity at possibly more significant levels.

If possible more detailed fieldwork identifying landslides that were not obvious on the aerial photographs would support and contribute to the overall values obtained. Since the vegetation in SPCW is so dense, most of the data were extracted from digital GIS data, past aerial photographs, and fieldwork along trails and roads, which was biased toward anthropogenic sources. More extensive surveys on private lands that have a moderate level of accessibility (Picardo, Shamrock, and Crespi Ranches) would add data and improve the accuracy of the hillslope sediment source analysis. Landslides along channel terraces that are obscured by thick vegetation would be obvious during fieldwork through a thorough channel assessment.

To achieve accurate quantitative values of surface erosion, a long-term monitoring study would need to be conducted. Either erosion pins or sediment traps could be used to measure the annual downslope movement of soil. Turbidity meters installed in tributaries would measure the delivery of sediment to the stream network. Figures 72a-b in Section 5.2.5 represent the significance of surface erosion over just one wet season and the possible contribution that was unable to be fully assessed from this study.

6.5 Contributions of the study

This study identified past, present, and likely future natural and anthropogenic sources delivering sediment to San Pedro Creek. It spatially traced changes in sediment production over time simultaneously with associated contributing natural and anthropogenic factors. Based on this research, sediment mitigation efforts aimed at enhancing steelhead trout habitat and ensuring the protection of the population can be effectively implemented. The reduction of sediment in the stream network also increases the water quality enhancing the overall value of the ecosystem. This study provides a comprehensive set of baseline data upon which future long-term sediment-related research in SPCW can be developed. Finally, as a result of this study, extensive literature was gathered, new GIS data were generated, and field data and photographs were collected and analyzed expanding the knowledge base of sediment production and sources in SPCW.

References

- Ahnert, F. 1996. *Introduction to Geomorphology*. London: Arnold Publishers.
- Amato, P. 2003. Effects of urbanization on storm response in the North Fork San Pedro Creek. MA Thesis. San Francisco State University. San Francisco.
- 2002. Storm response of water and turbidity levels in two tributaries in San Pedro Creek. In *San Pedro Creek Watershed Assessment and Enhancement Plan*. http://bss.sfsu.edu/jdavis/pedrocreek/Publications/SPCW_Assess_Enhance_Plan.pdf (10 October 2003).
- Aniya, M. 1985. Landslide-susceptibility mapping in the Amahata River Basin, Japan. *Annals of the Association of American Geographers*. 75: 102-114.
- Battad, D.T. 1993. Integration of Geographic Information Systems for simulation models for watershed erosion prediction. Doctoral dissertation, Range Science, Texas A&M University.
- Benda, L.E. and T. W. Cundy. 1990. Predicting deposition of debris flows in mountain channels. *Canadian Geotechnical Journal*. 27: 409-417.
- Brabb, E.E. and E.H. Pampeyan. 1972. Preliminary map of landslide deposits in San Mateo County, California, scale 1:62,500. *Miscellaneous Field Studies Map MF-344*. Washington, D.C.: U.S. Geological Survey.
- Brabb, E.E., E.H. Pampeyan, and M.G. Bonilla. 1972. Landslide susceptibility in San Mateo County, California, scale 1:62,500. *Miscellaneous Field Studies Map MF-360*. Washington, D.C.: U.S. Geological Survey.
- Brardinoni, F., O. Slaymaker, and M.A. Hassan. 2002. Landslide inventory in a rugged forested watershed: a comparison between air-photo and field survey data. *Geomorphology*. 1321:1-18.
- Budd, W.W., P.L. Cohen, P.R. Saunders, and F.R. Steiner. 1987. Stream corridor management in the Pacific Northwest: I. Determination of stream-corridor widths. *Environmental Management*. 11:587-597.
- Bullard, T. F., T. Minor, and R. Maholland. 2002. Sediment Source Assessment: Squaw Creek Watershed, Placer County, California, Final report. http://www.swrcb.ca.gov/rwqcb6/TMDL/Squaw/Squaw_Creek_Final_Report_6-02.pdf (13 May 2003).
- Caltrans. 2003. Devil's Slide at route 1 and Devil's Slide tunnel project. <http://www.dot.ca.gov/dist4/dslide.htm> (13 May 2003).
- Cannon, S.H. and S.D. Ellen. 1988. Rainfall that resulted in abundant debris-flow activity during the storm. In *Landslides, Floods, and Marine Effects of the Storm of January 3-5, 1982, in the San Francisco Bay Region, California*. U.S. Geological Survey Professional Paper 1434. Washington, D.C.: U.S. Geological Survey.
- Clapp, E.M., P.R. Bierman, and M. Caffee. 2002. Using ¹⁰Be and ²⁶Al to determine sediment generation rates and identify sediment source areas in arid region drainage basins. *Geomorphology*. 45: 89-104.

- Collins, A.L. and D.E. Walling. 2002. Selecting properties for discriminating potential suspended sediment sources in river basins. *Journal of Hydrology*. 261: 216-244.
- Collins, L., P. Amato, and D. Morton. 2001. San Pedro Creek Geomorphic Analysis. In *San Pedro Creek Watershed Assessment and Enhancement Plan*. http://bss.sfsu.edu/jdavis/pedrocreek/Publications/SPCW_Assess_Enhance_Plan.pdf (10 October 2003).
- Collins, L., J. Collins, R. Grossinger, L. McKee, and A. Riley. 2001. Wildcat Creek Watershed: A scientific study of physical processes and land use effects. San Francisco Estuary Institute. <http://www.sfei.org/watersheds/wildcatreport/wildcatindex.html> (13 April 2003).
- Couper, P.R. and I.P. Maddock. 2001. Subaerial river bank erosion processes and their interaction with other bank erosion mechanisms on the River Arrow, Warwickshire, UK. *Earth Surface Processes and Landforms*. 26: 631-646.
- Culp, J. 2002. Shell Mounds to Cul-de-Sacs: The Landscape of San Pedro Valley, Pacifica, California. Research Project. San Francisco State University. San Francisco.
- Davis, J. 2003. Personal Communication. San Francisco State University. San Francisco, California.
- 2002. Personal Communication. San Francisco State University. San Francisco, California.
- Dai, F.C. and C.F. Lee. 2001. Terrain-based mapping of landslide susceptibility using a geographic information system: a case study. *Canadian Geotechnical Journal*. 38: 911-923.
- DeRose, R.C., B. Gomez, M. Marden, and N.A. Trustrum. 1998. Gully erosion in Mangatu Forest, New Zealand, estimated from Digital Elevation Models. *Earth Surface Processes and Landforms*. 23: 1045-1053.
- Dietrich, W.E. and D.R. Montgomery. 1998. SHALSTAB: A digital terrain model for mapping shallow landslide potential. <http://ist-socrates.berkeley.edu/~geomorph/shalstab/> (6 April 2003).
- Dietrich, W.E., D. Bellugi, R. Real de Asua, and L. Stanziano. 1998. SHALSTAB Tools Tutorial: Using SHALSTAB to map shallow landslide potential. <http://ist-socrates.berkeley.edu/~geomorph/shalstab/> (6 April 2003).
- Ellen, S.D., G.F. Wieczorek, W.M. Brown, III, and D.G. Herd. 1988. Introduction. In *Landslides, Floods, and Marine Effects of the Storm of January 3-5, 1982, in the San Francisco Bay Region, California*. U.S. Geological Survey Professional Paper 1434. Washington, D.C.: U.S. Geological Survey.
- Ellen, S.D., R.K. Mark, G.F. Wieczorek, C.M. Wentworth, D.W. Ramsey and T.E. May. 1997. San Francisco Bay Region Landslide Portfolio Part E: Map of debris flow source areas in the San Francisco Bay Region, California. U.S. Geological Survey Open File Report 97-745. <http://wrgis.wr.usgs.gov/open-file/of97-745/of97-745e.html> (14 May 2003).

- ESRI (Earth Systems Research Institute). 2001. USA sample data packaged with ArcMap 8.1.
- Finco, M.V. and G.F. Hepner. 1998. Modeling agricultural nonpoint source sediment yield in Imperial Valley, California. *Photogrammetric Engineering and Remote Sensing*. 64: 1097-1105.
- Gilliam, J.W. and R.W. Skaggs. 1988. Nutrient and sediment removal in wetland buffers. In *Proceedings of National Symposium on Wetland Hydrology*, edited by J.A. Kusler. Berne, NY: Association of State Wetland Managers.
- Heisinger, Doug. 2003. Personal Communication. San Pedro County Park. Pacifica, CA.
- Hooke, J.M. 1979. An analysis of the processes of river bank erosion. *Journal of Hydrology*. (42): 39-62.
- Howard, T.R., J.E. Baldwin, II, and H.F. Donley. 1988. Landslides in Pacifica, California caused by the storm. In *Landslides, Floods, and Marine Effects of the Storm of January 3-5, 1982, in the San Francisco Bay Region, California*. U.S. Geological Survey Professional Paper 1434. Washington, D.C.: U.S. Geological Survey.
- KRIS (Klamath Resource Information System). 2002. Policy and Regulation: Total Maximum Daily Load (TMDL). <http://www.krisweb.com/krisredwood/krisdb/html/krisweb/policy/tmdl.htm> (12 May 2003).
- Kasai, M., T. Marutani, L.M. Reid, and N.A. Trustrum. 2001. Estimation of Temporally Averaged Sediment Delivery Ratio Using Aggradational Terraces in Headwater Catchments of the Waipaoa River, North Island, New Zealand. *Earth Surface Processes and Landforms*. (26): 1-16.
- Kashiwagi, J.H. and Hokholt, L.A. 1991. USDA Soil Conservation Service. Soil Survey of San Mateo County, Eastern part, and San Francisco County, California.
- Knighton, D. 1984. *Fluvial Forms and Processes*. London: Edward Arnold.
- Lynch, J.A., E.S. Corbett, and K. Mussallem. 1985. Best management practices for controlling nonpoint-source pollution on forested watersheds. *Journal of Soil and Water Conservation*. 40: 164-167.
- Magilligan, F.J. 1985. Historical floodplain sedimentation in the Galena River Basin, Wisconsin and Illinois. *Annals of the Association of American Geographers*. 75: 583-594.
- Marsh, W.M. 1998. *Landscape Planning: Environmental Applications*. New York: John Wiley & Sons.
- Meyer, L.D. 1986. Erosion Processes and Sediment Properties for Agricultural Cropland. In *Hillslope Processes: The Binghamton Symposia in Geomorphology: International Series*, edited by A.D. Abrahams. Winchester, M.A.: Allen & Unwin.
- Millward, A.A. and J.E. Mersey. 1999. Adapting the RUSLE to model soil erosion potential in a mountainous tropical watershed. *Catena*. 38: 109-129.
- Montgomery, D.R. 1994. Road surface drainage, channel initiation, and slope instability. *Water Resources Research*. 30(6): 1925-1932.

- Montgomery, D.R. and W.E. Dietrich. 1989. Source areas, drainage density, and channel initiation. *Water Resources Research*. 25(8): 1907-1918.
- Mount, J.R. 1995. *California Rivers and Streams*. Berkeley: University of California Press.
- Nilsen, T.H. 1986. Relative slope-stability mapping and land-use planning in the San Francisco Bay region, California. In *Hillslope Processes: The Binghamton Symposia in Geomorphology: International Series*, edited by A.D. Abrahams. Winchester, M.A.: Allen & Unwin.
- OMC (Oakland Museum of California). Guide to San Francisco Bay Area Creeks, San Pedro Creek, 1896. <http://www.museumca.org/creeks/76-TopoSPedro.html> (14 July 2003).
- Owens, P.N. and D.E. Wallings. 2002. Changes in sediment sources and floodplain deposition rates in the catchment of the River Tweed, Scotland, over the last 100 years: the impact of climate and land use changes. *Earth Surface Processes and Landforms*. 27: 403-423.
- PWA (Pacific Watershed Associates). 2003. Sediment Assessment of Roads and Trails within the Pescadero/Memorial/Sam McDonald County Park Complex, Pescadero Creek Watershed, San Mateo County, California Contract # 39000-02-C212, Final Report. http://www.co.sanmateo.ca.us/vgn/images/portal/cit_609/23704068sedimentassessment_body.pdf (13 May 2003).
- Pampeyan, E.H. 1994. Geologic map of the Montara Mountain and San Mateo 7-1/2' Quadrangles, San Mateo County, California, scale 1:24,000. *Miscellaneous Investigation Series Map I-2390*. Washington, D.C.: U.S. Geological Survey.
- Parsons, A.J. and Abrahams, A.D. 1993. *Overland Flow: Hydraulics and Erosion Mechanics*. New York: Chapman and Hall.
- Pasternack, G.B., G.S. Brush, and W.B. Hilgartner. 2001. Impact of historic land-use change on sediment delivery to a Chesapeake Bay subestuarine delta. *Earth Surface Processes and Landforms*. 26: 409-427.
- Petersen, R.C., L.B.M. Petersen, and J. Lacoursiere. 1992. A building block model for stream restoration. In *River Conservation and Management*, edited by P.J. Boon, P. Calow, and G.E. Petts. Chichester: John Wiley.
- Prosser, I.P., A.O. Hughes, and I.D. Rutherford. 2000. Bank Erosion of an incised upland channel by Subaerial Processes: Tasmania, Australia. *Earth Surface Processes and Landforms*. 25: 1085-1101.
- Rib, H.T. and Liang, T. 1978. Recognition and identification. In *Landslides: Analysis and Control, Special Report 176*. Edited by Schuster, R.L. and Krizek, R.J. Washington, D.C.: National Academy of Sciences. p. 34-80.
- Riley, A.L. 1998. *Restoring Streams in Cities: A Guide for Planners, Policymakers, and Citizens*. Washington, D.C.: Island Press.
- SPCWC (San Pedro Creek Watershed Coalition). 2002. In *San Pedro Creek Watershed Assessment and Enhancement Plan*. http://bss.sfsu.edu/jdavis/pedrocreek/Publications/SPCW_Assess_Enhance_Plan.pdf (10 October 2003).

- 2000. Management Plan-Draft. <http://www.pedrocreek.org/wshedplan.htm> (25 April 2003).
- Selby, M. J. 1993. *Hillslope Materials and Processes*. Oxford: Oxford University Press.
- Simanton, J.R. and K.G. Renard. 1993. Upland erosion research on rangeland. In *Overland Flow: Hydraulics and Erosion Mechanics*, edited by Parsons, A.J. and A.D. Abrahams. New York: Chapman and Hall.
- Smith, T.C. 1988. A method for mapping relative susceptibility to debris flows with an example from San Mateo County. In *Landslides, Floods, and Marine Effects of the Storm of January 3-5, 1982, in the San Francisco Bay Region, California*. U.S. Geological Survey Professional Paper 1434. Washington, D.C.: U.S. Geological Survey.
- Stillwater Sciences. 1999. South Fork Eel TMDL: Sediment source analysis, Final report. <http://www.epa.gov/region09/water/tmdl/sed4.pdf> (13 May 2003).
- Thorne, C.R. 1982. Processes and mechanisms of river bank erosion. In *Gravel-Bed Rivers: Fluvial Processes, Engineering, and Management*, edited by R.D. Hey et al. New York: John Wiley and Sons.
- USCB (US Census Bureau). 2001. Maps and cartographic products, county and county equivalent boundary files. http://www.census.gov/geo/www/cob/bdy_files.html (9 July 2003).
- USGS (US Geological Survey). 2003. San Francisco Bay Area Database, digital elevation models. http://bard.wr.usgs.gov/html/dir/dem_html/dem-sf.html (10 July 2003).
- 1998. Potential San Francisco Bay landslides during El Niño: 1982 debris flow, San Mateo County. <http://walrus.wr.usgs.gov/elnino/landslides-sfbay/debrpic.html> (18 July 2003).
- 1997. Montara Mountain, CA, 7.5-Minute Topographic Quadrangle, scale 1:24,000. Washington, D.C.: U.S. Geological Survey.
- VanderWerf, B. 1994. *Montara Mountain*. El Granada, CA: Gum Tree Land Books.
- Varnes, D.J. 1978. Slope movement types and processes. In *Landslides Analysis and Control*, edited by Schuster, R.L. and Krizek, R. Washington, D.C.: National Academy of Science.
- Vasey, M. 2001. On the trail. http://www.baynature.com/2001spring/ott_spring2001.html (14 July 2003).
- WFPB (Washington Forest Practice Board). 1997a. Watershed Analysis Manual: Mass Wasting, Department of Natural Resources, Forest Practices Division. <http://www.dnr.wa.gov/forestpractices/watershedanalysis/manual/masswast.pdf> (13 May 2003).
- 1997b. Watershed Analysis Manual: Surface Erosion, Department of Natural Resources, Forest Practices Division. <http://www.dnr.wa.gov/forestpractices/watershedanalysis/manual/erosion.pdf> (13 May 2003).
- Walling, D.E. 1983. The Sediment Delivery Problem. *Journal of Hydrology*. (65): 209-237.

- Wentworth, C.M. 1986. Maps of debris flow features evident after the storms of December 1956 and January 1982, Montara Mountain area, California. U.S. Geological Survey Open File Report 86-363, scale 1:24,000. Washington, D.C.: U.S. Geological Survey.
- Wieczorek, G.F., E.L. Harp, R.K. Mark, A.K. Bhattacharyya. 1988. Debris flows and other landslides in San Mateo, Santa Cruz, Contra Costa, Alameda, Napa, Solano, Sonoma, Lake, and Yolo Counties, and other factors influencing debris-flow distribution. In *Landslides, Floods, and Marine Effects of the Storm of January 3-5, 1982, in the San Francisco Bay Region, California*. U.S. Geological Survey Professional Paper 1434. Washington, D.C.: U.S. Geological Survey.

Appendix A: Aerial photograph inventory

Source	Date	Flight/ project number	Scale	Stereo/ mono	Photo number
<i>Whittier College</i>	3/23/1941	C-6660	24K	stereo	1
					2
					3
					13
					14
					15
					16

<i>Whittier College</i>	3/23/1941	C-6660	15,840	mono	86
					87

<i>Pacific Aerial Surveys</i>	5/6/1955	AV170	10K	stereo	01-14
					01-15
					01-16
					01-17
					01-18
	5/10/1955	AV170	10K	stereo	02-24
					02-25
					02-26
					02-27
					02-28
					02-29
					02-30
					03-28
					03-29
					03-30
					03-31
					03-32
					03-33
					03-34
					04-24
					04-25
					04-26
					04-27
					04-28

217

					04-29
--	--	--	--	--	-------

					04-30
--	--	--	--	--	-------

<i>Agricultural stabilization office</i>	5/27/1956	ddb-ir-32	20K	mono	sw
					se
					nw
					ne
					csw
					cse
					cne
					cnw
<i>USGS</i>	9/08/1956	gs-vlx	24K	mono	1.113
					1.114
					1.115

<i>Aerial Viewpoint</i>	7/9/1963	1330	12K	stereo	4-2197
					4-2198
					4-2199
					4-2200
					4-2201
					4-2202
					4-2203
					5-2139
					5-2140
					5-2141
					5-2142
					5-2143
					5-2144
					5-2145
					6-2129
					6-2130
					6-2131
					6-2132
					6-2133
					6-2134
					6-2135

218

<i>USGS</i>	4/18/1968	gs-vbzj	24K	mono	1-106
					1-107

<i>Pacific Aerial</i>	4/28/1975	AV1188	12K	stereo	01-20
-----------------------	-----------	--------	-----	--------	-------

<i>Surveys</i>					
					01-21
					01-22
					01-23
					02-25
					02-26
					02-27
					02-28
					02-29
					02-30
					03-22
					03-23
					03-24
					03-25
					03-26
					03-27

<i>Pacific Aerial Surveys</i>	6/6/1983	AV2265	12K	stereo	01-20
					01-21
					01-22
					01-23
					02-22
					02-23
					02-24
					02-25
					02-26
					02-27
					03-20
					03-21
					03-22
					03-23
					03-24
					03-25

<i>Pacific Aerial Surveys</i>	7/1/1991	AV4075	12K	stereo	03-25
-------------------------------	----------	--------	-----	--------	-------

219

					03-26
					03-27
					03-28
					03-29
					03-30

					03-31
					04-24
					04-25
					04-26
					04-27
					04-28
					04-29
	7/2/1991				02-22
					02-23
					02-24
					02-25
					02-26
					02-27

<i>USGS</i>	6/08/1991	gs-vfnz-c	24K	mono	3-131
					3-132

<i>Pacific Aerial Surveys</i>	6/23/1997	AV5434	12K	stereo	2-22
					2-23
					2-24
					2-25
					2-26
					3-19
					3-20
					3-21
					3-22
					104-19
					104-20
					104-21
					104-22

<i>USGS</i>	?	DOQ	1 meter pixels	mono	
-------------	---	-----	----------------	------	--

Appendix B: GIS layers used

Most of the data layers used were directly from federal sources with modifications either from the San Pedro Creek Watershed Coalition or by the author. Below is a complete list of GIS layers analyzed with source and any modifications. All orthorectifications were matched to the stream network. Most layers are in both vector and raster format, were clipped to match the study area, and analyzed in ArcView 3.2, ArcMap 8.2, and ArcInfo 4.0. All layers were projected to UTM zone 10N using North American Datum 1983.

Connectivity

Derived from buffer distances to the stream and slope gradients.

Contours

Derived from USGS data from the SPCWC.

Digital Elevation Model (DEM)

USGS data used to create hillshade, slope, aspect, flow direction, flow accumulation, and ultimately watershed and subwatershed boundaries.

Effective drainage density

Incorporates the total lengths of the stream network, roads, and trails with drainage channels stabilizing hillslopes. Roads and streams from SPCWC and trails and drainage channels digitized from USGS DEM.

Geology and Faults

A detailed USGS geology map by Pampayen (1994) with fault lines and some landslide deposits was digitized. The faults layer from SPCWC was modified to correspond with this map and others were added. Names were attributed where possible.

Landslides, Landslide Tracks, and Gullies

Landslide and gullies were traced from aerial photographic analysis. Additional landslides were digitized from Pampayen's geology map (1994) and detailed landslide maps by Smith (1988) and Wentworth (1986). Attributed with dates first visible on photos, type of source including obvious trigger mechanisms (natural v. anthropogenic), phase of event (fresh, mature, old), surface area of scars/gullies, volume of material displaced, and volume of material delivered to the stream network.

Past land use

Digitized developed, farmland, and natural areas from stereo aerial photographs for 1941, 1955, 1975, 1983, 1991, and 1997.

Perennial flow points

Digitized from field collected GPS data indicating perennial flow initiation points. Collected mostly in the fall of 2002 with few additions in the summer of 2003.

Perennial point drainage area

Derived drainages for known pour points of perennial flow initiation. Indicates drainage required to sustain perennial flow in SPCW.

Present land use and ownership

Land use and public land ownership available from SPCWC. Names of public landowners were attributed.

Prioritizations

Highlights areas per each subwatershed where sediment abatement management is needed.

Relative slope stability

Generated from SHALSTAB model based on USGS DEM and landslides digitized from stereo air photos. Indicates probable slope failure during varying levels of precipitation events.

Roads

USGS data attributed by the SPCWC and modified by the author. Roads far outside of the study area were deleted and roads within the watershed that are inaccessible to the general public and mainly used as trails were moved to the trails layer. Attributed with year of construction.

Sediment Erosion Model (SEM)

Derived from k factor and slope. Qualitatively indicates areas highly susceptible to surface erosion.

SEM connectivity

Qualitatively identifies areas of sediment delivery to the stream network through the vegetation buffer. Derived by merging the SEM with the vegetation buffer based on slope and distance to stream network.

Soils

US Department of Agriculture Soil Conservation Service data (Kashiwagi and Hokholt 1991) attributed by SPCWC.

Soil k-factor

Derived from soil layer by the k factor attribution. Weighted final value for K factor as a factor of percent composition per soil complex. Used in sediment erosion model (SEM).

Slope

Derived from USGS DEM data from SPCWC.

Stream buffers

Generated from literature review to surround the stream riparian corridors.

Stream network

Derived from hydrologic flow model and modified by SPCWC. Attributed perennial flow data and tributary codes. Modified lines in Pedro Point I and Shamrock to known drainage routes.

Subwatershed

Demarcates the boundaries of each subwatershed examined.

Trails

Traced from the Digital Orthophoto Quad and field collected GPS points. Attributed with levels of use, maintenance, year of construction, and names where applicable.

Vegetation

Detailed vegetation data was assessed and compiled under the direction of Mike Vasey and entered into GIS format by Brendan Thompson.

Appendix C: Past and current land use cover per subwatershed

Developed	1941		1955		1975		1983		1991		1997	
	m ²	% of total	m ²	% of total	m ²	% of total	m ²	% of total	m ²	% of total	m ²	% of total
North	15200	6.2%	16100	3.5%	2301300	69.2%	2316500	69.4%	2321600	68.9%	2321600	68.9%
Middle	1300	0.5%	3300	0.7%	9600	0.3%	8400	0.3%	8400	2.5%	8400	0.2%
Middle/South	6400	2.6%	22700	4.9%	78100	2.3%	77800	2.3%	83000	2.5%	83000	2.5%
South	0	0.0%	400	0.1%	20700	0.6%	20300	0.6%	20300	0.6%	20300	0.6%
Sanchez	0	0.0%	47100	10.3%	81200	2.4%	81800	2.4%	89000	2.6%	89000	2.6%
Shamrock	12400	5.0%	124300	27.1%	219100	6.6%	219100	6.6%	231800	6.9%	231800	6.9%
Hinton	211200	85.7%	33600	7.3%	367600	11.1%	367600	11.0%	367600	10.9%	367600	10.9%
Pedro Point I	0	0.0%	211400	46.1%	247800	7.5%	247800	7.4%	247800	7.4%	247800	7.4%
Pedro Point II	0	0.0%	0	0.0%	0	0.0%	0	0.0%	0	0.0%	0	0.0%
All subwatersheds	246,500		458,900		3,325,400		3,339,300		3,369,500		3,369,500	
<i>All subwatersheds total ha</i>	<i>24.7</i>		<i>45.9</i>		<i>332.5</i>		<i>333.9</i>		<i>337.0</i>		<i>337.0</i>	
<i>% of total land use for entire SPCW</i>		1.4%		2.6%		18.9%		19.0%		19.1%		19.1%

Farmland/ Ranchland	1941	1955	1975	1983	1991	1997

	m ²	% of total	m ²	% of total	m ²	% of total	m ²	% of total	m ²	% of total	m ²	% of total
North	563200	40.5%	439700	47.7%	18900	13.5%	18900	14.2%	18900	14.1%	18900	14.1%
Middle	172700	12.4%	99600	10.8%	6000	4.3%	0	0.0%	0	0.0%	0	0.0%
Middle/South	97800	7.0%	51900	5.6%	0	0.0%	0	0.0%	0	0.0%	0	0.0%
South	45400	3.3%	30600	3.3%	0	0.0%	0	0.0%	0	0.0%	0	0.0%
Sanchez	90100	6.5%	43200	4.7%	600	0.4%	0	0.0%	0	0.0%	0	0.0%
Shamrock	290100	20.9%	189100	20.5%	114400	81.8%	114400	85.8%	115500	85.9%	115500	85.9%
Hinton	78800	5.7%	0	0.0%	0	0.0%	0	0.0%	0	0.0%	0	0.0%
Pedro Point I	1600	0.1%	49100	5.3%	0	0.0%	0	0.0%	0	0.0%	0	0.0%
Pedro Point II	49300	3.5%	19500	2.1%	0	0.0%	0	0.0%	0	0.0%	0	0.0%
All subwatersheds	1,389,000		922,700		139,900		133,300		134,400		134,400	
<i>All subwatersheds total ha</i>	<i>138.9</i>		<i>92.3</i>		<i>14.0</i>		<i>13.3</i>		<i>13.4</i>		<i>13.4</i>	
<i>% of total land use for entire SPCW</i>		7.9%		5.2%		0.8%		0.8%		0.8%		0.8%

Other (Natural/ Undeveloped)	1941	1955	1975	1983	1991	1997

	m ²	% of total										
North	5560600	34.8%	5683200	35.0%	3818800	27.0%	3803600	26.9%	3798500	26.9%	3798500	26.9%
Middle	3106300	19.4%	3177400	19.6%	3264700	23.1%	3271900	23.1%	3271900	23.2%	3271900	23.2%
Middle/South	0	0.0%	29600	0.2%	26100	0.2%	26400	0.2%	21200	0.2%	21200	0.2%
South	2774600	17.4%	2789000	17.2%	2799300	19.8%	2799700	19.8%	2799700	19.8%	2799700	19.8%
Sanchez	2235600	14.0%	2235400	13.8%	2243900	15.9%	2243900	15.9%	2236700	15.9%	2236700	15.9%
Shamrock	1133900	7.1%	1123000	6.9%	1102900	7.8%	1102900	7.8%	1089100	7.7%	1089100	7.7%
Hinton	567800	3.6%	613000	3.8%	279000	2.0%	279000	2.0%	279000	2.0%	279000	2.0%
Pedro Point I	240600	1.5%	240600	1.5%	253300	1.8%	253300	1.8%	253300	1.8%	253300	1.8%
Pedro Point II	360100	2.3%	342200	2.1%	361700	2.6%	361700	2.6%	361700	2.6%	361700	2.6%
All subwatersheds	15,979,500		16,233,400		14,149,700		14,142,400		14,111,100		14,111,100	
<i>All subwatersheds total ha</i>	<i>1598.0</i>		<i>1623.3</i>		<i>1415.0</i>		<i>1414.2</i>		<i>1411.1</i>		<i>1411.1</i>	
<i>% of total land use for entire SPCW</i>		90.7%		92.2%		80.3%		80.3%		80.1%		80.1%

Appendix D: Current effective drainage density per subwatershed

Subwatershed	Total lengths per subwatershed												Total effective drainage density		
	Streams			Roads			Trails			Terraced culverts					
	m	% of total	density (km/km ²)	m	% of total	density (km/km ²)	m	% of total	density (km/km ²)	m	% of total	density (km/km ²)	m	% of total	density (km/km ²)
North	15197	31.0%	2.5	25352	61.7%	4.1	16761	29.5%	2.7	10770	100.0%	1.8	68080	43.2%	11.1
Middle	9444	19.3%	2.9	47	0.1%	0.0	10144	17.9%	3.1	0	0.0%	0.0	19635	12.5%	6.0
Middle/South	483	1.0%	4.8	1031	2.5%	10.3	0	0.0%	0.0	0	0.0%	0.0	1514	1.0%	15.1
South	7339	15.0%	2.6	255	0.6%	0.1	9141	16.1%	3.2	0	0.0%	0.0	16735	10.6%	5.9
Sanchez	7915	16.2%	3.4	1449	3.5%	0.6	8246	14.5%	3.5	0	0.0%	0.0	17610	11.2%	7.5
Shamrock	4389	9.0%	3.0	4402	10.7%	3.0	6241	11.0%	4.3	0	0.0%	0.0	15032	9.5%	10.4
Hinton	1817	3.7%	2.8	4322	10.5%	6.6	138	0.2%	0.2	0	0.0%	0.0	6277	4.0%	9.7
Pedro Point I	1148	2.3%	2.3	3529	8.6%	9.8	2439	4.3%	4.8	0	0.0%	0.0	7116	4.5%	16.8
Pedro Point II	1276	2.6%	3.5	674	1.6%	1.9	3643	6.4%	10.1	0	0.0%	0.0	5593	3.5%	15.5
All subwatersheds (total m)	49008			41061			56753			10770			157592		
<i>All subwatersheds (total km)</i>	<i>49.0</i>			<i>41.1</i>			<i>56.8</i>			<i>10.8</i>			<i>157.6</i>		
Total Density (km/km ²)	2.8			2.3			3.2			0.6			8.9		